

(12) INTERNATIONAL APPLICATION PUBLISHED UNDER THE PATENT COOPERATION TREATY (PCT)

(19) World Intellectual Property Organization
International Bureau(43) International Publication Date
6 December 2001 (06.12.2001)

PCT

(10) International Publication Number
WO 01/91807 A2(51) International Patent Classification⁷: **A61K 51/08**Beechurst Drive, Houston, TX 77030 (US). **KIM, E., Ed-mund** [US/US]; 7 Magnolia Bend, Houston, TX 77024 (US).

(21) International Application Number: PCT/US01/18060

(22) International Filing Date: 1 June 2001 (01.06.2001)

(74) Agent: **SCHULTZ, Teresa, J.**; Fulbright & Jaworski L.L.P., Suite 2400, 600 Congress Avenue, Austin, TX 78701 (US).

(25) Filing Language: English

(26) Publication Language: English

(30) Priority Data:
09/587,583 2 June 2000 (02.06.2000) US
09/599,152 21 June 2000 (21.06.2000) US(81) Designated States (*national*): AI, AG, AL, AM, AT, AU, AZ, BA, BB, BG, BR, BY, BZ, CA, CH, CN, CO, CR, CU, CZ, DE, DK, DM, DZ, EE, ES, FI, GB, GD, GE, GH, GM, HR, HU, ID, IL, IN, IS, JP, KE, KG, KP, KR, KZ, LC, LK, LR, LS, LT, LU, LV, MA, MD, MG, MK, MN, MW, MX, MZ, NO, NZ, PL, PT, RO, RU, SD, SE, SG, SI, SK, SL, TJ, TM, TR, TT, TZ, UA, UG, US, UZ, VN, YU, ZA, ZW.(63) Related by continuation (CON) or continuation-in-part (CIP) to earlier applications:
US 09/587,583 (CON)
Filed on 2 June 2000 (02.06.2000)
US 09/599,152 (CON)
Filed on 21 June 2000 (21.06.2000)(84) Designated States (*regional*): ARIPO patent (GH, GM, KI, LS, MW, MZ, SD, SL, SZ, TZ, UG, ZW), Eurasian patent (AM, AZ, BY, KG, KZ, MD, RU, TJ, TM), European patent (AT, BE, CH, CY, DE, DK, ES, FI, FR, GB, GR, IE, IT, LU, MC, NL, PT, SE, TR), OAPI patent (BF, BJ, CF, CG, CI, CM, GA, GN, GW, ML, MR, NE, SN, TD, TG).(71) Applicant (*for all designated States except US*): **BOARD OF REGENTS** [US/US]; The University of Texas System, 201 W. 7th St., Austin, TX 78701 (US).**Published:**— *without international search report and to be republished upon receipt of that report*

(72) Inventors; and

(75) Inventors/Applicants (*for US only*): **YANG, David, J.** [US/US]; 1123 Spinnaker Way, Sugarland, TX 77030 (US). **LIU, Chun-Wei** [US/US]; 3918 Millrock Circle, Sugarland, TX 77479 (US). **YU, Dong-Fang** [CN/US]; 15002*For two-letter codes and other abbreviations, refer to the "Guidance Notes on Codes and Abbreviations" appearing at the beginning of each regular issue of the PCT Gazette.*

(54) Title: ETHYLENEDICYSSTEINE (EC)-DRUG CONJUGATES, COMPOSITIONS AND METHODS FOR TISSUE SPECIFIC DISEASE IMAGING

(57) Abstract: The invention provides, in a general sense, a new labeling strategy employing ^{99m}Tc chelated with ethylenedicysteine (EC). EC is conjugated with a variety of ligands and chelated to ^{99m}Tc for use as an imaging agent for tissue-specific diseases. The drug conjugates of the invention may also be used as a prognostic tool or as a tool to deliver therapeutics to specific sites within a mammalian body. Kits for use in tissue-specific disease imaging are also provided.

WO 01/91807 A2

DESCRIPTIONETHYLENEDICYSSTEINE (EC)-DRUG CONJUGATES, COMPOSITIONS AND
METHODS FOR TISSUE SPECIFIC DISEASE IMAGINGBACKGROUND OF THE INVENTION

The government does not own rights in the present invention.

1. Field of the Invention

The present invention relates generally to the fields of labeling, radioimaging and chemical synthesis. More particularly, it concerns a strategy for radiolabeling target ligands. It further concerns methods of using those radiolabeled ligands in tumor imaging and tissue-specific disease imaging.

2. Description of Related Art

Improvement of scintigraphic tumor imaging is extensively determined by development of more tumor specific radiopharmaceuticals. Due to greater tumor specificity, radiolabeled ligands as well as radiolabeled antibodies have opened a new era in scintigraphic detection of tumors and undergone extensive preclinical development and evaluation. (Mathias *et al.*, 1996, 1997a, 1997b). Radionuclide imaging modalities (positron emission tomography, PET; single photon emission computed tomography, SPECT) are diagnostic cross-sectional imaging techniques that map the location and concentration of radionuclide-labeled radiotracers. Although CT and MRI provide considerable anatomic information about the location and the extent of tumors, these imaging modalities cannot adequately differentiate invasive lesions from edema, radiation necrosis, grading or gliosis. PET and SPECT can be used to localize and characterize tumors by measuring metabolic activity.

The development of new tumor hypoxia agents is clinically desirable for detecting primary and metastatic lesions as well as predicting radioresponsiveness and time to recurrence. None of the contemporary imaging modalities accurately measures hypoxia since the diagnosis of tumor hypoxia requires pathologic examination. It is often difficult to predict the outcome of a therapy for hypoxic tumor without knowing at least the baseline of hypoxia in each tumor treated. Although the Eppendorf polarographic oxygen microelectrode can measure the oxygen

tension in a tumor, this technique is invasive and needs a skillful operator. Additionally, this technique can only be used on accessible tumors (e.g., head and neck, cervical) and multiple readings are needed. Therefore, an accurate and easy method of measuring tumor hypoxia will be useful for patient selection. However, tumor to normal tissue uptake ratios vary depending upon the radiopharmaceuticals used. Therefore, it would be rational to correlate tumor to normal tissue uptake ratio with the gold standard Eppendorf electrode measures of hypoxia when new radiopharmaceuticals are introduced to clinical practice.

[^{18}F]FMISO has been used to diagnose head and neck tumors, myocardial infarction, inflammation, and brain ischemia (Martin *et al.* 1992; Yeh *et al.* 1994; Yeh *et al.* 1996; Liu *et al.* 1994). Tumor to normal tissue uptake ratio was used as a baseline to assess tumor hypoxia (Yet *et al.* 1996). Although tumor hypoxia using [^{18}F]FMISO was clearly demonstrated, introducing new imaging agents into clinical practice depends on some other factors such as easy availability and isotope cost. Although tumor metabolic imaging using [^{18}F]FDG was clearly demonstrated, introducing molecular imaging agents into clinical practice depends on some other factors such as easy availability and isotope cost. [^{18}F]fluorodeoxyglucose (FDG) has been used to diagnose tumors, myocardial infarction, and neurological disease. In addition, PET radiosynthesis must be rapid because of short half-life of the positron isotopes. ^{18}F chemistry is also complex. The ^{18}F chemistry is not reproducible in different molecules. Thus, it would be ideal to develop a chelator which could conjugate to various drugs. The preferred isotope would be $^{99\text{m}}\text{Tc}$ due to low cost (\$0.21/mCi vs. \$50/mCi for ^{18}F) and low energy (140 Kev vs. 571 Kev for ^{18}F). $^{99\text{m}}\text{Tc}$ is easily obtained from a ^{99}Mo generator. Due to favorable physical characteristics as well as extremely low price, $^{99\text{m}}\text{Tc}$ has been preferred to label radiopharmaceuticals.

Several compounds have been labeled with $^{99\text{m}}\text{Tc}$ using nitrogen and sulfur chelates (Blondeau *et al.*, 1967; Davison *et al.*, 1980). Bis-aminoethanethiol tetradentate ligands, also called diaminodithiol compounds, are known to form very stable Tc(V)O complexes on the basis of efficient binding of the oxotechnetium group to two thiolsulfur and two amine nitrogen atoms. $^{99\text{m}}\text{Tc-L,L-ethylenedicysteine}$ ($^{99\text{m}}\text{Tc-EC}$) is a recent and successful example of N_2S_2 chelates. EC can be labeled with $^{99\text{m}}\text{Tc}$ easily and efficiently with high radiochemical purity and stability, and is excreted through the kidney by active tubular transport (Surma *et al.*, 1994; Van Nerom *et al.*, 1990, 1993; Verbruggen *et al.*, 1990, 1992). Other applications of EC would be chelated with gallium-68 (a positron emitter, $t_{1/2}=68$ min) for PET and gadolinium, iron or manganese for

magnetic resonance imaging (MRI). ^{99m}Tc -EC-neomycin and ^{99m}Tc -EC-deoxyglucose were developed and their potential use in tumor characterization was evaluated.

SUMMARY OF THE INVENTION

The present invention overcomes these and other drawbacks of the prior art by providing a new radiolabeling strategy to target tissues for imaging. The invention provides radiolabeled tissue-specific ligands, as well as methods for making the radiolabeled ligands and for using them to image tissue-specific diseases.

The present invention provides compositions for tissue specific disease imaging. The imaging compositions of the invention generally include a radionuclide label chelated with ethylenedicysteine and a tissue specific ligand conjugated to the ethylenedicysteine on one or both of its acid arms. The ethylenedicysteine forms an N_2S_2 chelate with the radionuclide label. Of course, the chelated compound will include an ionic bond between the radionuclide and the chelating compound. The terms "EC-tissue specific ligand conjugate," "EC-derivative" and "EC-drug conjugate" are used interchangeably herein to refer to the unlabeled ethylenedicysteine-tissue specific ligand compound. As used herein, the term "conjugate" refers to a covalently bonded compound.

Ethylenedicysteine is a bis-aminoethanethiol (BAT) tetradentate ligand, also known as diaminodithiol (DADT) compounds. Such compounds are known to form very stable Tc(V)O- complexes on the basis of efficient binding of the oxotechnetium group to two thiol-sulphur and two amine-nitrogen atoms. The ^{99m}Tc labeled diethylester ($^{99m}\text{Tc-L,L-EC}$) is known as a brain agent. $^{99m}\text{Tc-L,L-ethylenedicysteine}$ ($^{99m}\text{Tc-L,L-EC}$) is its most polar metabolite and was discovered to be excreted rapidly and efficiently in the urine. Thus, $^{99m}\text{Tc-L,L-EC}$ has been used as a renal function agent. (Verbruggen *et al.* 1992).

A tissue specific ligand is a compound that, when introduced into the body of a mammal or patient, will specifically bind to a specific type of tissue. It is envisioned that the compositions of the invention may include virtually any known tissue specific compound. Preferably, the tissue specific ligand used in conjunction with the present invention will be an anticancer agent, DNA topoisomerase inhibitor, antimetabolite, tumor marker, folate receptor targeting ligand, tumor apoptotic cell targeting ligand, tumor hypoxia targeting ligand, DNA

intercalator, receptor marker, peptide, nucleotide, organ specific ligand, antimicrobial agent, such as an antibiotic or an antifungal, glutamate pentapeptide or an agent that mimics glucose. The agents that mimic glucose may also be referred to as "sugars."

5 Preferred anticancer agents include methotrexate, doxorubicin, tamoxifen, paclitaxel, topotecan, LHRH, mitomycin C, etoposide, tomudex, podophyllotoxin, mitoxantrone, captothecin, colchicine, endostatin, fludarabine and gemcitabine. Preferred tumor markers include PSA, ER, PR, AFP, CA-125, CA-199, CEA, interferons, BRCA1, cytoxin, p53, VEGF, integrins, endostatin, HER-2/neu, antisense markers or a monoclonal antibody. It is envisioned
10 that any other known tumor marker or any monoclonal antibody will be effective for use in conjunction with the invention. Preferred folate receptor targeting ligands include folate, methotrexate and tomudex. Preferred tumor apoptotic cell or tumor hypoxia targeting ligands include annexin V, colchicine, nitroimidazole, mitomycin or metronidazole. Preferred antimicrobials include ampicillin, amoxicillin, penicillin, cephalosporin, clidamycin,
15 gentamycin, kanamycin, neomycin, natamycin, nafcillin, rifampin, tetracyclin, vancomycin, bleomycin, and doxycyclin for gram positive and negative bacteria and amphotericin B, amantadine, nystatin, ketoconazole, polymycin, acyclovir, and ganciclovir for fungi. Preferred agents that mimic glucose, or sugars, include neomycin, kanamycin, gentamycin, paromycin, amikacin, tobramycin, netilmicin, ribostamycin, sisomicin, micromicin, lividomycin, dibekacin,
20 isepamicin, astromicin, aminoglycosides, glucose or glucosamine.

In certain embodiments, it will be necessary to include a linker between the ethylenedicycysteine and the tissue specific ligand. A linker is typically used to increase drug solubility in aqueous solutions as well as to minimize alteration in the affinity of drugs. While
25 virtually any linker which will increase the aqueous solubility of the composition is envisioned for use in conjunction with the present invention, the linkers will generally be either a poly-amino acid, a water soluble peptide, or a single amino acid. For example, when the functional group on the tissue specific ligand, or drug, is aliphatic or phenolic-OH, such as for estradiol, topotecan, paclitaxel, or raloxifen etoposide, the linker may be poly-glutamic acid (MW about
30 750 to about 15,000), poly-aspartic acid (MW about 2,000 to about 15,000), bromo ethylacetate, glutamic acid or aspartic acid. When the drug functional group is aliphatic or aromatic-NH₂ or peptide, such as in doxorubicin, mitomycin C, endostatin, annexin V, LHRH, octreotide, and VIP, the linker may be poly-glutamic acid (MW about 750 to about 15,000), poly-aspartic acid (MW about 2,000 to about 15,000), glutamic acid or aspartic acid. When the drug functional

group is carboxylic acid or peptide, such as in methotrexate or folic acid, the linker may be ethylenediamine, or lysine.

While the preferred radionuclide for imaging is ^{99m}Tc , it is envisioned that other radionuclides may be chelated to the EC-tissue specific ligand conjugates, or EC-drug conjugates of the invention, especially for use as therapeutics. For example, other useful radionuclides are ^{188}Re , ^{186}Re , ^{153}Sm , ^{166}Ho , ^{90}Y , ^{89}Sr , ^{67}Ga , ^{68}Ga , ^{111}In , ^{153}Gd , and ^{59}Fe . These compositions are useful to deliver the therapeutic radionuclides to a specific lesion in the body, such as breast cancer, ovarian cancer, prostate cancer (using for example, $^{186/188}\text{Re-EC-folate}$) and head and neck cancer (using for example, $^{186/188}\text{Re-EC-nitroimidazole}$).

Specific embodiments of the present invention include $^{99m}\text{Tc-EC-annexin V}$, $^{99m}\text{Tc-EC-colchicine}$, $^{99m}\text{Tc-EC-nitroimidazole}$, $^{99m}\text{Tc-EC-glutamate pentapeptide}$, $^{99m}\text{Tc-EC-metronidazole}$, $^{99m}\text{Tc-EC-folate}$, $^{99m}\text{Tc-EC-methotrexate}$, $^{99m}\text{Tc-EC-tomodex}$, $^{99m}\text{Tc-EC-neomycin}$, $^{99m}\text{Tc-EC-kanamycin}$, $^{99m}\text{Tc-EC-aminoglycosides}$, (glucosamine, EC-deoxyglucose), $^{99m}\text{Tc-EC-gentamycin}$, and $^{99m}\text{Tc-EC-tobramycin}$.

The present invention further provides a method of synthesizing a radiolabeled ethylenedicycysteine drug conjugate or derivative for imaging or therapeutic use. The method includes obtaining a tissue specific ligand, admixing the ligand with ethylenedicycysteine (EC) to obtain an EC-tissue specific ligand derivative, and admixing the EC-tissue specific ligand derivative with a radionuclide and a reducing agent to obtain a radionuclide labeled EC-tissue specific ligand derivative. The radionuclide is chelated to the EC via an N_2S_2 chelate. The tissue specific ligand is conjugated to one or both acid arms of the EC either directly or through a linker as described above. The reducing agent is preferably a dithionite ion, a stannous ion or a ferrous ion.

The present invention further provides a method for labeling a tissue specific ligand for imaging, therapeutic use or for diagnostic or prognostic use. The labeling method includes the steps of obtaining a tissue specific ligand, admixing the tissue specific ligand with ethylenedicycysteine (EC) to obtain an EC-ligand drug conjugate, and reacting the drug conjugate with ^{99m}Tc in the presence of a reducing agent to form an N_2S_2 chelate between the ethylenedicycysteine and the ^{99m}Tc .

For purposes of this embodiment, the tissue specific ligand may be any of the ligands described above or discussed herein. The reducing agent may be any known reducing agent, but will preferably be a dithionite ion, a stannous ion or a ferrous ion.

5 In another embodiment, the present invention provides a method of imaging a site within a mammalian body. The imaging method includes the steps of administering an effective diagnostic amount of a composition comprising a ^{99m}Tc labeled ethylenedicysteine-tissue specific ligand conjugate and detecting a radioactive signal from the ^{99m}Tc localized at the site. The detecting step will typically be performed from about 10 minutes to about 4 hours after
10 introduction of the composition into the mammalian body. Most preferably, the detecting step will be performed about 1 hour after injection of the composition into the mammalian body.

In certain preferred embodiments, the site will be an infection, tumor, heart, lung, brain, liver, spleen, pancreas, intestine or any other organ. The tumor or infection may be located
15 anywhere within the mammalian body but will generally be in the breast, ovary, prostate, endometrium, lung, brain, or liver. The site may also be a folate-positive cancer or estrogen-positive cancer.

The invention also provides a kit for preparing a radiopharmaceutical preparation. The
20 kit generally includes a sealed *via* or bag, or any other kind of appropriate container, containing a predetermined quantity of an ethylenedicysteine-tissue specific ligand conjugate composition and a sufficient amount of reducing agent to label the conjugate with ^{99m}Tc . In certain cases, the ethylenedicysteine-tissue specific ligand conjugate composition will also include a linker between the ethylenedicysteine and the tissue specific ligand. The tissue specific ligand may be
25 any ligand that specifically binds to any specific tissue type, such as those discussed herein. When a linker is included in the composition, it may be any linker as described herein.

The components of the kit may be in any appropriate form, such as in liquid, frozen or dry form. In a preferred embodiment, the kit components are provided in lyophilized form. The
30 kit may also include an antioxidant and/or a scavenger. The antioxidant may be any known antioxidant but is preferably vitamin C. Scavengers may also be present to bind leftover radionuclide. Most commercially available kits contain glucoheptonate as the scavenger. However, glucoheptonate does not completely react with typical kit components, leaving approximately 10-15% left over. This leftover glucoheptonate will go to a tumor and skew

imaging results. Therefore, the inventors prefer to use EDTA as the scavenger as it is cheaper and reacts more completely.

Another aspect of the invention is a prognostic method for determining the potential usefulness of a candidate compound for treatment of specific tumors. Currently, most tumors are treated with the "usual drug of choice" in chemotherapy without any indication whether the drug is actually effective against that particular tumor until months, and many thousands of dollars, later. The imaging compositions of the invention are useful in delivering a particular drug to the site of the tumor in the form of a labeled EC-drug conjugate and then imaging the site within hours to determine whether a particular drug.

In that regard, the prognostic method of the invention includes the steps of determining the site of a tumor within a mammalian body, obtaining an imaging composition which includes a radionuclide chelated to EC which is conjugated to a tumor specific cancer chemotherapy drug candidate, administering the composition to the mammalian body and imaging the site to determine the effectiveness of the candidate drug against the tumor. Typically, the imaging step will be performed within about 10 minutes to about 4 hours after injection of the composition into the mammalian body. Preferably, the imaging step will be performed within about 1 hour after injection of the composition into the mammalian body.

The cancer chemotherapy drug candidate to be conjugated to EC in the prognostic compositions may be chosen from known cancer chemotherapy drugs. Such drugs appear in Table 2. There are many anticancer agents known to be specific for certain types of cancers. However, not every anticancer agent for a specific type of cancer is effective in every patient. Therefore, the present invention provides for the first time a method of determining possible effectiveness of a candidate drug before expending a lot of time and money on treatment.

Yet another embodiment of the present invention is a reagent for preparing a scintigraphic imaging agent. The reagent of the invention includes a tissue specific ligand, having an affinity for targeted sites *in vivo* sufficient to produce a scintigraphically-detectable image, covalently linked to a ^{99m}Tc binding moiety. The ^{99m}Tc binding moiety is either directly attached to the tissue specific ligand or is attached to the ligand through a linker as described above. The ^{99m}Tc binding moiety is preferably an N_2S_2 chelate between ^{99m}Tc in the +4 oxidation state and ethylenedicysteine (EC). The tissue specific ligand will be covalently linked

to one or both acid arms of the EC, either directly or through a linker as described above. The tissue specific ligand may be any of the ligands as described above.

BRIEF DESCRIPTION OF THE DRAWINGS

The following drawings form part of the present specification and are included to further demonstrate certain aspects of the present invention. The invention may be better understood by reference to one or more of these drawings in combination with the detailed description of specific embodiments presented herein.

FIG. 1. Synthetic scheme of ^{99m}Tc -EC-folate.

FIG. 2. Synthetic scheme of ^{99m}Tc -EC-MTX (methotrexate).

FIG. 3. Synthetic scheme of ^{99m}Tc -EC-TDX (tomudex).

FIG. 4. Biodistribution studies for ^{99m}Tc -EC and ^{99m}Tc -EC-folate.

FIG. 5. Blocking studies for tumor/muscle and tumor/blood count ratios with ^{99m}Tc -EC-folate.

FIG. 6A and 6B. Scintigraphic images of tumor in ^{99m}Tc -EC-folate injected group as compared to ^{99m}Tc -EC injected group.

FIG. 7. Synthetic scheme of EC-MN (metronidazole)

FIG. 8A and FIG. 8B. For EC-NIM, FIG. 8A shows the synthetic scheme and FIG. 8B illustrates the ^1H -NMR confirmation of the structure.

FIG. 9. Biodistribution studies (tumor/blood ratios) for ^{99m}Tc -EC-MN, $[^{18}\text{F}]\text{FMISO}$ and $[^{131}\text{I}]\text{IMISO}$.

FIG. 10. Biodistribution studies (tumor/muscle ratios) for ^{99m}Tc -EC, $[^{18}\text{F}]\text{FMISO}$ and $[^{131}\text{I}]\text{IMISO}$.

FIG. 11A and 11B. Scintigraphic images of tumor in ^{99m}Tc -EC-MN (FIG. 11A) and ^{99m}Tc -EC (FIG. 11B) injected groups.

5 **FIG. 12.** Autoradiograms performed at 1 hour after injection with ^{99m}Tc -EC-MN.

FIG. 13. Illustrates stability of ^{99m}Tc -EC-NIM in dog serum samples.

10 **FIG. 14A and FIG. 14B.** Illustrates breast tumor uptake of ^{99m}Tc -EC-NIM vs. ^{99m}Tc -EC in rats (FIG. 14A) and in rats treated with paclitaxel compared to controls (FIG. 14B).

15 **FIG. 15A, FIG. 15B, FIG. 15C, and FIG. 15D.** Illustrates ovarian tumor uptake of ^{99m}Tc -EC-NIM vs. ^{99m}Tc -EC in rats (FIG. 15A) The tumor uptake in rats treated with paclitaxel (FIG. 15B) was less than tumor uptake in rats not treated with paclitaxel (FIG. 15A). Also illustrated is tumor uptake of ^{99m}Tc -EC-NIM in rats having sarcomas. FIG. 15C shows tumor uptake in sarcoma bearing rats treated with paclitaxel while FIG. 15D shows tumor uptake in rats not treated with paclitaxel. There was a decreased uptake of ^{99m}Tc -EC-NIM after treatment with paclitaxel.

20 **FIG. 16.** Synthetic scheme of EC-GAP (pentaglutamate).

FIG. 17. Scintigraphic images of breast tumors in ^{99m}Tc -EC-GAP injected group.

25 **FIG. 18.** Scintigraphic images of breast tumors in ^{99m}Tc -EC-ANNEX V injected group at different time intervals.

FIG. 19A and FIG. 19B. Comparison of uptake difference of ^{99m}Tc -EC-ANNEX V between pre- (FIG. 19A) and post- (FIG. 19B) paclitaxel treatment in ovarian tumor bearing group.

30 **FIG. 20A and FIG. 20B.** Comparison of uptake difference of ^{99m}Tc -EC-ANNEX V between pre- (FIG. 20A) and post- (FIG. 20B) paclitaxel treatment in sarcoma tumor bearing group.

FIG. 21. Synthetic scheme of EC-COL (colchicine).

FIG. 22. Illustration that no degradation products observed in EC-COL synthesis.

FIG. 23. Ratios of tumor to muscle and tumor to blood as function of time for ^{99m}Tc -EC-COL.

FIG. 24. Ratios of tumor to muscle and tumor to blood as function of time for ^{99m}Tc -EC.

FIG. 25. In vivo imaging studies in breast tumor bearing rats with ^{99m}Tc -EC-COL.

FIG. 26. In vivo imaging studies in breast tumor bearing rats with ^{99m}Tc -EC.

FIG. 27. Computer outlined region of interest after injection of ^{99m}Tc -EC-COL vs. ^{99m}Tc -EC.

FIG. 28. SPECT with ^{99m}Tc -EC-MN of 59 year old male patient who suffered stroke. Images taken one hour post-injection.

FIG. 29. MRI T1 weighted image of same patient as FIG. 28.

FIG. 30. SPECT with ^{99m}Tc -EC-MN of 73 year old male patient one day after stroke at one hour post-injection.

FIG. 31. SPECT with ^{99m}Tc -EC-MN of same 73 year old patient as imaged in FIG. 30 twelve days after stroke at one hour post-injection.

FIG. 32. CT of same 73 year old male stroke patient as imaged in FIG. 30, one day after stroke.

FIG. 33. CT of same 73 year old male stroke patient as imaged in FIG. 32, twelve days after stroke. Note, no marked difference between days one and twelve using CT for imaging.

FIG. 34. SPECT with ^{99m}Tc -EC-MN of 72 year old male patient who suffered a stroke at one hour post-injection.

FIG. 35. CT of same 72 year old stroke patient as imaged in FIG. 34. Note how CT image exaggerates the lesion size.

FIG. 36. Synthetic scheme of ^{99m}Tc -EC-neomycin.

FIG. 37A. Scintigraphic image of breast tumor-bearing rats after administration of ^{99m}Tc -EC and ^{99m}Tc -EC-neomycin (100 $\mu\text{Ci}/\text{rat}$, iv.) showed that the tumor could be well visualized from 0.5-4 hours postinjection.

FIG. 37B. Scintimammography with ^{99m}Tc -EC- neomycin (30 mCi, iv.) of a breast cancer patient. Images taken two hours post-injection.

FIG. 38A. ^1H -NMR of EC.

FIG. 38B. ^1H -NMR of neomycin.

FIG. 38C. ^1H -NMR of EC-neomycin.

FIG. 39A and FIG. 39B. Mass spectrometry of EC-neomycin ($M+ 1112.55$).

FIG. 40A. UV wavelength scan of EC.

FIG. 40B. UV wavelength scan of neomycin.

FIG. 40C. UV wavelength scan of EC-neomycin.

FIG. 41. Radio-TLC analysis of ^{99m}Tc -EC-neomycin.

FIG. 42. HPLC analysis of ^{99m}Tc -EC-neomycin (radioactive detector).

FIG. 43. HPLC analysis of ^{99m}Tc -EC-neomycin (UV 254 nm).

FIG. 44. HPLC analysis of ^{18}F -FDG (radioactive detector).

5 **FIG. 45.** IIPLC analysis of ^{18}F -FDG (UV 254 nm).

FIG. 46. *In vitro* cellular uptake assay of a series of ^{99m}Tc -EC-drug conjugates in lung cancer cell line. ^{99m}Tc -EC- neomycin showed highest uptake in the agents tested.

10 **FIG. 47.** Effect of glucose on cellular (A549) uptake of ^{99m}Tc -EC- neomycin and ^{18}F -FDG.

FIG. 48A and FIG. 48B. Effect of glucose on cellular (H1299) uptake of ^{99m}Tc -EC- neomycin and ^{18}F -FDG illustrated as percent of drug uptake (FIG. 48A) and as percent of change with glucose loading (FIG. 48B).

15

FIG. 49. Synthetic scheme of ^{99m}Tc -EC-Glucosamine

FIG. 50. Hexokinase assay of glucose.

20

FIG. 51. Hexokinase assay of glucosamine.

FIG. 52. Hexokinase assay of EC-glucosamine.

25 **FIG. 53.** Hexokinase assay of EC-GAP-glucosamine.

FIG. 54. Synthetic scheme of ^{99m}Tc -EC-GAP-glucosamine.

FIG. 55A, FIG. 55B, FIG. 55C. *In vitro* cellular uptake assay of ^{99m}Tc -EC (FIG. 56A), ^{99m}Tc -EC-deoxyglucose-GAP (FIG. 56B), and ^{18}F -FDG (FIG. 56C) in lung cancer cell line (A549). ^{99m}Tc -EC-DG showed similar uptake compared to ^{18}F -FDG.

30

FIG. 56. Tumor-to-tissue count density ratios of ^{99m}Tc -EC-GAP in breast tumor-bearing rats.

FIG. 57 *In vitro* cellular uptake of ^{18}F PDG with glucose loading at 2 hours post-injection in breast cancer cell line (13762).

- 5 **FIG. 58.** *In vivo* tissue uptake of ^{99m}Tc -EC-neomycin in breast tumor-bearing mice.
- FIG. 59.** Synthetic scheme of ^{99m}Tc -EC-deoxyglucose.
- FIG. 60.** Mass spectrometry of EC-deoxyglucose.
- 10 **FIG. 61.** ^1H -NMR of EC-deoxyglucose (EC-DG).
- FIG. 62.** ^1H -NMR of glucosamine.
- FIG. 63.** Radio-TLC analysis of ^{99m}Tc -EC-DG.
- 15 **FIG. 64.** HPLC analysis of ^{99m}Tc -EC-deoxyglucose and ^{99m}Tc -EC- (radioactive detector).
- FIG. 65.** HPLC analysis of ^{99m}Tc -EC-deoxyglucose and ^{99m}Tc -EC (radioactive detector, mixed).
- 20 **FIG. 66.** Hexokinase assay of glucose.
- FIG. 67.** Hexokinase assay of FDG.
- 25 **FIG. 68.** Hexokinase assay of EC-DG.
- FIG. 69.** *In vitro* cellular uptake assay of ^{99m}Tc -EC-deoxyglucose, ^{99m}Tc -EC and ^{18}F -FDG in lung cancer cell line (A549). ^{99m}Tc -EC-DG showed similar uptake compared to ^{18}F -FDG.
- 30 **FIG. 70.** Effect of d- and l-glucose on breast cellular (13762 cell line) uptake of ^{99m}Tc -EC- DG.

- FIG. 71. Effect of d- and l-glucose on breast cellular (13762 cell line) uptake of ^{18}F -FDG.
- 5 FIG. 72. Effect of d- and l-glucose on lung cellular (A549 cell line) uptake of ^{18}F -FDG.
- FIG. 73. Effect of d- and l-glucose on breast cellular (A549 cell line) uptake of $^{99\text{m}}\text{Tc}$ -EC- DG.
- 10 FIG. 74. Effect of *in vivo* blood glucose level induced by glucosamine and EC-DG (1.2 mmol/kg, i.v.).
- FIG. 75. Effect of *in vivo* blood glucose level induced by FDG (1.2 and 1.9 mmol/kg, i.v.) and insulin.
- 15 FIG. 76. Tumor-to-tissue count density ratios of $^{99\text{m}}\text{Tc}$ -EC-deoxyglucose in breast tumor-bearing rats.
- FIG. 77. *In vivo* biodistribution of $^{99\text{m}}\text{Tc}$ -EC-deoxyglucose in breast tumor-bearing rats.
- 20 FIG. 78. *In vivo* tissue uptake of $^{99\text{m}}\text{Tc}$ -EC-deoxyglucose in lung tumor-bearing mice.
- FIG. 79. *In vivo* tissue uptake of $^{99\text{m}}\text{Tc}$ -EC-neomycin in lung tumor-bearing mice.
- 25 FIG. 80. *In vivo* tissue uptake of ^{18}F -FDG in lung tumor-bearing mice.
- FIG. 81. Planar image of breast tumor-bearing rats after administration of $^{99\text{m}}\text{Tc}$ -EC and $^{99\text{m}}\text{Tc}$ -EC-deoxyglucose (100 $\mu\text{Ci}/\text{rat}$, iv.) showed that the tumor could be well visualized from 0.5-4 hours postinjection.
- 30 FIG. 82A. MRI of a patient with malignant astrocytoma.

FIG. 82B. SPECT with ^{99m}Tc -EC-DG of a patient with malignant astrocytoma.

FIG. 83A. MRI of a patient with hemorrhagic astrocytoma.

5 **FIG. 83B.** SPECT with ^{99m}Tc -EC-DG of a patient with malignant astrocytoma.

FIG. 84A. MRI of a patient with benign meningioma.

10 **FIG. 84B.** SPECT with ^{99m}Tc -EC-DG of a patient with benign meningioma showed no focal intensified uptake.

FIG. 85A. CT of a patient with TB in lung.

15 **FIG. 85B.** SPECT with ^{99m}Tc -EC-DG of a patient with TB showed no focal intensified uptake.

FIG. 86A. CT of patient with lung cancer.

FIG. 86B. Whole body images of ^{99m}Tc -EC-DG of a patient with lung cancer.

20 **FIG. 86C.** SPECT with ^{99m}Tc -EC-DG of a patient with lung cancer, the tumor showed focal intensified uptake.

DESCRIPTION OF ILLUSTRATIVE EMBODIMENTS

In the field of nuclear medicine, certain pathological conditions are localized, or their extent is assessed, by detecting the distribution of small quantities of internally-administered radioactively labeled tracer compounds (called radiotracers or radiopharmaceuticals). Methods for detecting these radiopharmaceuticals are known generally as imaging or radioimaging methods.

In radioimaging, the radiolabel is a gamma-radiation emitting radionuclide and the radiotracer is located using a gamma-radiation detecting camera (this process is often referred to as gamma scintigraphy). The imaged site is detectable because the radiotracer is chosen either to localize at a pathological site (termed positive contrast) or, alternatively, the radiotracer is chosen specifically not to localize at such pathological sites (termed negative contrast).

A variety of radionuclides are known to be useful for radioimaging, including ^{67}Ga , $^{99\text{m}}\text{Tc}$, ^{111}In , ^{123}I , ^{125}I , ^{169}Yb or ^{186}Re . Due to better imaging characteristics and lower price, attempts have been made to replace the ^{123}I , ^{131}I , ^{67}Ga and ^{111}In labeled compounds with corresponding $^{99\text{m}}\text{Tc}$ labeled compounds when possible. Due to favorable physical characteristics as well as extremely low price (\$0.21/mCi), $^{99\text{m}}\text{Tc}$ has been preferred to label radiopharmaceuticals. Although it has been reported that DTPA-drug conjugate could be labeled with $^{99\text{m}}\text{Tc}$ effectively (Mathias *et al.*, 1997), DTPA moiety does not chelate with $^{99\text{m}}\text{Tc}$ as stable as with ^{111}In . (Goldsmith, 1997).

A number of factors must be considered for optimal radioimaging in humans. To maximize the efficiency of detection, a radionuclide that emits gamma energy in the 100 to 200 keV range is preferred. To minimize the absorbed radiation dose to the patient, the physical half-life of the radionuclide should be as short as the imaging procedure will allow. To allow for examinations to be performed on any day and at any time of the day, it is advantageous to have a source of the radionuclide always available at the clinical site. $^{99\text{m}}\text{Tc}$ is a preferred radionuclide because it emits gamma radiation at 140 keV, it has a physical half-life of 6 hours, and it is readily available on-site using a molybdenum-99/technetium-99m generator.

Bis-aminoethanethiol tetradentate ligands, also called diaminodithiol compounds, are known to form very stable $\text{Tc}(\text{V})\text{O}$ -complexes on the basis of efficient binding of the

oxotechnetium group to two thiolsulfur and two amine nitrogen atoms. (Davison *et al.*, 1980;1981; Verbruggen *et al.*, 1992). ^{99m}Tc -L,L-ethylenedicycysteine (^{99m}Tc -EC) is the most recent and successful example of N_2S_2 chelates. (Verbruggen *et al.*, 1992; Van Nerom *et al.*, 1993; Surma *et al.*, 1994). EC, a new renal imaging agent, can be labeled with ^{99m}Tc easily and efficiently with high radiochemical purity and stability and is excreted through kidney by active tubular transport. (Verbruggen *et al.*, 1992; Van Nerom *et al.*, 1993; Surma *et al.*, 1994; Verbruggen *et al.*, 1990; Van Nerom *et al.*, 1990; Jamar *et al.*, 1993). Other applications of EC would be chelated with gallium-68 (a positron emitter, $t_{1/2} = 68$ minutes) for PET and gadolinium, iron or manganese for magnetic resonance imaging (MRI).

The present invention utilizes ^{99m}Tc -EC as a labeling agent to target ligands to specific tissue types for imaging. The advantage of conjugating the EC with tissue targeting ligands is that the specific binding properties of the tissue targeting ligand concentrates the radioactive signal over the area of interest. While it is envisioned that the use of ^{99m}Tc -EC as a labeling strategy can be effective with virtually any type of compound, some suggested preferred ligands are provided herein for illustration purposes. It is contemplated that the ^{99m}Tc -EC-drug conjugates of the invention may be useful to image not only tumors, but also other tissue-specific conditions, such as infection, hypoxic tissue (stroke), myocardial infarction, apoptotic cells, Alzheimer's disease and endometriosis.

Radiolabeled proteins and peptides have been reported in the prior art. (Ege *et al.*, U.S. Patent No. 4,832,940, Abrams *et al.*, 1990; Bakker *et al.*, 1990; Goldsmith *et al.*, 1995, 1997; Olexa *et al.* 1982; Ranby *et al.* 1988; Hadley *et al.* 1988; Lees *et al.* 1989; Sobel *et al.* 1989; Stuttle, 1990; Maraganore *et al.* 1991; Rodwell *et al.* 1991; Tubis *et al.* 1968; Sandrehagen 1983). However, ^{99m}Tc -EC has not been used in conjunction with any ligands, other than as the diethylester (Kabasakal, 2000), prior to the present invention. The diethylester of EC was used as a cerebral blood flow agent (Kikukawa, *et al.*, 2000).

Although optimal for radioimaging, the chemistry of ^{99m}Tc has not been as thoroughly studied as the chemistry of other elements and for this reason methods of radiolabeling with ^{99m}Tc are not abundant. ^{99m}Tc is normally obtained as ^{99m}Tc pertechnetate (TcO_4^- ; technetium in the +7 oxidation state), usually from a molybdenum-99/technetium-99m generator. However, pertechnetate does not bind well with other compounds. Therefore, in order to radiolabel a compound, ^{99m}Tc pertechnetate must be converted to another form. Since technetium does not

form a stable ion in aqueous solution, it must be held in such solutions in the form of a coordination complex that has sufficient kinetic and thermodynamic stability to prevent decomposition and resulting conversion of ^{99m}Tc either to insoluble technetium dioxide or back to pertechnetate.

For the purpose of radiolabeling, it is particularly advantageous for the ^{99m}Tc complex to be formed as a chelate in which all of the donor groups surrounding the technetium ion are provided by a single chelating ligand – in this case, ethylenedicysteine. This allows the chelated ^{99m}Tc to be covalently bound to a tissue specific ligand either directly or through a single linker between the ethylenedicysteine and the ligand.

Technetium has a number of oxidation states: +1, +2, +4, +5, +6 and +7. When it is in the +1 oxidation state, it is called Tc MIBI. Tc MIBI must be produced with a heat reaction. (Seabold *et al.* 1999). For purposes of the present invention, it is important that the Tc be in the +4 oxidation state. This oxidation state is ideal for forming the N_2S_2 chelate with EC. Thus, in forming a complex of radioactive technetium with the drug conjugates of the invention, the technetium complex, preferably a salt of ^{99m}Tc pertechnetate, is reacted with the drug conjugates of the invention in the presence of a reducing agent.

The preferred reducing agent for use in the present invention is stannous ion in the form of stannous chloride (SnCl_2) to reduce the Tc to its +4 oxidation state. However, it is contemplated that other reducing agents, such as dithionate ion or ferrous ion may be useful in conjunction with the present invention. It is also contemplated that the reducing agent may be a solid phase reducing agent. The amount of reducing agent can be important as it is necessary to avoid the formation of a colloid. It is preferable, for example, to use from about 10 to about 100 μg SnCl_2 per about 100 to about 300 mCi of Tc pertechnetate. The most preferred amount is about 0.1 mg SnCl_2 per about 200 mCi of Tc pertechnetate and about 2 ml saline. This typically produces enough Tc-EC-tissue specific ligand conjugate for use in 5 patients.

It is often also important to include an antioxidant in the composition to prevent oxidation of the ethylenedicysteine. The preferred antioxidant for use in conjunction with the present invention is vitamin C (ascorbic acid). However, it is contemplated that other antioxidants, such as tocopherol, pyridoxine, thiamine or rutin, may also be useful.

In general, the ligands for use in conjunction with the present invention will possess either amino or hydroxy groups that are able to conjugate to EC on either one or both acid arms. If amino or hydroxy groups are not available (e.g., acid functional group), a desired ligand may still be conjugated to EC and labeled with ^{99m}Tc using the methods of the invention by adding a linker, such as ethylenediamine, amino propanol, diethylenetriamine, aspartic acid, polyaspartic acid, glutamic acid, polyglutamic acid, or lysine. Ligands contemplated for use in the present invention include, but are not limited to, angiogenesis/antiangiogenesis ligands, DNA topoisomerase inhibitors, glycolysis markers, antimetabolite ligands, apoptosis/hypoxia ligands, DNA intercalators, receptor markers, peptides, nucleotides, antimicrobials such as antibiotics or antifungals, organ specific ligands and sugars or agents that mimic glucose.

EC itself is water soluble. It is necessary that the EC-drug conjugate of the invention also be water soluble. Many of the ligands used in conjunction with the present invention will be water soluble, or will form a water soluble compound when conjugated to EC. If the tissue specific ligand is not water soluble, however, a linker which will increase the solubility of the ligand may be used. Linkers may attach to an aliphatic or aromatic alcohol, amine or peptide or to a carboxylic acid or peptide. Linkers may be either poly amino acid (peptide) or amino acid such as glutamic acid, aspartic acid or lysine. Table 1 illustrates desired linkers for specific drug functional groups.

Table 1

Drug Functional Group	Linker	Example
Aliphatic or phenolio-OH	EC-Poly (glutamic acid) (MW. 750-15,000) or EC-poly(aspartic acid) (MW. 2000-15,000) or bromo ethylacetate or EC-glutamic acid or EC-aspartic acid.	A
Aliphatic or aromatic-NH ₂ or peptide	EC-poly(glutamic acid) (MW. 750-15,000) or EC-poly(aspartic acid) (MW. 2000-15,000) or EC-glutamic acid (mono- or diester) or EC-aspartic acid.	B
Carboxylic acid or peptide	Ethylene diamine, lysine	C

Examples:

- A. estradiol, topotecan, paclitaxel, raloxifen etoposide
- B. doxorubicin, mitomycin C, endostatin, annexin V. LHRH, octreotide, VIP
- C. methotrexate, folic acid

It is also envisioned that the EC-tissue specific ligand drug conjugates of the invention may be chelated to other radionuclides and used for radionuclide therapy. Generally, it is believed that virtually any α , β -emitter, γ -emitter, or β , γ -emitter can be used in conjunction with the invention. Preferred β , γ -emitters include ^{166}Ho , ^{188}Re , ^{186}Re , ^{153}Sm , and ^{89}Sr . Preferred β -emitters include ^{90}Y and ^{225}Ac . Preferred γ -emitters include ^{67}Ga , ^{68}Ga , ^{64}Cu , ^{62}Cu and ^{111}In . Preferred α -emitters include ^{211}At and ^{212}Bi . It is also envisioned that para-magnetic substances, such as Gd, Mn and Fe can be chelated with EC for use in conjunction with the present invention.

Complexes and means for preparing such complexes are conveniently provided in a kit form including a sealed vial containing a predetermined quantity of an EC-tissue specific ligand conjugate of the invention to be labeled and a sufficient amount of reducing agent to label the conjugate with ^{99m}Tc . ^{99m}Tc labeled scintigraphic imaging agents according to the present invention can be prepared by the addition of an appropriate amount of ^{99m}Tc or ^{99m}Tc complex into a vial containing the EC-tissue specific ligand conjugate and reducing agent and reaction under conditions described in Example 1 hereinbelow. The kit may also contain conventional pharmaceutical adjunct materials such as, for example, pharmaceutically acceptable salts to adjust the osmotic pressure, buffers, preservatives, antioxidants, and the like. The components of the kit may be in liquid, frozen or dry form. In a preferred embodiment, kit components are provided in lyophilized form.

Radioactively labeled reagents or conjugates provided by the present invention are provided having a suitable amount of radioactivity. In forming ^{99m}Tc radioactive complexes, it is generally preferred to form radioactive complexes in solutions containing radioactivity at concentrations of from about 0.01 millicurie (mCi) to about 300 mCi per mL.

^{99m}Tc labeled scintigraphic imaging agents provided by the present invention can be used for visualizing sites in a mammalian body. In accordance with this invention, the ^{99m}Tc labeled scintigraphic imaging agents are administered in a single unit injectable dose. Any of the common carriers known to those with skill in the art, such as sterile saline solution or plasma, can be utilized after radiolabeling for preparing the injectable solution to diagnostically image various organs, tumors and the like in accordance with this invention. Generally, the unit dose to be administered has a radioactivity of about 0.01 mCi to about 300 mCi, preferably 10 mCi to about 200 mCi. The solution to be injected at unit dosage is from about 0.01 mL to about 10

mL. After intravenous administration, imaging of the organ or tumor in vivo can take place, if desired, in hours or even longer, after the radiolabeled reagent is introduced into a patient. In most instances, a sufficient amount of the administered dose will accumulate in the area to be imaged within about 0.1 of an hour to permit the taking of scintiphotos. Any conventional
5 method of scintigraphic imaging for diagnostic or prognostic purposes can be utilized in accordance with this invention.

The ^{99m}Tc -EC labeling strategy of the invention may also be used for prognostic purposes. It is envisioned that EC may be conjugated to known drugs of choice for cancer
10 chemotherapy, such as those listed in Table 2. These EC-drug conjugates may then be radio labeled with ^{99m}Tc and administered to a patient having a tumor. The labeled EC-drug conjugates will specifically bind to the tumor. Imaging may be performed to determine the effectiveness of the cancer chemotherapy drug against that particular patient's particular tumor. In this way, physicians can quickly determine which mode of treatment to pursue, which chemotherapy drug
15 will be most effective. This represents a dramatic improvement over current methods which include choosing a drug and administering a round of chemotherapy. This involves months of the patient's time and many thousands of dollars before the effectiveness of the drug can be determined.

The ^{99m}Tc labeled EC-tissue specific ligand conjugates and complexes provided by the
20 invention may be administered intravenously in any conventional medium for intravenous injection such as an aqueous saline medium, or in blood plasma medium. Such medium may also contain conventional pharmaceutical adjunct materials such as, for example, pharmaceutically acceptable salts to adjust the osmotic pressure, buffers, preservatives,
25 antioxidants and the like. Among the preferred media are normal saline and plasma.

Specific, preferred targeting strategies are discussed in more detail below.

Tumor Folate Receptor Targeting

30 The radiolabeled ligands, such as pentetreotide and vasoactive intestinal peptide, bind to cell receptors, some of which are overexpressed on tumor cells (Britton and Granowska, 1996; Krenning *et al.*, 1995; Reubi *et al.*, 1992; Goldsmith *et al.*, 1995; Virgolini *et al.*, 1994). Since

these ligands are not immunogenic and are cleared quickly from the plasma, receptor imaging would seem to be more promising compared to antibody imaging.

Folic acid as well as antifolates such as methotrexate enter into cells *via* high affinity folate receptors (glycosylphosphatidylinositol-linked membrane folate-binding protein) in addition to classical reduced-folate carrier system (Westerhof *et al.*, 1991; Orr *et al.*, 1995; Hsueh and Dolnick, 1993). Folate receptors (FRs) are overexpressed on many neoplastic cell types (*e.g.*, lung, breast, ovarian, cervical, colorectal, nasopharyngeal, renal adenocarcinomas, malign melanoma and ependymomas), but primarily expressed only several normal differentiated tissues (*e.g.*, choroid plexus, placenta, thyroid and kidney) (Orr *et al.*, 1995; Weitman *et al.*, 1992a; Campbell *et al.*, 1991; Weitman *et al.*, 1992b; Holm *et al.*, 1994; Ross *et al.*, 1994; Franklin *et al.*, 1994; Weitman *et al.*, 1994). FRs have been used to deliver folate-conjugated protein toxins, drug/antisense oligonucleotides and liposomes into tumor cells overexpressing the folate receptors (Ginobbi *et al.*, 1997; Leamon and Low, 1991; Leamon and Low, 1992; Leamon *et al.*, 1993; Lee and Low, 1994). Furthermore, bispecific antibodies that contain anti-FR antibodies linked to anti-T cell receptor antibodies have been used to target T cells to FR-positive tumor cells and are currently in clinical trials for ovarian carcinomas (Canevari *et al.*, 1993; Bolhuis *et al.*, 1992; Patrick *et al.*, 1997; Coney *et al.*, 1994; Kranz *et al.*, 1995). Similarly, this property has been inspired to develop radiolabeled folate-conjugates, such as ^{67}Ga -deferoxamine-folate and ^{111}In -DTPA-folate for imaging of folate receptor positive tumors (Mathias *et al.*, 1996; Wang *et al.*, 1997; Wang *et al.*, 1996; Mathias *et al.*, 1997b). Results of limited *in vitro* and *in vivo* studies with these agents suggest that folate receptors could be a potential target for tumor imaging. In this invention, the inventors developed a series of new folate receptor ligands. These ligands are ^{99m}Tc -EC-folate, ^{99m}Tc -EC-methotrexate (^{99m}Tc -EC-MTX), ^{99m}Tc -EC-tomodex (^{99m}Tc -EC-TDX).

Tumor Hypoxia Targeting

Tumor cells are more sensitive to conventional radiation in the presence of oxygen than in its absence; even a small percentage of hypoxic cells within a tumor could limit the response to radiation (Hall, 1988; Bush *et al.*, 1978; Gray *et al.*, 1953). Hypoxic radioresistance has been demonstrated in many animal tumors but only in few tumor types in humans (Dische, 1991; Gatenby *et al.*, 1988; Nordmark *et al.*, 1996). The occurrence of hypoxia in human tumors, in most cases, has been inferred from histology findings and from animal tumor studies. *In vivo* demonstration of hypoxia requires tissue measurements with oxygen electrodes and the invasiveness of these techniques has limited their clinical application.

Misonidazole (MISO) is a hypoxic cell sensitizer, and labeling MISO with different radioisotopes (*e.g.*, ^{18}F , ^{123}I , $^{99\text{m}}\text{Tc}$) may be useful for differentiating a hypoxic but metabolically active tumor from a well-oxygenated active tumor by PET or planar scintigraphy. [^{18}F]Fluoromisonidazole (FMISO) has been used with PET to evaluate tumors hypoxia. Recent studies have shown that PET, with its ability to monitor cell oxygen content through [^{18}F]FMISO, has a high potential to predict tumor response to radiation (Koh *et al.*, 1992; Valk *et al.*, 1992; Martin *et al.*, 1989; Rasey *et al.*, 1989; Rasey *et al.*, 1990; Yang *et al.*, 1995). PET gives higher resolution without collimation, however, the cost of using PET isotopes in a clinical setting is prohibitive. Although labeling MISO with iodine was the choice, high uptake in thyroid tissue was observed. Therefore, it is desirable to develop compounds for planar scintigraphy that the isotope is less expensive and easily available in most major medical facilities. In this invention, the inventors present the synthesis of $^{99\text{m}}\text{Tc}$ -EC-2- nitroimidazole and $^{99\text{m}}\text{Tc}$ -EC-metronidazole and demonstrate their potential use as tumor hypoxia markers.

Peptide Imaging of Cancer

Peptides and amino acids have been successfully used in imaging of various types of tumors (Wester *et al.*, 1999; Coenen and Stocklin, 1988; Raderer *et al.*, 1996; Lambert *et al.*, 1990; Bakker *et al.*, 1990; Stella and Mathew, 1990; Butterfield *et al.*, 1998; Piper *et al.*, 1983; Moehizuki *et al.*, Dickinson and Hiltner, 1981). Glutamic acid based peptide has been used as a drug carrier for cancer treatment (Stella and Mathew, 1990; Butterfield *et al.*, 1998; Piper *et al.*, 1983; Moehizuki *et al.*, 1985; Dickinson and Hiltner, 1981). It is known that glutamate moiety of folate degraded and formed polyglutamate *in vivo*. The polyglutamate is then re- conjugated

to folate to form folyl polyglutamate, which is involved in glucose metabolism. Labeling glutamic acid peptide may be useful in differentiating the malignancy of the tumors. In this invention, the inventors report the synthesis of EC-glutamic acid pentapeptide and evaluate its potential use in imaging tumors.

Imaging Tumor Apoptotic Cells

Apoptosis occurs during the treatment of cancer with chemotherapy and radiation (Lennon *et al.*, 1991; Abrams *et al.*, 1990; Blakenberg *et al.*, 1998; Blakenberg *et al.*, 1999; Tait and Smith, 1991). Annexin V is known to bind to phosphatidylserin, which is overexpressed by tumor apoptotic cells (Blakenberg *et al.*, 1999; Tait and Smith, 1991). Assessment of apoptosis by annexin V would be useful to evaluate the efficacy of therapy such as disease progression or regression. In this invention, the inventors synthesize ^{99m}Tc -EC-annexin V (EC- ANNEX) and evaluate its potential use in imaging tumors.

Imaging Tumor Angiogenesis

Angiogenesis is in part responsible for tumor growth and the development of metastasis. Antimitotic compounds are antiangiogenic and are known for their potential use as anticancer drugs. These compounds inhibit cell division during the mitotic phase of the cell cycle. During the biochemical process of cellular functions, such as cell division, cell motility, secretion, ciliary and flagellar movement, intracellular transport and the maintenance of cell shape, microtubules are involved. It is known that antimitotic compounds bind with high affinity to microtubule proteins (tubulin), disrupting microtubule assembly and causing mitotic arrest of the proliferating cells. Thus, antimitotic compounds are considered as microtubule inhibitors or as spindle poisons (Lu, 1995).

Many classes of antimitotic compounds control microtubule assembly-disassembly by binding to tubulin (Lu, 1995; Goh *et al.*, 1998; Wang *et al.*, 1998; Rowinsky *et al.*, 1990; Imbert, 1998). Compounds such as colchicinoids interact with tubulin on the colchicine-binding sites and inhibit microtubule assembly (Lu, 1995; Goh *et al.*, 1998; Wang *et al.*, 1998). Among colchicinoids, colchicine is an effective anti-inflammatory drug used to treat prophylaxis of acute gout. Colchicine also is used in chronic myelocytic leukemia. Although colchicinoids are potent against certain types of tumor growth, the clinical therapeutic potential is limited due to inability to separate the therapeutic and toxic effects (Lu, 1995). However, colchicine may be

useful as a biochemical tool to assess cellular functions. In this invention, the inventors developed ^{99m}Tc -EC-colchicine (EC-COL) for the assessment of biochemical process on tubulin functions.

5 **Imaging Tumor Apoptotic Cells**

Apoptosis occurs during the treatment of cancer with chemotherapy and radiation. Annexin V is known to bind to phosphatidylserin, which is overexpressed by tumor apoptotic cells. Assessment of apoptosis by annexin V would be useful to evaluate the efficacy of therapy
10 such as disease progression or regression. Thus, ^{99m}Tc -EC-annexin V (EC-ANNEX) was developed.

Imaging Tumor Hypoxia

15 The assessment of tumor hypoxia by an imaging modality prior to radiation therapy would provide rational means of selecting patients for treatment with radiosensitizers or bioreductive drugs (e.g., tirapazamine, mitomycin C). Such selection of patients would permit more accurate treatment patients with hypoxic tumors. In addition, tumor suppressor gene (P53) is associated with multiple drug resistance. To correlate the imaging findings with the
20 overexpression of P53 by histopathology before and after chemotherapy would be useful in following-up tumor treatment response. ^{99m}Tc -EC-2-nitroimidazole and ^{99m}Tc -EC-metronidazole were developed.

Imaging Tumor Angiogenesis

25 Angiogenesis is in part responsible for tumor growth and the development of metastasis. Antimitotic compounds are antiangiogenic and are known for their potential use as anticancer drugs. These compounds inhibit cell division during the mitotic phase of the cell cycle. During the biochemical process of cellular functions, such as cell division, cell motility, secretion,
30 ciliary and flagellar movement, intracellular transport and the maintenance of cell shape, microtubules are involved. It is known that antimitotic compounds bind with high affinity to microtubule proteins (tubulin), disrupting microtubule assembly and causing mitotic arrest of the proliferating cells. Thus, antimitotic compounds are considered as microtubule inhibitors or as spindle poisons. Colchicine, a potent antiangiogenic agent, is known to inhibit microtubule

polymerization and cell arrest at metaphase. Colchicine (COL) may be useful as a biochemical tool to assess cellular functions. ^{99m}Tc -EC-COL was then developed.

Imaging Hypoxia Due to Stroke

Although tumor cells are more or less hypoxic, it requires an oxygen probe to measure the tensions. In order to mimic hypoxic conditions, the inventors imaged 11 patients who had experienced stroke using ^{99m}Tc -EC-metronidazole (^{99m}Tc -EC-MN). Metronidazole is a tumor hypoxia marker. Tissue in the area of a stroke becomes hypoxic due to lack of oxygen. The SPECT images were conducted at 1 and 3 hours post injection with ^{99m}Tc -EC-MN. All of these imaging studies positively localized the lesions. CT does not show the lesions very well or accurately. MRI and CT in some cases exaggerate the lesion size. The following are selected cases from three patients.

Case 1. A 59 year old male patient suffered a stroke in the left basal ganglia. SPECT ^{99m}Tc -EC-MN identified the lesions at one hour post-injection (FIG. 28), which corresponds to MRI T1 weighted image (FIG. 29).

Case 2. A 73 year old male patient suffered a stroke in the left medium cerebral artery (MCA) territory. SPECT ^{99m}Tc -EC-MN was obtained at day 1 and day 12 (FIGs. 30 and 31) at one hour post-injection. The lesions showed significant increased uptake at day 12. CT showed extensive cerebral hemorrhage in the lesions. No marked difference was observed between days 1 and 12 (FIGs. 32 and 33). The findings indicate that the patient symptoms improved due to the tissue viability (from anoxia to hypoxia). SPECT ^{99m}Tc -EC-MN provides functional information which is better than CT images.

Case 3. A 72 year old male patient suffered a stroke in the right MCA and PCA area. SPECT ^{99m}Tc -EC-MN identified the lesions at one hour post-injection (FIG. 34). CT exaggerates the lesion size. (FIG. 35).

Tumor Glycolysis Targeting

The radiolabeled ligands, such as polysaccharide (neomycin, kanamycin, tobramycin) and monosaccharide (glucosamine) bind to cell glucose transporter, followed by phosphorylation which are overexpressed on tumor cells (Rogers *et al.*, 1968; Fanciulli *et al.*, 1994; Popovici *et al.*, 1971; Jones *et al.*, 1973; Hermann *et al.*, 2000). Polysaccharide (neomycin, kanamycin, tobramycin) and monosaccharide (glucosamine) induced glucose level could be suppressed by insulin (Harada *et al.*, 1995; Moller *et al.*, 1991; Offield *et al.*, 1996; Shankar *et al.*, 1998; Yoshino *et al.*, 1999; Villevalois-Cam *et al.*, 2000). Since these ligands are not immunogenic and are cleared quickly from the plasma, metabolic imaging would seem to be more promising compared to antibody imaging.

The following examples are included to demonstrate preferred embodiments of the invention. It should be appreciated by those of skill in the art that the techniques disclosed in the examples which follow represent techniques discovered by the inventor to function well in the practice of the invention, and thus can be considered to constitute preferred modes for its practice. However, those of skill in the art should, in light of the present disclosure, appreciate that many changes can be made in the specific embodiments which are disclosed and still obtain a like or similar result without departing from the spirit and scope of the invention.

EXAMPLE 1: TUMOR FOLATE RECEPTOR TARGETING

Synthesis of EC

EC was prepared in a two-step synthesis according to the previously described methods (Ratner and Clarke, 1937; Blondeau *et al.*, 1967; each incorporated herein by reference). The precursor, L-thiazolidine-4-carboxylic acid, was synthesized (m.p. 195°, reported 196-197°). EC was then prepared (m.p. 237°, reported 251-253°). The structure was confirmed by ¹H-NMR and fast-atom bombardment mass spectroscopy (FAB-MS).

Synthesis of aminoethylamido analogue of methotrexate (MTX- NH₂)

MIX (227 mg, 0.5 mmol) was dissolved in 1 ml of HCl solution (2N). The pH value was <3. To this stirred solution, 2 ml of water and 4 ml of N-ethoxycarbonyl-2-ethoxy-1,2-dihydroquinoline (EEDQ, 6.609% in methanol, 1 mmol) were added at room temperature.

Ethylenediamine (EDA, 0.6 ml, 10 mmol) was added slowly. The reaction mixture was stirred overnight and the solvent was evaporated in vacuo. The raw solid material was washed with diethyl ether (10 ml), acetonitrile (10 ml) and 95% ethyl alcohol (50 ml) to remove the unreacted EEDQ and EDA. The product was then dried by lyophilization and used without further purification. The product weighed 210 mg (84.7%) as a yellow powder. m.p. of product: 195-198 °C (dec, MIX); ¹H-NMR (D₂O) δ 2.98-3.04 (d, 8H, - (CH₂)₂CONH(CH₂)₂NH₂), 4.16-4.71 (m, 6H, -CH₂- pteridinyl, aromatic-NCH₃, NH-CH-COOH glutamate), 6.63-6.64 (d, 2H, aromatic-CO), 7.51-7.53 (d, 2H. aromatic-N), 8.36 (s, 1H, pteridinyl). FAB MS m/z calcd for C₂₂H₂₈N₁₀O₄(M)⁺ 496.515, found 496.835.

Synthesis of aminoethylamido analogue of folate (Folate- NH₂)

Folic acid dihydrate (1 g, 2.0 mmol) was added in 10 ml of water. The pH value was adjusted to 2 using HCl (2 N). To this stirred solution, N-ethoxycarbonyl-2-ethoxy-1,2-dihydroquinoline (EEDQ, 1 g in 10 ml methanol, 4.0 mmol) and ethylenediamine (EDA, 1.3 ml, 18 mmol) were added slowly. The reaction mixture was stirred overnight at room temperature. The solvent was evaporated in vacuo. The product was precipitated in methanol (50 ml) and further washed with acetone (100 ml) to remove the unreacted EEDQ and EDIT. The product was then freeze-dried and used without further purification. Ninhydrin (2% in methanol) spray indicated the positivity of amino group. The product weighed 0.6 g (yield 60%) as a yellow powder. m.p. of product: 250° (dec). ¹H-NMR (D₂O) δ 1.97-2.27 (m, 2H, -CH₂ glutamate of folate), 3.05-3.40 (d, 6H, -CH₂CONH(CH₂)₂NH₂), 4.27-4.84 (m, 3H, -CH₂-pteridinyl, NH-CH-COOH glutamate), 6.68-6.70 (d, 2H, aromatic-CO), 7.60-7.62 (d, 2H, aromatic-N), 8.44 (s, 1H, pteridinyl). FAB MS m/z calcd for C₂₁H₂₅N₉O₅(M)⁺ 483, found 483.21.

Synthesis of ethylenedicysteine- folate (EC- Folate)

To dissolve EC, NaOH (2N, 0.1 ml) was added to a stirred solution of EC (114 mg, 0.425 mmol) in water (1.5 ml). To this colorless solution, sulfo-NHS (92.3 mg, 0.425 mmol) and EDC (81.5 mg, 0.425 mmol) were added. Folate-NH₂ (205 mg, 0.425 mmol) was then added. The mixture was stirred at room temperature for 24 hours. The mixture was dialyzed for 48 hours using Spectra/POR molecular porous membrane with molecule cut-off at 500 (Spectrum Medical Industries Inc., Houston, TX). After dialysis, the product was freeze dried. The product weighed 116 mg (yield 35%). m.p. 195° (dec); ¹H-NMR (D₂O) δ 1.98-2.28 (m, 2H, -CH₂

glutamate of folate), 2.60-2.95 (m, 4H and $-\text{CH}_2\text{-SH}$ of EC). 3.24-3.34 (m, 10H, $-\text{CH}_2\text{-CO}$, ethylenediamine of folate and ethylenediamine of EC), 4.27-4.77 (m, 5H, $-\text{CH-pteridinyI}$, NH-CH-COOH glutamate of folate and NH-CH-COOH of EC), 6.60-6.62 (d, 2H, aromatic-CO), 7.58-7.59 (d, 2H, aromatic-N), 8.59 (s, 1H, pteridinyI). Anal. calcd for $\text{C}_{29}\text{H}_{37}\text{N}_{11}\text{S}_2\text{O}_8$
 5 $\text{Na}_2(8\text{H}_2\text{O})$, FAB MS m/z (M)⁺ 777.3 (free of water). C, 37.79; H, 5.75; N, 16.72; S, 6.95. Found: m/z (M)⁺ 777.7 (20), 489.4 (100). C, 37.40; H, 5.42; N, 15.43; S, 7.58.

Radiolabeling of EC-folate and EC with ^{99m}Tc

10 Radiosynthesis of ^{99m}Tc -EC-folate was achieved by adding required amount of ^{99m}Tc -pertechnetate into home-made kit containing the lyophilized residue of EC-folate (3 mg), SnCl_2 (100 μg), Na_2HPO_4 (13.5 mg), ascorbic acid (0.5 mg) and NaEDTA (0.5 mg). Final pH of preparation was 7.4. ^{99m}Tc -EC was also obtained by using home-made kit containing the lyophilized residue of EC (3 mg), SnCl_2 (100 μg), Na_2IPO_4 (13.5 mg), ascorbic acid (0.5 mg)
 15 and NaEDTA (0.5 mg) at pH 10. Final pH of preparation was then adjusted to 7.4. Radiochemical purity was determined by TLC (ITLC SG, Gelman Sciences, Ann Arbor, MI) eluted with, respectively, acetone (system A) and ammonium acetate (1M in water):methanol (4:1) (system B). From radio-TLC (Bioscan, Washington, DC) analysis, the radiochemical purity was >95% for both radiopharmaceuticals. Radio-TLC data are summarized in Table 2.
 20 Synthesis of ^{99m}Tc -EC-folate is shown in FIG. 1.

TABLE 2

DRUGS OF CHOICE FOR CANCER CHEMOTHERAPY

25 The tables that follow list drugs used for treatment of cancer in the USA and Canada and their major adverse effects. The Drugs of Choice listing based on the opinions of Medical Letter consultants. Some drugs are listed for indications for which they have not been approved by the US Food and Drug Administration. Anticancer drugs and their adverse effects follow. For purposes of the present invention, these lists are meant to be exemplary and not exhaustive.

DRUGS OF CHOICE

Cancer	Drugs of Choice	Some alternatives
Adrenocortical**	Mitotane Cisplatin	Doxorubicin, streptozocin, etoposide

Cancer	Drugs of Choice	Some alternatives
Bladder*	<i>Local:</i> Instillation of BCG <i>Systemic:</i> Methotrexate + vinblastine + doxorubicin + claptatin (MVAC) Claptatin + Methotrexate + vinblastine (CMV)	Instillation of mitomycin, doxorubicin or thiotape Pecitaxel, substitution of carboplatin for claptatin in combinations
Brain		
Anaplastic astrocytoma*	Procarbazine + lamuatine + vincristine	Carmustine, Claptatin
Anaplastic oligodendro-Giloma*	Procarbazine + lamustine + vincristine	Carmustine, Claptatin
Gilablastome**		Procarbazine, claptatin
Medulloblastoma	Carmustine or lamustine Vincristine + carmustine ± mechlorethamine ± methotrexate Mechlorethamine + vincristine + procarbazine + prednisone (MOPP) Vincristine + claptatin ± cyclophosphamide	Etoposide
Primary central nervous system lymphoma	Methotrexate (high dose Intravenous and/or Intrathecal) ± cytarabine (Intravenous and/or Intrathecal) Cyclophosphamide + Doxorubicin + vincristine + prednisone (CHOP)	
Breast	<i>Adjuvant</i> ¹ : Cyclophosphamide + methotrexate + fluorouracil (CMF); Cyclophosphamide + Doxorubicin ± fluorouracil (AC or CAF); Tamoxifen <i>Metastatic:</i> Cyclophosphamide + metho-trexate + fluorouracil (CMF) or Cyclophosphamide + duxorubicin ± fluorouracil (AC or CAF) for receptor-negative and/or hormone-refractory; Tamoxifen for receptor-positive and/or hormone-sensitive ²	Paclitaxel; thiotepa + Doxorubicin + vinblastine; mitomycin + vinblastine; mitomycin + methotrexate + mitoxantrone; fluorouracil by continuous infusion; Bone marrow transplant ³
Cervix**	Claptatin Ifosfamide with means Bleomycin + ifosfamide with means	Chlorambucil, vincristine, fluorouracil, Doxorubicin, methotrexate, altretamine

* Chemotherapy has only moderate activity.

** Chemotherapy has only minor activity.

¹ Tamoxifen with or without chemotherapy is generally recommended for postmenopausal estrogen-receptor-positive, mode-positive patients and chemotherapy with or without tamoxifen for premenopausal mode-positive patients. Adjuvant treatment with chemotherapy and/or tamoxifen is recommended for mode-negative patients with larger tumors or other adverse prognostic indicators.

² Megastrol and other hormonal agents may be effective in some patients with tamoxifen fails.

³ After high-dose chemotherapy (Medical Letter, 34:79, 1982).

Cancer	Drugs of Choice	Some alternatives
	+ claptatin	
Chorlocarcinoma	Methotrexate ± leucovorin Dactinomycin	Methotrexate + dactinomycin + cyclophosphamide (MAC) Etoposide + methotrexate + dactinomycin + cyclophosphamide + vincristine
Colorectal*	<i>Adjuvant colon</i> ⁴ : Fluorouracil + levam-isole; fluorouracil + leucovorin <i>Metastatic</i> : fluorouracil + leucovorin	<i>Hepatic metastases</i> : Intrahepatic-arterial flouxuridine Mitomycin
Embryonal rhabdomyosarcoma ⁵	Vincristine + dactinomycin ± cyclophosphamide Vincristine + ifosfamide with means + etoposide	Same + Doxorubicin
Endometrial**	Megastrol or another progestin Doxorubicin + claptatin ± cyclophosphamide	fluorouracil, tamoxifen, altretamine
Esophageal*	Claptatin + fluorouracil	Doxorubicin, methotrexate, mitomycin
Ewing's sarcoma ⁵	Cyclophosphamide (or ifosfamide with means) + Doxorubicin + vincristine (CAV) ± dactinomycin	CAV + etoposide
Gastric**	Fluorouracil ± leucovorin	Claptatin Doxorubicin, etoposide, methotrexate + leucovorin, mitomycin
Head and neck squamous cell ⁶	Claptatin + fluorouracil Methotrexate	Blomycin, carboplatin, paclitaxel
Islet cell**	Streptozocin + Doxorubicin	Streptozocin + fluorouracil; chlorozotocin [†] ; octreotide
Kaposi's sarcoma* (Aids-related)	Etoposide or interferon alfa or vinblastine Doxorubicin + bleomycin + vincristine or vinblastine (ABV)	Vincristine, Doxorubicin, bleomycin
Leukemia Acute lymphocytic leukemia (ALL) ⁷	<i>Induction</i> : Vincristine + prednisone + asparaginase ± daunorubicin	<i>Induction</i> : same ± high- dose methotrexate ±

⁴ For rectal cancer, postoperative adjuvant treatment with fluorouracil plus radiation, preceded and followed by treatment with fluorouracil alone.

⁵ Drugs have major activity only when combined with surgical resection, radiotherapy or both.

⁶ The vitamin A analog isotretinoin (Accutane) can control pre-neoplastic lesions (leukoplakia) and decreases the rate of second primary tumors (SE Banner et al, J Natl Cancer Inst, 88:140 1994).

[†] Available in the USA only for investigational use.

Cancer	Drugs of Choice	Some alternatives
	<i>CNS prophylaxis:</i> Intrathecal methotrexate ± systemic high-dose methotrexate with leucovorin ± Intrathecal cytarabine ± Intrathecal hydrocortisone <i>Maintenance:</i> Methotrexate + mercapto-purine Bone marrow transplant. ^{3,8}	cytarabine; pegaspargase instead of asparaginase Teniposide or etoposide High-dose cytarabine <i>Maintenance:</i> same + periodic vincristine + prednisone
Acute myeloid leukemia (AML) ⁹	<i>Induction:</i> Cytarabine + either daunorubicin or idarubicin <i>Post Induction:</i> High-dose cytarabine ± other drugs such as etoposide Bone marrow transplant ³ .	Cytarabine + mitoxentron High-dose cytarabine
Chronic lymphocytic leukemia (CLL)	Chlorambucil ± prednisone Fludarabine	Cladribine, cyclophosphamide, pentostatin, vincristine, Doxorubicin
Chronic myeloid leukemia (CML) ¹⁰		
Chronic phase	Bone marrow transplant ³ Interferon alfa Hydroxyures	Busulfan
Accelerated ¹¹	Bone marrow transplant ³	Hydroxyures, busulfen
Blast crisis ¹¹	<i>Lymphoid:</i> Vincristine + prednisone + L-separaginase + intrathecal methotrexate (± maintenance with methotrexate + 8-	Tretinoin [†] Amscrine, † azacitidine Vincristine + plicamycin

7 High-risk patients (e.g., high counts, cytogenetic abnormalities, adults) may require additional drugs for induction, maintenance and “Intensification” (use of additional drugs after achievement of remission). Additional drugs include cyclophosphamida, mitoxantrone and thioguanine. The results of one large controlled trial in the United Kingdom suggest that Intensification may improve survival in all children with ALL (JM Chassele et al, Lancet, 34B:143, Jan 21, 1995).

Patients with a poor prognosis initially or those who relapse after remission. Some patients with acute promyelocytic leukemia have had complete responses to tratinoin. Such treatment can cause a toxic syndrome characterized by fever and respiratory distress (RP Warrell, Jr et al, *N Engl J Med*. 328:177, 1993).

Allogeneic HLA-identical sibling bone marrow transplantation can cure 40% to 70% of patients with CML in chronic phase, 18% to 28% of patients with accelerated phase CML, and 15% patients in blast crisis. Disease-free survival after bone marrow transplantations adversely influenced by age > 50 years, duration of disease > 3 years from diagnosis, and use of one-antigen-mismatched or matched-unrelated donor marrow. Interferon also may be curative in patients with chronic phase CML who achieve a complete cytogenetic response (about 10%); it is the treatment of choice for patients > 80 years old with newly diagnosed chronic phase CML and for all patients who are not candidates for an allogeneic bone marrow transplant. Chemotherapy alone is palliative.

¹¹ If a second chronic phase is achieved with any of these combinations, allogeneic bone marrow transplant should be considered. Bone marrow transplant in second chronic phase may be curative for 30% to 35% of patients with CML.

Cancer	Drugs of Choice	Some alternatives
	marcapotpurine)	
Hairy cell Leukemia	Pentostatin or cladribine	Interferon alfa, chlorambucil, fludarabine
Liver**	Doxorubicin Fluorouracil	Intrahepatic-arterial floxuridine or claptatin
Lung, small cell (cat cell)	Claptatin + etoposide (PE) Cyclophosphamide + doxorubicin + vincristine (CAV) PE alternated with CAV Cyclophosphamide + etoposide + claptatin (CEP) Duxorubicin + cyclophosphamide + etoposide (ACE)	Ifosfamide with means + carboplatin + etoposide (ICE) Daily oral etoposide Etoposide + ifosfamide with means + claptatin (VIP) Paclitaxel
Lung (non-small cell) **	Claptatin + etoposide Claptatin + Vinblastine ± mitomycin Claptatin + vincristine	Claptatin + fluorouracil + leucovorin Carboplatin + paclitaxel
Lymphomas Hodgkin's ¹²	Doxorubicin + bleomycin + vinblastine + dacarbazine (ABVD) ABVD alternated with MOPP Mechlorethamine + vincristine + procarbazine (± prednisone) + doxorubicin + bleomycin + vinblastine (MOP[P]-ABV)	Mechlorethamine + vincristine + procarbazine + prednisone (MOPP) Chlorambucil + vinblastine + procarbazine + prednisone ± carmustine Etoposide + vinblastine + doxorubicin Bone marrow transplant ³
Non-Hodgkin's Burkitt's lymphoma	Cyclophosphamide + vincristine + methotrexate Cyclophosphamide + high-dose cytarabine ± methotrexate with leutovorin Intrathecal methotrexate or cytarabine	Ifosfamide with means Cyclophosphamide + doxorubicin + vincristine + prednisone (CHOP)
Difuse large-cell lymphoma	Cyclophosphamide + doxorubicin + vincristine + prednisone (CHOP)	Dexamethasone sometimes substituted for prednisone Other combination regimens, which may include methotrexate, etoposide, cytarabine, bleomycin, procarbazine, ifosfamide and mitoxantrone Bone marrow transplant ³
Follicular lymphoma	Cyclophosphamide or chlorambucil	Same ± vincristine and prednisone, ± etoposide Interferon alfa, cladribine, fludarabine Bone marrow transplant ³ Cyclophosphamide + doxorubicin + vincristine + prednisone (CHOP)
Melanoma**	Interferon Alfa Dacarbazine	Carmustine, lomustine, cisplatin Dacarbazine + claptatin + carmustine + tamoxifen Aldesleukin
Mycosis fungoides*	PUVA (psoralen + ultraviolet A) Mechlorethamine (topical) Interferon alfa	Isotretinoin, topical carmustine, pentostatin, fludarabine, cladribine, photopheresis (extra-

¹² Limited-stage Hodgkin's disease (stages 1 and 2) is curable by radiotherapy. Disseminated disease (stages 3b and 4) require chemotherapy. Some intermediate stages and selected clinical situations may benefit from both.

Cancer	Drugs of Choice	Some alternatives
	Electron beam radiotherapy Methotrexate	corporeal photochemotherapy), chemotherapy as in non- Hodgkin's lymphoma
Mysloma*	Melphelan (or cyclophosphamide) + prednisons Melphalan ± carmustine + cyclophosphamide + prednisons + vincristine Dexamethasone + doxorubicin + vincristine (VAD) Vincristine + carmustine + doxorubicin + prednisons (VBAP)	Interferon alfa Bone marrow transplant ³ High-dose dexamethasone
Neuroblastoma*	Doxorubicin + cyclophosphamide + claplatin + etoposide or etoposide doxorubicin + cyclophosphamide Claplatin + cyclophosphamide	Carboplatin, etoposide Bone marrow transplant ³
Osteogenic sarcoma ⁵	Doxorubicin + claplatin ± etoposide ± ifosfamide	Ifosfamide with means, etoposide, carboplatin, high- dose methotrexate with leucovorin Cyclophosphamide + etoposide
Cancer	Drugs of Choice	Some alternatives
Ovary	Claplatin (or carboplatin) + paclitaxel Claplatin (or carboplatin) + cyclophosphamide (CP) ± doxorubicin (CAP)	Ifosfamide with means, paclitaxel, tamoxifen, melphalan, altretamine
Pancreatic **	Fluorouracil ± leucovorin	Gemoltabine
Prostate	Leuprolide (or goserelin) ± flutamide	Estramustine ± vinblastine, aminoglutethimide + hydrocortisone, estramustine + etoposide, diethylstilbestrol, nilutamide
Renal **	Aldesleukin Interferon alfa	Vinblastine, floxuridine
Retinoblastoma**	Doxorubicin + cyclophosphamide ± claplatin ± etoposide ± vincristine	Carboplatin, etoposide, Ifosfamide with means
Sarcomas, soft tissue, adult *	Doxorubicin ± decarbazine ± cyclophosphamide ± Ifosfamide with means	Mitomycin + doxorubicin + claplatin Vincristine, etoposide
Testicular	Claplatin + etoposide ± bleomycin (PEB)	Vinblastine (or etoposide) + Ifosfamide with means + claplatin (VIP) Bone marrow transplant ³
Wilms' tumor ⁵	Dactinomycin + vincristine ± doxorubicin ± cyclophosphamide	Ifosfamide with means, etoposide, carboplatin

+ Available in the USA only for investigational use.

ANTICANCER DRUGS AND HORMONES

Drug	Acute Toxicity ‡	Delayed toxicity ‡
Aldesleukin (Interleukin-2; Proleukin - Cetus Oncology)	Fever; fluid retention; hypertension; respiratory distress; rash; anemia; thrombocytopenia; nausea and vomiting; diarrhea; capillary leak syndrome; nephrotoxicity; myocardial toxicity; hepatotoxicity; erythema nodosum; neutrophil chemotactic defects	Neuropsychiatric disorders; hypothyroidism; nephrotic syndrome; possibly acute leukoencephalopathy; brachial plexopathy; bowel perforation
Altretamine (hexamethylmelamine; Hexalen - U Bioscience)	Nausea and vomiting	Bone marrow depression; CNS depression; peripheral neuropathy; visual hallucinations; stexis; tremors, alopecia; rash
Aminoglutethimide (Cytadren - Ciba)	Drowsiness; nausea; dizziness; rash	Hypothyroidism (rare); bone marrow depression; fever; hypotension; masculinization
†Amsacrine (m-AMSA; amaine; AMSP P-D-Parke-Davis, Amsidyl-Warner-Lambert)	Nausea and vomiting; diarrhea; pain or phlebitis on infusion; anaphylaxis	Bone marrow depression; hepatic injury; convulsions; stomatitis; ventricular fibrillation; alopecia; congestive heart failure; renal dysfunction
Asparaginase (Elspar-merck; Kidrolase in Canada)	Nausea and vomiting; fever; chills; headache; hypersensitivity, anaphylaxis; abdominal pain; hyperglycemia leading to coma	CNS depression or hyperexcitability; acute hemorrhagic pancreatitis; coagulation defects; thromboses; renal damage; hepatic damage
Cervix **	Claplatin Ifosfamide with means Bleomycin patin Ifosfamide with means	Chlorambucil, vincristine, fluorouracil, doxorubicin, methotrexate, altretamine
Chorlocarcinoma	Methotrexate ± leucovorin Dactinomycin	Methotrexate + dactinomycin + cyclophosphamide (MAC) Etoposide + methotrexate + dactinomycin + cyclophosphamide + vincristine
Colorectal *	Adjuvant colon ⁴ : Fluorouracil + lavamleole; fluorouracil + leucovorin Metastatic: Fluorouracil + leucovorin	Hepatic metastases: Intrahepatic-arterial flouxiridine Mitomycin
Embryonal rhabdomyosarcoma ⁶	Vincristine + dactinomycin ± cyclophosphamide Vincristine + Ifosfamide with means + etoposide	Same + doxorubicin

Endometrial **	Megastrol or another progestin Doxorubicin + claptatin ± cyclophosphamide	Fluorouracil, tamoxifen, altretamine
Cancer	Drugs of Choice	Some alternatives
Esophageal *	Claptatin + Fluorouracil	Doxorubicin,
Ewing's sarcoma ⁵	Cyclophosphamide (or ifosfamide with means) + doxorubicin + vincristine (CAV) ± dactinomycin	methotrexate, mitomycin CAV + etoposide
Gastric **	Fluorouracil ± leucovorin	Claptatin, doxorubicin, etoposide, methotrexate + leucovorin, mitomycin
Head and neck squamous cell ⁵	Claptatin + fluorouracil	Blaomycin, carboplatin, pactitaxel
Islet cell **	Methotrexate	Streptozocin + fluorouracil;
	Streptozocin + doxorubicin	chlorozotocin; actreotide
Kaposi's sarcoma* (AIDS-related)	Etoposide or Interferon alfa or vinorelbine Doxorubicin + bleomycin + vincristine or vinorelbine (ABV)	Vincristine, doxorubicin, bleomycin
Leukemias	<i>Induction:</i> Vincristine + prednisone + asparaginase ± daunorubicin	<i>Induction:</i> same ± high- dose methotrexate ± cytarabine; pegaspargase
Acute lymphocytic leukemia (ALL) ⁷	CNS prophylaxis; Intrathecal methotrexate ± systemic high-dose methotrexate with leucovorin ± Intrathecal cytarabine ± Intrathecal hydrocortisone	instead of asparaginase Teniposide or etoposide High-dose cytarabine
	Maintenance: methotrexate ± mercaptopurine	Maintenance: same + periodic vincristine + prednisone
Acute myeloid leukemia (AML) ⁹	Bone marrow transplant ³ Induction: Cytarabine + either daunorubicin or idarubicin Post Induction: High-dose cytarabine ± other drugs such as etoposide Bone marrow transplant ³	Cytarabine + mitoxantrone High-dose cytarabine
Chronic lymphocytic leukemia (CLL)	Chlorambucil ± prednisone Fludarabine	Claptatin, cyclophosphamide, pentostatin, vincristine, doxorubicin

† Available in the USA only for investigational use.

‡ Dose-limiting effects are in bold type. Cutaneous reactions (sometimes severe), hyperpigmentation, and ocular toxicity have been reported with virtually all nonhormonal anticancer drugs. For adverse interactions with other drugs, see *the Medical Letter Handbook of Adverse Drug Interactions, 1995*.

1. Available in the USA only for investigational use.

2. Megestrol and other hormonal agents may be effective in some patients when tamoxifen fails.

3. After high-dose chemotherapy (Medical Letter, 34:78, 1992).

4. For rectal cancer, postoperative adjuvant treatment with fluorouracil plus radiation, preceded and followed by treatment with fluorouracil alone.

5. Drugs have major activity only when combined with surgical resection, radiotherapy or both.

6. The vitamin A analog isotretinoin (Accutane) can control pre-neoplastic lesions (leukoplakia) and decreases the rates of second primary tumors (SE Senner et al., J Natl Cancer Inst. 88:140, 1994).
7. High-risk patients (e.g., high counts, cytogenetic abnormalities, adults) may require additional drugs for induction, maintenance and "intensification" (use of additional drugs after achievement of remission). Additional drugs include cyclophosphamide, mitoxantrone and thioguanine. The results of one large controlled trial in the United Kingdom suggest that intensification may improve survival in all children with ALL (Jim Chassella et al., Lancet, 348: 143, Jan 21, 1998).
8. Patients with a poor prognosis initially or those who relapse after remission
9. Some patients with acute promyelocytic leukemia have had complete responses to tretinoin. Such treatment can cause a toxic syndrome characterized primarily by fever and respiratory distress (RP Warrell, Jr et al. N Eng J. Med, 329:177, 1993).
10. Allogeneic HLA identical sibling bone marrow transplantation can cure 40% to 70% of patients with CML in chronic phase, 15% to 25% of patients with accelerated phase CML, and < 15% patients in blast crisis. Disease-free survival after bone marrow transplantation is adversely influenced by age > 50 years, duration of disease > 3 years from diagnosis, and use of one antigen mismatched or matched-unrelated donor marrow. Interferon alpha may be curative in patients with chronic phase CML who achieve a complete cytogenetic response (about 10%); It is the treatment of choice for patients > 50 years old with newly diagnosed chronic phase CML and for all patients who are not candidates for an allogeneic bone marrow transplant. Chemotherapy alone is palliative.

Radiolabeling of EC-MTX and EC-TDX with ^{99m}Tc

Use the same method described for the synthesis of EC-folate, EC-MTX and EC-TDX were prepared. The labeling procedure is the same as described for the preparation of ^{99m}Tc -EC-folate except EC-MTX and EC-TDX were used. Synthesis of ^{99m}Tc -EC-MTX and ^{99m}Tc -EC-TDX is shown in FIG. 2 and FIG. 3.

Stability assay of ^{99m}Tc -EC-folate, ^{99m}Tc -EC-MTX and ^{99m}Tc -EC-TDX

Stability of ^{99m}Tc -EC-Folate, ^{99m}Tc -EC-MTX and ^{99m}Tc -EC-TDX was tested in serum samples. Briefly, 740 KBq of 1 mg ^{99m}Tc -EC-Folate, ^{99m}Tc -EC-MIX and ^{99m}Tc -EC-TDX was incubated in dog serum (200 μl) at 37 °C for 4 hours. The serum samples were diluted with 50% methanol in water and radio-TLC repeated at 0.5, 2 and 4 hours as described above.

Tissue distribution studies

Female Fischer 344 rats (150 \pm 25 g) (Harlan Sprague-Dawley, Indianapolis, IN) were inoculated subcutaneously with 0.1 ml of mammary tumor cells from the 13762 tumor cell line suspension (10⁶ cells/rat, a tumor cell line specific to Fischer rats) into the hind legs using 25-gauge needles. Studies performed 14 to 17 days after implantation when tumors reached

approximately 1 cm diameter. Animals were anesthetized with ketamine (10-15 mg/rat, intraperitoneally) before each procedure.

In tissue distribution studies, each animal injected intravenously with 370-550 KBq of ^{99m}Tc -EC-folate or ^{99m}Tc -EC (n=3/time point). The injected mass of each ligand was 10 μg per rat. At 20 min, 1, 2 and 4 h following administration of the radiopharmaceuticals, the anesthetized animals were sacrificed and the tumor and selected tissues were excised, weighed and counted for radioactivity by a gamma counter (Packard Instruments, Downers Grove, IL). The biodistribution of tracer in each sample was calculated as percentage of the injected dose per gram of tissue wet weight (%ID/g). Counts from a diluted sample of the original injectate were used for reference. Tumor/nontarget tissue count density ratios were calculated from the corresponding %ID/g values. Student-t test was used to assess the significance of differences between two groups.

In a separate study, blocking studies were performed to determine receptor-mediated process. In blocking studies, for ^{99m}Tc -EC-folate was co-administrated (i.v.) with 50 and 150 $\mu\text{mol/kg}$ folic acid to tumor bearing rats (n=3/group). Animals were killed 1 h post-injection and data was collected.

Scintigraphic imaging and autoradiography studies

Scintigraphic images, using a gamma camera (Siemens Medical Systems, Inc., Hoffman Estates, IL) equipped with low-energy, parallel-hole collimator, were obtained 0.5, 2 and 4 hrs after i.v. injection of 18.5 MBq of ^{99m}Tc -labeled radiotracer.

Whole-body autoradiogram were obtained by a quantitative image analyzer (Cyclone Storage Phosphor System, Packard, Meridian, CI.). Following i.v. injection of 37 MBq of ^{99m}Tc -EC-folate, animal killed at 1 h and body was fixed in carboxymethyl cellulose (4%). The frozen body was mounted onto a cryostat (LKB 2250 cryomicrotome) and cut into 100 μm coronal sections. Each section was thawed and mounted on a slide. The slide was then placed in contact with multipurpose phosphor storage screen (MP, 7001480) and exposed for 15 h ^{99m}Tc -labeled). The phosphor screen was excited by a red laser and resulting blue light that is proportional with previously absorbed energy was recorded.

RESULTS

Chemistry and Stability of ^{99m}Tc -EC-Folate

A simple, fast and high yield aminoethylamido and EC analogues of folate, MTX and TDX were developed. The structures of these analogues were confirmed by NMR and mass spectroscopic analysis. Radiosynthesis of EC-folate with ^{99m}Tc was achieved with high (>95%) radiochemical purity. ^{99m}Tc -EC-folate was found to be stable at 20 min. 1, 2 and 4 hours in dog serum samples.

Biodistribution of ^{99m}Tc -EC-folate

Biodistribution studies showed that tumor/blood count density ratios at 20 min-4 h gradually increased for ^{99m}Tc -EC-folate, whereas these values decreased for ^{99m}Tc -EC in the same time period (FIG. 4). %ID/g uptake values, tumor/blood and tumor/muscle ratios for ^{99m}Tc -EC-folate and ^{99m}Tc -EC were given in Tables 3 and 4, respectively.

TABLE 3
Biodistribution of ^{99m}Tc -EC-folate in Breast Tumor-Bearing Rats

	% of injected ^{99m}Tc -EC-folate dose per organ or tissue			
	20 min	1 h	2 h	4 h
Blood	0.370±0.049	0.165±0.028	0.086±0.005	0.058±0.002
Lung	0.294±0.017	0.164±0.024	0.092±0.002	0.063±0.003
Liver	0.274±0.027	0.185±0.037	0.148±0.042	0.105±0.002
Stomach	0.130±0.002	0.557±0.389	0.118±0.093	0.073±0.065
Kidney	4.328±0.896	4.052±0.488	5.102±0.276	4.673±0.399
Thyroid	0.311±0.030	0.149±0.033	0.095±0.011	0.066±0.011
Muscle	0.058±0.004	0.0257±0.005	0.016±0.007	0.008±0.0005
Intestine	0.131±0.013	0.101±0.071	0.031±0.006	0.108±0.072
Urine	12.637±2.271	10.473±3.083	8.543±2.763	2.447±0.376
Tumor	0.298±0.033	0.147±0.026	0.106±0.029	0.071±0.006
Tumor/Blood	0.812±0.098	0.894±0.069	1.229±0.325	1.227±0.129
Tumor/Muscle	5.157±0.690	5.739±0.347	6.876±2.277	8.515±0.307

Values shown represent the mean ± standard deviation of data from 3 animals

Scintigraphic Imaging and Autoradiography Studies

Scintigraphic images obtained at different time points showed visualization of tumor in ^{99m}Tc -EC-folate injected group. Contrary, there was no apparent tumor uptake in ^{99m}Tc -EC

injected group (FIG. 6). Both radiotracer showed evident kidney uptake in all images. Autoradiograms performed at 1 h after injection of ^{99m}Tc -EC-folate clearly demonstrated tumor activity.

EXAMPLE 2: TUMOR HYPOXIA TARGETING

Synthesis of 2-(2-methyl-5-nitro- ^1H imidazolyl)ethylamine (amino analogue of metronidazole, MN- NH_2)

Amino analogue of metronidazole was synthesized according to the previously described methods (Hay *et al.*, 1994). Briefly, metronidazole was converted to a mesylated analogue (m.p. 149-150°C, reported 153-154°C, TLC:ethyl acetate, $R_f=0.45$), yielded 75%. Mesylated metronidazole was then reacted with sodium azide to afford azido analogue (TLC:ethyl acetate, $R_f=0.52$), yielded 80%. The azido analogue was reduced by triphenyl phosphine and yielded (60%) the desired amino analogue (m.p. 190-192°C, reported 194-195°C, TLC:ethyl acetate, $R_f=0.15$). Ninhydrin (2% in methanol) spray indicated the positivity of amino group of MN- NH_2 . The structure was confirmed by ^1H -NMR and mass spectroscopy (FAB-MS) m/z 171(M^+H , 100).

Synthesis of Ethylenedicysteine-Metronidazole (EC- MN)

Sodium hydroxide (2N, 0.2 ml) was added to a stirred solution of EC (134 mg, 0.50 mmol) in water (5 ml). To this colorless solution, sulfo-NHS (217 mg, 1.0 mmol) and 1- C (192 mg, 1.0 mmol) were added. MN- NH_2 : dihydrochloride salt (340 mg, 2.0 mmol) was then added. The mixture was stirred at room temperature for 24 hours. The mixture was dialyzed for 48 hrs using Spectra/POR molecular porous membrane with cut-off at 500 (Spectrum Medical Industries Inc., Houston, TX). After dialysis, the product was frozen dried using lyophilizer (Labconco, Kansas City, MO). The product weighed 315 mg (yield 55%). ^1H -NMR (D_2O) δ 2.93 (s, 6H, nitroimidazole- CH_3), 2.60-2.95 (m, 4H and - CH_2 -SH of EC), 3.30-3.66 (m, 8H, ethylenediamine of EC and nitromidazole- CH_2 - CH_2 - NH_2), 3.70-3.99 (t, 2H, NH-CH-CO of EC), 5.05 (t, 4H, metronidazole- CH_2 - CH_2 - NH_2) (s, 2H, nitroimidazole C= CH). FAB MS m/z 572 (M^+ , 20). The synthetic scheme of EC-MN is shown in FIG. 7.

Synthesis of 3-(2-nitro-¹H-imidazolyl)propylamine (amino analogue of nitroimidazole, NIM- NH₂)

To a stirred mixture containing 2-nitroimidazole (1g, 8.34 mmol) and Cs₂CO₃ (2.9g, 8.90 mmol) in dimethylformamide (DMF, 50 ml), 1,3-ditosylpropane (3.84 g, 9.99 mmol) was added. The reaction was heated at 80°C for 3 hours. The solvent was evaporated under vacuum and the residue was suspended in ethylacetate. The solid was filtered, the solvent was concentrated, loaded on a silica gel-packed column and eluted with hexane:ethylacetate (1:1). The product, 3-tosylpropyl-(2-nitroimidazole), was isolated (1.67g, 57.5%) with m.p. 108-111°C. ¹H-NMR (CDCl₃) δ 2.23 (m, 2H), 2.48 (s, 3H), 4.06 (t, 2H, J=5.7Hz), 4.52 (t, 2H, J=6.8Hz), 7.09 (s, 1H), 7.24 (s, 1H), 7.40 (d, 2H, J=8.2Hz), 7.77 (d, 2H, J=8.2Hz).

Tosylated 2-nitroimidazole (1.33g, 4.08 mmol) was then reacted with sodium azide (Q29 g, 4.49 mmol) in DMF (10 ml) at 100°C for 3 hours. After cooling, water (20 ml) was added and the product was extracted from ethylacetate (3x20 ml). The solvent was dried over MgSO₄ and evaporated to dryness to afford azido analogue (0.6 g, 75%, TLC: hexane:ethyl acetate; 1:1, R_f=0.42). ¹H-NMR (CDCl₃) δ 2.14 (m, 2H), 3.41 (t, 2H, J=6.2Hz), 4.54 (t, 2H, J=6.9Hz), 7.17 (s, 2H).

The azido analogue (0.57 g, 2.90 mmol) was reduced by triphenyl phosphine (1.14 g, 4.35 mmol) in tetrahydrofuran (THF) at room temperature for 4 hours. Concentrated HCl (12 ml) was added and heated for additional 5 hours. The product was extracted from ethylacetate and water mixture. The ethylacetate was dried over MgSO₄ and evaporated to dryness to afford amine hydrochloride analogue (360 mg, 60%). Ninhydrin (2% in methanol) spray indicated the positivity of amino group of NIM- NH₂. ¹H-NMR (D₂O) δ 2.29 (m, 2H), 3.13 (t, 2H, J=7.8Hz), 3.60 (br, 2H), 4.35 (t, 2H, J=7.4Hz), 7.50 (d, 1H, J=2.1Hz), 7.63 (d, 1H, J=2.1Hz).

Synthesis of ethylenedicycysteine-nitroimidazole (EC- NIM)

Sodium hydroxide (2N, 0.6 ml) was added to a stirred solution of EC (134 mg, 0.50 mmol) in water (2ml). To this colorless solution, sulfo-NHS (260.6 mg, 1.2 mmol), EDC (230 mg, 1.2 mmol) and sodium hydroxide (2N, 1 ml) were added. NIM-NH₂ hydrochloride salt (206.6 mg, 1.0 mmol) was then added. The mixture was stirred at room temperature for 24 hours. The mixture was dialyzed for 48 hrs using Spectra/POR molecular porous membrane

with cut-off at 500 (Spectrum Medical Industries Inc., Houston, TX). After dialysis, the product was frozen dried using lyophilizer (Labconco, Kansas City, MO). The product weighed 594.8 mg (yield 98%). The synthetic scheme of EC-NIM is shown in FIG. 8A. The structure is confirmed by $^1\text{H-NMR}$ (D_2O) (FIG. 8B).

Radiolabeling of EC-MN and EC-NIM with $^{99\text{m}}\text{Tc}$

Radiosynthesis of $^{99\text{m}}\text{Tc-EC-MN}$ and $^{99\text{m}}\text{Tc-EC-NIM}$ were achieved by adding required amount of pertechnetate into home-made kit containing the lyophilized residue of EC-MN or EC-NIM (3 mg), SnCl_2 (100 μg), Na_2HPO_4 (13.5 mg), ascorbic acid (0.5 mg) and NaEDTA (0.5 mg). Final pH of preparation was 7.4. Radiochemical purity was determined by TLC (ITLAC SG, Gelman Sciences, Ann Arbor, MI) eluted with acetone (system A) and ammonium acetate (1M in water):methanol (4:1) (system B), respectively. From radio-TLC (Bioscan, Washington, DC) analysis, the radiochemical purity was >96% for both radiotracers.

Synthesis of [^{18}F]FMISO and [^{131}I]IMISO

[Should this be ^{18}F] fluoride was produced by the cyclotron using proton irradiation of enriched ^{18}O -water in a small-volume silver target. The tosyl MISO (Hay *et al.*, 1994) (20 mg) was dissolved in acetonitrile (1.5 ml), added to the kryptofix-fluoride complex. After heating, hydrolysis and column purification, A yield of 25-40% (decay corrected) of pure product was isolated with the end of bombardment (EOB) at 60 min. HPLC was performed on a C-18 ODS-20T column, 4.6 x 25 mm (Waters Corp., Milford, Mass), with water/acetonitrile, (80/20), using a flow rate of 1 ml/min. The no-carrier-added product corresponded to the retention time (6.12 min) of the unlabeled FMISO under similar conditions. The radiochemical purity was greater than 99%. Under the UV detector (310 nm), there were no other impurities. The specific activity of [^{18}F]FMISO determined was 1 Ci/ μmol based upon UV and radioactivity detection of a sample of known mass and radioactivity.

[^{131}I]IMISO was prepared using the same precursor (Cherif *et al.*, 1994), briefly, 5 mg of tosyl MISO was dissolved in acetonitrile (1 ml), and Na^{131}I (1 mCi in 0.1 ml IN NaOH) (Dupont New England Nuclear, Boston. MA) was added. After heating and purification, the product (60-70% yield) was obtained. Radio-TLC indicated the R_f values of 0.01 for the final product using chloroform methanol (7:3) as an eluant.

Stability assay of ^{99m}Tc -EC-MN and ^{99m}Tc -EC-NIM

Stability of labeled ^{99m}Tc -EC-MN and ^{99m}Tc -EC-NIM were tested in serum samples. Briefly, 740 KBq of 1 mg ^{99m}Tc -EC-MN and ^{99m}Tc -EC-NIM were incubated in dog serum (200 μl) at 37 °C for 4 hours. The serum samples were diluted with 50% methanol in water and radio-TLC repeated at 0.5, 2 and 4 hours as described above.

Tissue distribution studies of ^{99m}Tc -EC-MN

Female Fischer 344 rats (150 \pm 25 g) (Harlan Sprague-Dawley, Indianapolis, IN) were inoculated subcutaneously with 0.1 ml of mammary tumor cells from the 13762 tumor cell line suspension (10^6 cells/rat, a tumor cell line specific to Fischer rats) into the hind legs using 25-gauge needles. Studies performed 14 to 17 days after implantation when tumors reached approximately 1 cm diameter. Rats were anesthetized with ketamine (10-15 mg/rat, intraperitoneally) before each procedure.

In tissue distribution studies, each animal was injected intravenously with 370- 550 KBq of ^{99m}Tc -EC-MN or ^{99m}Tc -EC (n=3/time point). The injected mass of ^{99m}Tc -EC-MN was 10 μg per rat. At 0.5, 2 and 4 hrs following administration of the radiotracers, the rats were sacrificed and the selected tissues were excised, weighed and counted for radioactivity. The biodistribution of tracer in each sample was calculated as percentage of the injected dose per gram of tissue wet weight (%ID/g). Tumor/nontarget tissue count density ratios were calculated from the corresponding %ID/g values. The data was compared to [^{18}F]FMISO and [^{131}I]IMISO using the same animal model. Student t-test was used to assess the significance of differences between groups.

Scintigraphic imaging and autoradiography studies

Scintigraphic images, using a gamma camera (Siemens Medical Systems, Inc., Hoffman Estates, IL) equipped with low-energy, parallel-hole collimator, were obtained 0.5, 2 and 4 hrs after i.v. injection of 18.5 MBq of each radiotracer.

Whole-body autoradiogram was obtained by a quantitative image analyzer (Cyclone Storage Phosphor System, Packard, Meridian, CT). Following i.v. injection of 37 MBq of ^{99m}Tc -EC-MN, the animals were killed at 1 h and the body were fixed in carboxymethyl cellulose (4%) as previously described (Yang *et al.*, 1995). The frozen body was mounted onto a cryostat (LKB 2250 cryomicrotome) and cut into 100 μm coronal sections. Each section was thawed and mounted on a slide. The slide was then placed in contact with multipurpose phosphor storage screen (MP, 7001480) and exposed for 15 hrs.

To ascertain whether ^{99m}Tc -EC-NIM could monitor tumor response to chemotherapy, a group of rats with tumor volume 1.5 cm and ovarian tumor-bearing mice were treated with paclitaxel (40 mg/kg/rat, 80mg/kg/mouse, i.v.) at one single dose. The image was taken on day 4 after paclitaxel treatment. Percent of injected dose per gram of tumor weight with or without treatment was determined.

Polarographic oxygen microelectrode pO_2 measurements

To confirm tumor hypoxia, intratumoral pO_2 measurements were performed using the Eppendorf computerized histographic system. Twenty to twenty-five pO_2 measurements along each of two to three linear tracks were performed at 0.4 mm intervals on each tumor (40-75 measurements total). Tumor pO measurements were made on three tumor-bearing rats. Using an on-line computer system, the pot measurements of each track were expressed as absolute values relative to the location of the measuring point along the track, and as the relative frequencies within a pO_2 histogram between 0 and 100 mmHg with a class width of 2.5 mm.

RESULTS

Radiosynthesis and stability of ^{99m}Tc -EC-MN and ^{99m}Tc -EC-NIM

Radiosynthesis of EC-MN and EC-NIM with ^{99m}Tc were achieved with high (>95%) radiochemical purity. Radiochemical yield was 100%. ^{99m}Tc -EC-MN and ^{99m}Tc -EC-NIM (FIG. 13) were found to be stable at 0.5, 2 and 4 hrs in dog serum samples. There was no degradation products observed. Radiofluorination and radioiodination of MISO were achieved easily using the same precursor. In both labeled MISO analogues, the radiochemical purity was greater than 99%.

In vivo tissue distribution studies

The tissue distribution of ^{99m}Tc -EC-MN and ^{99m}Tc -EC in the tumor-bearing rats is shown in Tables 4 and 5. Due to high affinity for ionic ^{99m}Tc , there was no significant and consistent thyroid uptake, suggesting the in vivo stability of ^{99m}Tc -EC-MN (Table 5).

TABLE 4
Biodistribution of ^{99m}Tc -EC in Breast Tumor-Bearing Rats

	% of injected ^{99m}Tc -EC dose per organ or tissue			
	20min	1 h	2 h	4 h
Blood	0.435±0.029	0.273±0.039	0.211±0.001	0.149±0.008
Lung	0.272±0.019	0.187±0.029	0.144±0.002	0.120±0.012
Liver	0.508±0.062	0.367±0.006	0.286±0.073	0.234±0.016
Stomach	0.136±0.060	0.127±0.106	0.037±0.027	0.043±0.014
Kidney	7.914±0.896	8.991±0.268	9.116±0.053	7.834±1.018
Thyroid	0.219±0.036	0.229±0.118	0.106±0.003	0.083±0.005
Muscle	0.060±0.006	0.043±0.002	0.028±0.009	0.019±0.001
Intestine	0.173±0.029	0.787±0.106	0.401±0.093	0.103±0.009
Urine	9.124±0.808	11.045±6.158	13.192±4.505	8.693±2.981
Tumor	0.342±0.163	0.149±0.020	0.115±0.002	0.096±0.005
Tumor/Blood	0.776±0.322	0.544±0.004	0.546±0.010	0.649±0.005
Tumor/Muscle	5.841±3.253	3.414±0.325	4.425±1.397	5.093±0.223

Values shown represent the mean± standard deviation of data from 3 animals

In blocking studies, tumor/muscle and tumor/blood count density ratios were significantly decreased ($p<0.01$) with folic acid co-administrations (FIG. 5).

TABLE 5
Biodistribution of ^{99m}Tc -EC-metronidazole conjugate in breast tumor bearing rats¹

	30 Min.	2 Hour	4 Hour
Blood	1.46±0.73	1.19±0.34	0.76±0.14
Lung	0.79±0.39	0.73±0.02	0.52±0.07
Liver	0.83±0.36	0.91±0.11	0.87±0.09
Spleen	0.37±0.17	0.41±0.04	0.37±0.07
Kidney	4.30±1.07	5.84±0.43	6.39±0.48
Muscle	0.08±0.03	0.09±0.01	0.07±0.01
Intestine	0.27±0.12	0.39±0.24	0.22±0.05
Thyroid	0.051±0.16	0.51±0.09	0.41±0.02
Tumor	0.034±0.13	0.49±0.02	0.50±0.09

1. Each rat received 99m Tc-EC-metronidazole (10 μCi , iv). Each value is percent of injected dose per gram weight (n=3)/time interval. Each data represents mean of three measurements with standard deviation.

Biodistribution studies showed that tumor/blood and tumor/muscle count density ratios at 0.54 hr gradually increased for ^{99m}Tc -EC-MN, [^{18}F]FMISO and [^{131}I]IMISO, whereas these values did not alter for ^{99m}Tc -EC in the same time period (FIG. 9 and FIG. 10). [^{18}F]FMISO showed the highest tumor-to-blood uptake ratio than those with [^{131}I]IMISO and ^{99m}Tc -EC-MN at 30 min, 2 and 4 hrs post-injection. Tumor/blood and tumor/muscle ratios for ^{99m}Tc -EC-MN and [^{131}I]IMISO at 2 and 4 hrs postinjection were not significantly different (p<0.05).

Scintigraphic imaging and autoradiographic studies

Scintigraphic images obtained at different time points showed visualization of tumor in ^{99m}Tc -EC-MN and ^{99m}Tc -EC-NIM groups. Contrary, there was no apparent tumor uptake in ^{99m}Tc -EC injected group (FIG. 11). Autoradiograms performed at 1 hr after injection of ^{99m}Tc -EC-MN clearly demonstrated tumor activity (FIG. 12). Compare to ^{99m}Tc -EC-NM, ^{99m}Tc -EC-NIM appeared to provide better scintigraphic images due to higher tumor-to-background ratios. In breast tumor-bearing rats, tumor uptake was markedly higher in ^{99m}Tc -EC-NIM group compared to ^{99m}Tc -EC (FIG. 14A). Data obtained from percent of injected dose of ^{99m}Tc -EC-NIM per gram of tumor weight indicated that a 25% decreased uptake in the rats treated with paclitaxel when compared to control group (FIG. 14B).

In ovarian tumor-bearing mice, there was a decreased tumor uptake in mice treated with paclitaxel (FIG. 15A and FIG. 15B). Similar results were observed in sarcoma-bearing

(FIG. 15C and FIG. 15D). Thus, ^{99m}Tc -EC-NIM could be used to assess tumor response to paclitaxel treatment.

Polarographic oxygen microelectrode pO_2 measurements

Intratumoral PO_2 measurements of tumors indicated the tumor oxygen tension ranged 4.6 ± 1.4 mmHg as compared to normal muscle of 35 ± 10 mmHg. The data indicate that the tumors are hypoxic.

EXAMPLE 3: PEPTIDE IMAGING OF CANCER

Synthesis of Ethylenedicysteine-Pentaglutamate (EC- GAP)

Sodium hydroxide (1N, 1 ml) was added to a stirred solution of EC (200 mg, 0.75 mmol) in water (10 ml). To this colorless solution, sulfo-NHS (162 mg, 0.75 mmol) and EDC (143 mg, 0.75 mmol) were added. Pentaglutamate sodium salt (M.W. 750-1500, Sigma Chemical Company) (500 mg, 0.67 mmol) was then added. The mixture was stirred at room temperature for 24 hours. The mixture was dialyzed for 48 hrs using Spectra/POR molecular porous membrane with cut-off at 500 (Spectrum Medical Industries Inc., Houston, TX). After dialysis, the product was frozen dried using lyophilizer (Labconco, Kansas City, MO). The product in the salt form weighed 0.95 g. The synthetic scheme of EC-GAP is shown in FIG. 16.

Stability Assay of ^{99m}Tc -EC-GAP

Radiolabeling of EC-GAP with ^{99m}Tc was achieved using the same procedure described previously. The radiochemical purity was 100%. Stability of labeled ^{99m}Tc -EC-GAP was tested in serum samples. Briefly, 740 KBq of 1 mg ^{99m}Tc -EC-GAP was incubated in dog serum (200 μl) at 37°C for 4 hours. The serum samples were diluted with 50% methanol in water and radio-TLC repeated at 0.5, 2 and 4 hours as described above.

Scintigraphic Imaging Studies

Scintigraphic images, using a gamma camera equipped with low-energy, parallel-hole collimator, were obtained 0.5, 2 and 4 hrs after i.v. injection of 18.5 MBq of each radiotracer.

RESULTS

Stability Assay of ^{99m}Tc -EC-GAP

- 5 ^{99m}Tc -EC-GAP found to be stable at 0.5, 2 and 4 hrs in dog serum samples. There was no degradation products observed.

Scintigraphic imaging studies

- 10 Scintigraphic images obtained at different time points showed visualization of tumor in ^{99m}Tc -EC-GAP group. The optimum uptake is at 30min to 1 hour post-administration (FIG. 17).

EXAMPLE 4: IMAGING TUMOR APOPTOTIC CELLS

15 Synthesis of Ethylenedicysteine-Annexin V (EC-ANNEX)

- Sodium bicarbonate (1N, 1 ml) was added to a stirred solution of EC (5 mg, 0.019 mmol). To this colorless solution, sulfo-NHS (4 mg, 0.019 mmol) and EDC (4 mg, 0.019 mmol) were added. Annexin V (M.W. 33 kD, human, Sigma Chemical Company) (0.3 mg) was then
20 added. The mixture was stirred at room temperature for 24 hours. The mixture was dialyzed for 48 hrs using Spectra/POR molecular porous membrane with cut-off at 10,000 (Spectrum Medical Industries Inc., Houston, TX). After dialysis, the product was frozen dried using lyophilizer (Labconco, Kansas City, MO). The product in the salt form weighed 12 mg.

25 Stability Assay of ^{99m}Tc -EC-ANNEX

- Radiolabeling of EC-ANNEX with ^{99m}Tc was achieved using the same procedure described in EC-GAP. The radiochemical purity was 100%. Stability of labeled
30 ^{99m}Tc -EC-ANNEX was tested in serum samples. Briefly, 740 KBq of 1 mg ^{99m}Tc -EC-ANNEX was incubated in dog serum (200 μl) at 37 °C for 4 hours. The serum samples were diluted with 50% methanol in water and radio-TLC repeated at 0.5, 2 and 4 hours as described above.

Scintigraphic Imaging Studies

Scintigraphic images, using a gamma camera equipped with low-energy, parallel-hole collimator, were obtained 0.5, 2 and 4 hrs after i.v. injection of 18.5 MBq of the radiotracer. The animal models used were breast, ovarian and sarcoma. Both breast and ovarian-tumor bearing rats are known to overexpress high apoptotic cells. The imaging studies were conducted on day 14 after tumor cell inoculation. To ascertain the tumor treatment response, the pre-imaged mice were administered paclitaxel (80 mg/Kg, iv, day 14) and the images were taken on day 18.

RESULTS

Stability Assay of ^{99m}Tc -EC-ANNEX

^{99m}Tc -EC-ANNEX found to be stable at 0.5, 2 and 4 hrs in dog serum samples. There was no degradation products observed.

Scintigraphic imaging studies

Scintigraphic images obtained at different time points showed visualization of tumor in ^{99m}Tc -EC-ANNEX group (FIGs. 18-20). The images indicated that highly apoptotic cells have more uptake of ^{99m}Tc -EC-ANNEX. There was no marked difference of tumor uptake between pre- and post-paclitaxel treatment in the high apoptosis (ovarian tumor-bearing) group (FIG. 19A and FIG. 19B) and in the low apoptosis (sarcoma tumor-bearing) group (FIG. 20A and FIG. 20B).

EXAMPLE 5: IMAGING TUMOR ANGIOGENESIS

Synthesis of (Amino Analogue of Colchicine, COL-NH₂)

Demethylated amino and hydroxy analogue of colchicine was synthesized according to the previously described methods (Orr *et al.*, 1995). Briefly, colchicine (4 g) was dissolved in 100 ml of water containing 25% sulfuric acid. The reaction mixture was heated for 5 hours at 100°C. The mixture was neutralized with sodium carbonate. The product was filtered and dried over freeze dryer, yielded 2.4 g (70%) of the desired amino analogue (m.p. 153-155°C, reported 155-157°C). Ninhydrin (2% in methanol) spray indicated the positivity of amino group of

COL-NH₂. The structure was confirmed by ¹H-NMR and mass spectroscopy (FAB-MS).

¹H-NMR (CDCl₃) δ 8.09 (s, 1H), 7.51 (d, 1H, J=12 Hz), 7.30 (d, 1H, J=12Hz), 6.56 (s, 1H), 3.91 (s, 6H), 3.85 (m, 1H), 3.67 (s, 3H), 2.25-2.52 (m, 4H). m/z 308.2(M⁺, 20), 307.2 (100).

Synthesis of Ethylenedicysteine-Colchicine (EC-COL)

Sodium hydroxide (2N, 0.2 ml) was added to a stirred solution of EC (134 mg, 0.50 mmol) in water (5 ml). To this colorless solution, sulfo-NHS (217 mg, 1.0 mmol) and EDC (192 mg, 1.0 mmol) were added. COL-NH₂ (340 mg, 2.0 mmol) was then added. The mixture was stirred at room temperature for 24 hours. The mixture was dialyzed for 48 hrs using Spectra/POR molecular porous membrane with cut-off at 500 (Spectrum Medical Industries Inc., Houston, TX). After dialysis, the product was frozen dried using lyophilizer (Labconco, Kansas City, MO). The product weighed 315 mg (yield 55%). ¹H-NMR (D₂O) δ 7.39 (s, 1H), 7.20 (d, 1H, J=12Hz), 7.03 (d, 1H, J=12Hz), 6.78 (s, 1H), 4.25-4.40 (m, 1H), 3.87 (s, 3H, -OCH₃), 3.84 (s, 3H, -OCH₃), 3.53 (s, 3H, -OCH₃), 3.42-3.52 (m, 2H), 3.05-3.26 (m, 4H), 2.63-2.82 (m, 4H), 2.19-2.25 (m, 4H). FAB MS m/z 580 (sodium salt, 20). The synthetic scheme of EC-COL is shown in FIG. 21.

Radiolabeling of EC-COL and EC with ^{99m}Tc

Radiosynthesis of ^{99m}Tc-EC-COL was achieved by adding required amount of ^{99m}Tc-pertechnetate into home-made kit containing the lyophilized residue of EC-COL (5 mg), SnCl₂ (100 µg), Na₂HPO₄ (13.5 mg), ascorbic acid (0.5 mg) and NaEDTA (0.5 mg). Final pH of preparation was 7.4. ^{99m}Tc-EC was also obtained by using home-made kit containing the lyophilized residue of EC (5 mg), SnCl₂ (100 µg), Na₂HPO₄ (13.5 mg), ascorbic acid (0.5 mg) and NaEDTA (0.5 mg) at pH 10. Final pH of preparation was then adjusted to 7.4. Radiochemical purity was determined by TLC (ITLC SG, Gelman Sciences, Ann Arbor, MI) eluted with ammonium acetate (1M in water):methanol (4:1). Radio-thin layer chromatography (TLC, Bioscan, Washington, DC) was used to analyze the radiochemical purity for both radiotracers.

Stability Assay of ^{99m}Tc-EC-COL

Stability of labeled ^{99m}Tc -EC-COL was tested in serum samples. Briefly, 740 KBq of 5 mg ^{99m}Tc -EC-COL was incubated in the rabbit serum (500 μl) at 37 °C for 4 hours. The serum samples were diluted with 50% methanol in water and radio-TLC repeated at 0.5, 2 and 4 hours as described above.

Tissue Distribution Studies

Female Fischer 344 rats (150 \pm 25 g) (Harlan Sprague-Dawley, Indianapolis, IN) were inoculated subcutaneously with 0.1 ml of mammary tumor cells from the 13762 tumor cell line suspension (10 cells/rat, a tumor cell line specific to Fischer rats) into the hind legs using 25-gauge needles. Studies performed 14 to 17 days after implantation when tumors reached approximately 1 cm diameter. Rats were anesthetized with ketamine (10-15 mg/rat, intraperitoneally) before each procedure.

In tissue distribution studies, each animal was injected intravenously with 370-550 KBq of ^{99m}Tc -EC-COL or ^{99m}Tc -EC (n=3/time point). The injected mass of ^{99m}Tc -EC-COL was 10 μg per rat. At 0.5, 2 and 4 hrs following administration of the radiotracers, the rats were sacrificed and the selected tissues were excised, weighed and counted for radioactivity. The biodistribution of tracer in each sample was calculated as percentage of the injected dose per gram of tissue wet weight (%ID/g). Tumor/nontarget tissue count density ratios were calculated from the corresponding %ID/g values. Student t-test was used to assess the significance of differences between groups.

Scintigraphic Imaging Studies

Scintigraphic images, using a gamma camera (Siemens Medical Systems, Inc., Hoffman Estates, IL) equipped with low-energy, parallel-hole collimator, were obtained 0.5, 2 and 4 hrs after i.v. injection of 300 μCi of ^{99m}Tc -EC-COL and ^{99m}Tc -EC. Computer outlined region of interest (ROI) was used to quantitate (counts per pixel) the tumor uptake versus normal muscle uptake.

RESULTS

Radiosynthesis and stability of $^{99m}\text{Tc-EC-COL}$

Radiosynthesis of EC-COL with ^{99m}Tc was achieved with high (>95%) radiochemical purity (FIG. 21). $^{99m}\text{Tc-EC-COL}$ was found to be stable at 0.5, 2 and 4 hrs in rabbit serum samples. There was no degradation products observed (FIG. 22).

In Vivo Biodistribution

In vivo biodistribution of $^{99m}\text{Tc-EC-COL}$ and $^{99m}\text{Tc-EC}$ in breast-tumor-bearing rats are shown in Tables 4 and 6. Tumor uptake value (%ID/g) of $^{99m}\text{Tc-EC-COL}$ at 0.5, 2 and 4 hours was 0.436 ± 0.089 , 0.395 ± 0.154 and 0.221 ± 0.006 (Table 6), whereas those for $^{99m}\text{Tc-EC}$ were 0.342 ± 0.163 , 0.115 ± 0.002 and 0.097 ± 0.005 , respectively (Table 4). Increased tumor-to-blood (0.52 ± 0.12 to 0.72 ± 0.07) and tumor-to-muscle (3.47 ± 0.40 to 7.97 ± 0.93) ratios as a function of time were observed in $^{99m}\text{Tc-EC-COL}$ group (FIG. 23). Conversely, tumor-to-blood and tumor-to-muscle values showed time-dependent decrease with $^{99m}\text{Tc-EC}$ when compared to $^{99m}\text{Tc-EC-COL}$ group in the same time period (FIG. 24).

TABLE 6
Biodistribution of $^{99m}\text{Tc-EC-Colchicine}$ in Breast Tumor Bearing Rats

	30 Min.	2 Hour	4 Hour
Blood	0.837 ± 0.072	0.606 ± 0.266	0.307 ± 0.022
Lung	0.636 ± 0.056	0.407 ± 0.151	0.194 ± 0.009
Liver	1.159 ± 0.095	1.051 ± 0.213	0.808 ± 0.084
Spleen	0.524 ± 0.086	0.559 ± 0.143	0.358 ± 0.032
Kidney	9.705 ± 0.608	14.065 ± 4.007	11.097 ± 0.108
Muscle	0.129 ± 0.040	0.071 ± 0.032	0.028 ± 0.004
Stomach	0.484 ± 0.386	0.342 ± 0.150	0.171 ± 0.123
Uterus	0.502 ± 0.326	0.343 ± 0.370	0.133 ± 0.014
Thyroid	3.907 ± 0.997	2.297 ± 0.711	1.709 ± 0.776
Tumor	0.436 ± 0.089	0.395 ± 0.154	0.221 ± 0.006

* Each rat received ^{99m}Tc-EC-Colchicine (10 μCi, iv.). Each value is the percent of injected dose per gram tissue weight (n=3)/time interval. Each data represents mean of three measurements with standard deviation.

5

TABLE 7
Rf Values Determined by Radio-TLC (ITLC-SG) Studies

	System A*	System B†
^{99m} Tc-EC-folate	0	1(>95%)
^{99m} Tc-EC-	0	1(>95%)
Free ^{99m} Tc	1	1
Reduced ^{99m} Tc	0	0

* Acetone

† Ammonium Acetate (1M in water):Methanol (4:1)

10 **Gamma Scintigraphic Imaging of ^{99m}Tc-EC-COL in Breast Tumor-Bearing Rats**

In vivo imaging studies in three breast-tumor-bearing rats at 1 hour post-administration indicated that the tumor could be visualized well with ^{99m}Tc-EC-COL group (FIG. 25), whereas, less tumor uptake in the ^{99m}Tc-EC group was observed (FIG. 26). Computer outlined region of interest (ROI) showed that tumor/background ratios in ^{99m}Tc-EC-COL group were significantly higher than ^{99m}Tc-EC group (FIG. 27).

15

TUMOR GLYCOLYSIS TARGETING

20 **EXAMPLE 6: DEVELOPMENT OF ^{99m}Tc-EC-NEOMYCIN**

Synthesis of EC

EC was prepared in a two-step synthesis according to the previously described methods (Ratner and Clarke, 1937; Blondeau *et al.*, 1967). The precursor, L-thiazolidine-4-carboxylic acid, was synthesized (m.p. 195°, reported 196-197°). EC was then prepared (m.p. 237°, reported 251-253°). The structure was confirmed by ¹H-NMR and fast-atom bombardment mass spectroscopy (FAB-MS).

25

Synthesis of Ethylenedicysteine-neomycin (EC-neomycin)

Sodium hydroxide (2N, 0.2 ml) was added to a stirred solution of EC (134 mg, 0.50 mmol) in water (5 ml). To this colorless solution, sulfo-NHS (217 mg, 1.0 mmol) and EDC (192 mg, 1.0 mmol) were added. Neomycin trisulfate salt (909 mg, 1.0 mmol) was then added. The mixture was stirred at room temperature for 24 hours. The mixture was dialyzed for 48 hours using Spectra/POR molecular porous membrane with cut-off at 500 (Spectrum Medical Industries Inc., Houston, TX). After dialysis, the product was frozen dried using lyophilizer (Labconco, Kansas City, MO). The product weighed 720 mg (yield 83%). The synthetic scheme of EC-neomycin is shown in FIG. 36. The structure is confirmed by $^1\text{H-NMR}$ (FIGS. 38A-B), mass spectrometry (FIGS. 39A-B) and elemental analysis (Galbraith Laboratories, Inc. Knoxville, TN). Elemental analysis $\text{C}_{39}\text{H}_{75}\text{N}_{10}\text{S}_4\text{O}_{19} \cdot 15\text{H}_2\text{O}$ ($\text{C}, \text{H}, \text{N}, \text{S}$), Calc. C:33.77, H:7.58, N:10.11, S:9.23; found C:32.44, H:5.90, N:10.47, S:10.58. UV wavelength of EC-neomycin was shifted to 270.5 nm when compared to EC and neomycin (FIGS. 40A-C)

Radiolabeling of EC-MN and EC-neomycin with $^{99\text{m}}\text{Tc}$

Radiosynthesis of $^{99\text{m}}\text{Tc-EC}$ and $^{99\text{m}}\text{Tc-EC-neomycin}$ were achieved by adding required amount of $^{99\text{m}}\text{Tc-pertechetate}$ into home-made kit containing the lyophilized residue of EC or EC-neomycin (10 mg), SnCl_2 (100 μg), Na_2HPO_4 (13.5 mg) and ascorbic acid (0.5 mg). NaEDTA (0.5 mg) in 0.1 ml of water was then added. Final pH of preparation was 7.4. Radiochemical purity was determined by TLC (ITLC SG, Gelman Sciences, Ann Arbor, MI) eluted with ammonium acetate (1M in water):methanol (4:1). From radio-TLC (Bioscan, Washington, DC) analysis (FIG. 41) and HPLC analysis (FIGS. 42-45), the radiochemical purity was >95% for both radiotracers.

Stability assay of $^{99\text{m}}\text{Tc-EC}$ and $^{99\text{m}}\text{Tc-EC-neomycin}$

Stability of labeled $^{99\text{m}}\text{Tc-EC}$ and $^{99\text{m}}\text{Tc-EC-neomycin}$ were tested in dog serum samples. Briefly, 740 KBq of 1 mg $^{99\text{m}}\text{Tc-EC}$ and $^{99\text{m}}\text{Tc-EC-neomycin}$ were incubated in dog serum (200 μl) at 37°C for 4 hours. The serum samples were diluted with 50% methanol in water and radio-TLC repeated at 0.5, 2 and 4 hours as described above.

Tissue distribution studies of $^{99\text{m}}\text{Tc-EC-neomycin}$

Female Fischer 344 rats (150 ± 25 g) (Harlan Sprague-Dawley, Indianapolis, IN) were inoculated subcutaneously with 0.1 ml of mammary tumor cells from the 13762 tumor cell line suspension (10^6 cells/rat, a tumor cell line specific to Fischer rats) into the hind legs using 25-gauge needles. Studies performed 14 to 17 days after implantation when tumors reached

approximately 1 cm diameter. Rats were anesthetized with ketamine (10-15 mg/rat, intraperitoneally) before each procedure.

In tissue distribution studies, each animal was injected intravenously with 10-20 μCi of $^{99\text{m}}\text{Tc}$ -EC or $^{99\text{m}}\text{Tc}$ -EC-neomycin ($n=3/\text{time point}$). The injected mass of $^{99\text{m}}\text{Tc}$ -EC-neomycin was 200 μg per rat. At 0.5, 2 and 4 hours following administration of the radiotracers, the rats were sacrificed and the selected tissues were excised, weighed and counted for radioactivity. The biodistribution of tracer in each sample was calculated as percentage of the injected dose per gram of tissue wet weight (%ID/g). Tumor/nontarget tissue count density ratios were calculated from the corresponding %ID/g values. When compared to $^{99\text{m}}\text{Tc}$ -EC (Table 4) and free technetium (Table 9), tumor-to tissue ratios increased as a function of time in $^{99\text{m}}\text{Tc}$ -EC-neomycin group (Table 8).

Scintigraphic imaging studies

Scintigraphic images, using a gamma camera (Siemens Medical Systems, Inc., Hoffman Estates, IL) equipped with low-energy, parallel-hole collimator, were obtained 0.5, 2 and 4 hours after i.v. injection of 100 μCi of each radiotracer. Compare to $^{99\text{m}}\text{Tc}$ -EC, high uptake in the tumors was observed (FIG. 37A). Preliminary clinical imaging studies were conducted in a patient with breast cancer. The tumor was visualized well at 2 hours post-administration of $^{99\text{m}}\text{Tc}$ -EC-neomycin (FIG. 37B).

TABLE 8
Biodistribution of $^{99\text{m}}\text{Tc}$ -EC-neomycin in Breast Tumor Bearing Rats

	30 Min.	1 Hour	2 Hour	4 Hour
Blood	0.463 \pm 0.007	0.262 \pm 0.040	0.139 \pm 0.016	0.085 \pm 0.004
Lung	0.344 \pm 0.011	0.202 \pm 0.030	0.114 \pm 0.014	0.080 \pm 0.003
Liver	0.337 \pm 0.012	0.269 \pm 0.013	0.221 \pm 0.020	0.195 \pm 0.012
Stomach	0.279 \pm 0.039	0.147 \pm 0.001	0.061 \pm 0.008	0.054 \pm 0.008
Spleen	0.159 \pm 0.008	0.114 \pm 0.013	0.095 \pm 0.007	0.089 \pm 0.003
Kidney	8.391 \pm 0.395	8.804 \pm 0.817	8.356 \pm 0.408	8.638 \pm 0.251
Thyroid	0.349 \pm 0.008	0.202 \pm 0.028	0.114 \pm 0.007	0.086 \pm 0.001
Muscle	0.093 \pm 0.001	0.049 \pm 0.010	0.021 \pm 0.006	0.010 \pm 0.001
Intestine	0.159 \pm 0.004	0.093 \pm 0.014	0.061 \pm 0.004	0.266 \pm 0.200
Urine	25.402 \pm 8.621	21.786 \pm 2.690	0.224 \pm 0.000	2.609 \pm 2.377
Tumor	0.419 \pm 0.023	0.279 \pm 0.042	0.166 \pm 0.023	0.131 \pm 0.002

Brain	0.022±0.001	0.014±0.003	0.010±0.001	0.007±0.001
Heart	0.147±0.009	0.081±0.012	0.040±0.004	0.029±0.002
Tumor/Blood	0.906±0.039	1.070±0.028	1.196±0.061	1.536±0.029
Tumor/Muscle	4.512±0.220	5.855±0.458	8.364±1.469	12.706±0.783
Tumor/Brain	19.495±1.823	20.001±0.890	17.515±2.035	20.255±1.693

Values shown represent the mean ± standard deviation of data from 3 animals.

TABLE 9
Biodistribution of ^{99m}Tc Pertechnetate in Breast Tumor Bearing Rats

	30 Min.	2 Hour	4 Hour
Blood	1.218±0.328	0.666±0.066	0.715±0.052
Lung	0.646±0.291	0.632±0.026	0.387±0.024
Liver	0.541±0.232	0.304±0.026	0.501±0.081
Spleen	0.331±0.108	0.187±0.014	0.225±0.017
Kidney	0.638±0.197	0.489±0.000	0.932±0.029
Thyroid	24.821±5.181	11.907±15.412	17.232±5.002
Muscle	0.130±0.079	0.076±0.002	0.063±0.003
Intestine	0.153±0.068	0.186±0.007	0.344±0.027
Tumor	0.591±0.268	0.328±0.016	0.423±0.091
Brain	0.038±0.014	0.022±0.002	0.031±0.009
Heart	0.275±0.089	0.145±0.015	0.166±0.012
Tumor/Blood	0.472±0.093	0.497±0.073	0.597±0.144
Tumor/Muscle	4.788±0.833	4.302±0.093	6.689±1.458
Tumor/Liver	1.084±0.023	1.084±0.115	0.865±0.270

Values shown represent the mean ± standard deviation of data from 3 animals.

In vitro cellular uptake of ^{99m}Tc -EC-drug conjugates

To evaluate the cellular uptake of ^{99m}Tc -EC-drug conjugates, each well containing 80,000 cells (A549 lung cancer cell line) was added with 2 μCi of ^{99m}Tc -EC-neomycin and ^{18}F -FDG. After incubation at 0.5-4 hours, the cells were washed with phosphate buffered saline 3 times and followed by trypsin to lose the cells. The cells were then counted by a gamma counter. ^{99m}Tc -EC-neomycin showed highest uptake among those agents tested in human lung cancer cell line (FIG. 46).

Effect of glucose on cellular uptake of ^{99m}Tc -EC-neomycin and ^{18}F -FDG

Neomycin is known to influence glucose absorption (Rogers et al., 1968; Fanciulli et al., 1994). Previous experiments have shown that ^{99m}Tc -EC-neomycin has higher uptake than ^{18}F -FDG in human lung cancer cell line (A549). To determine if uptake of ^{99m}Tc -EC-neomycin is mediated via glucose-related mechanism, glucose (0.1 mg-2.0 mg) was added to each well containing either 50,000 (breast) cells or 80,000 cells (lung) along with 2 μCi of ^{99m}Tc -EC-neomycin and ^{18}F -FDG. After incubation, the cells were washed with phosphate buffered saline 3 times and followed by trypsin to lose the cells. The cells were then counted by a gamma counter.

By adding glucose at the concentration of 0.1-2.0 mg/well, decreased uptake of ^{99m}Tc -EC-neomycin in two lung cancer cell lines and one breast cell line was observed. Similar results were observed in ^{18}F -FDG groups. ^{99m}Tc -EC (control) showed no uptake. The findings suggest that the cellular uptake of ^{99m}Tc -EC-neomycin may be mediated via glucose-related mechanism (FIGS. 47, 48A and 48B).

EXAMPLE 7: TUMOR METABOLIC IMAGING WITH ^{99m}Tc -EC-DEOXYGLUCOSE**Synthesis of EC-deoxyglucose (EC-DG)**

Sodium hydroxide (1N, 1ml) was added to a stirred solution of EC (110 mg, 0.41 mmol) in water (5 ml). To this colorless solution, sulfo-NHS (241.6 mg, 1.12 mmol) and EDC (218.8 mg, 1.15 mmol) were added. D-Glucosamine hydrochloride salt (356.8 mg, 1.65 mmol) was then added. The mixture was stirred at room temperature for 24 hours. The mixture was dialyzed for 48 hours using Spectra/POR molecular porous membrane with cut-off at 500 (Spectrum Medical Industries Inc., Houston, TX). After dialysis, the product was frozen dried using lyophilizer (Labconco, Kansas City, MO). The product in the salt form weighed 568.8 mg. The synthetic scheme is shown in Figure 59. The structure was confirmed by mass spectrometry (FIG. 60) and proton NMR (FIGS. 61 and 62). Radiochemical purity of ^{99m}Tc -EC-DG was 100% as determined by radio-TLC (FIG. 63) and HPLC (FIGS. 64 and 65) analysis.

Hexokinase assay

To determine if EC-DG mimics glucose phosphorylation, a hexokinase assay was conducted. Using a ready made kit (Sigma Chemical Company), EC-DG, glucosamine and glucose (standard) were assayed at UV wavelength 340 nm. Glucose, EC-DG and glucosamine showed positive hexokinase assay (FIGS. 66-68).

In vitro cellular uptake assay

In vitro cellular uptake assay was conducted by using a human lung cancer cell line (A549). Two μCi of ^{99m}Tc -EC-DG and ^{18}F -FDG were added to wells containing 80,000 cells each. After incubation at 0.5-4 hours, the cells were washed with phosphate buffered saline 3 times and followed by trypsin to lose the cells. The cells were then counted by a gamma counter. The uptake of ^{99m}Tc -EC-DG was comparable to FDG (FIG. 69).

Effect of d- and l-glucose on cellular uptake of ^{99m}Tc -EC-deoxyglucose and ^{18}F -FDG

To evaluate if the uptake of ^{99m}Tc -EC-deoxyglucose is mediated via d-glucose mechanism, d- and l-glucose (1 mg and 2.0 mg) were added to, each well containing either breast or lung cancer cells (50,000/0.5 ml/well), along with $2\mu\text{Ci}$ of ^{99m}Tc -EC-deoxyglucose and ^{18}F -FDG. After 2 hours incubation, the cells were washed with phosphate buffered saline 3 times and followed by trypsin to lose the cells. The cells were counted by a gamma counter.

By adding glucose at the concentration of 1-2.0 mg/well, a decreased uptake of ^{99m}Tc -EC-deoxyglucose and ^{18}F -FDG by d-glucose in breast and lung cancer cells was observed. However, there was no influence on both agents by l-glucose (FIG. 70-73). The findings suggest that the cellular uptake of ^{99m}Tc -EC-deoxyglucose is mediated via d-glucose mechanism.

Effect of EC-deoxyglucose loading on blood glucose level in normal rats

Previous experiments have shown that cellular uptake of ^{99m}Tc -EC-deoxyglucose is similar to FDG. For instance, the hexokinase assay (glucose phosphorylation) was positive. The uptake of ^{99m}Tc -EC-deoxyglucose is mediated via d-glucose mechanism. This study is to determine whether blood glucose level could be induced by either FDG or EC-deoxyglucose and suppressed by insulin.

Normal healthy Fischer 344 rats (weight 145-155 g) were fasting overnight prior to the experiments. The concentration of glucosamine hydrochloride, FDG and EC-deoxyglucose prepared was 60% and 164% (mg/ml). The blood glucose level (mg/dl) was determined by a glucose meter (Glucometer DEX, Bayer Corporation, Elkhart, IN). Prior to the study, the baseline of blood glucose level was obtained. Each rat ($n=3/\text{group}$) was administered 1.2 mmol/kg of glucosamine, FDG and EC-deoxyglucose. In a separate experiment, a group of rats was administered EC-deoxyglucose and FDG. Insulin (5 units) was administered after 30

minutes. Blood samples were collected from the tail vein every 30 minutes up to 6 hours post-administration.

Blood glucose level was induced by bolus intravenous administration of glucosamine, FDG and EC-deoxyglucose. This increased blood glucose level could be suppressed by co-administration of EC-deoxyglucose or FDG and insulin (FIGS. 74 and 75).

Tissue distribution studies of ^{99m}Tc -EC-DG

For breast tumor-bearing animal model, female Fischer 344 rats (150 ± 25 g) (Harlan Sprague-Dawley, Indianapolis, IN) were inoculated subcutaneously with 0.1 ml of mammary tumor cells from the 13762 tumor cell line suspension (10^6 cells/rat, a tumor cell line specific to Fischer rats) into the hind legs using 25-gauge needles. Studies were performed 14 to 17 days after implantation when tumors reached approximately 1 cm diameter. Rats were anesthetized with ketamine (10-15 mg/rat, intraperitoneally) before each procedure.

For lung tumor-bearing animal model, each athymic nude mouse (20-25g) was inoculated subcutaneously with 0.1 ml of human lung tumor cells from the A549 tumor cell line suspension (10^6 cells/mouse) into the hind legs using 25-gauge needles. Studies were performed 17 to 21 days after implantation when tumors reached approximately 0.6 cm diameter.

In tissue distribution studies, each animal was injected intravenously with 10-20 μCi (per rat) or 1-2 μCi (per mouse) of ^{99m}Tc -EC or ^{99m}Tc -EC-DG ($n=3/\text{time point}$). The injected mass of ^{99m}Tc -EC-DG was 1 mg per rat. At 0.5, 2 and 4 hours following administration of the radiotracers, the rodents were sacrificed and the selected tissues were excised, weighed and counted for radioactivity. The biodistribution of tracer in each sample was calculated as percentage of the injected dose per gram of tissue wet weight (%ID/g). Tumor/nontarget tissue count density ratios were calculated from the corresponding %ID/g values. When compared to ^{99m}Tc -EC (Table 4) and free technetium (Table 9), tumor-to tissue ratios increased as a function of time in ^{99m}Tc -EC-DG group (FIGS. 76-80).

Scintigraphic Imaging Studies

Scintigraphic images, using a gamma camera equipped with low-energy, parallel-hole collimator, were obtained 0.5, 2 and 4 hours after i.v. injection of 100 μCi of the radiotracer. The animal model used was breast tumor-bearing rats. Tumor could be visualized well when

compared to ^{99m}Tc -EC (control group) (FIG. 81). Preliminary clinical studies were conducted in 5 patients (3 brain tumors and 2 lung diseases). The images were obtained at 1-2 hours post-administration. ^{99m}Tc -EC-DG was able to differentiate benign versus malignant tumors. For instance, malignant astrocytoma showed high uptake (FIGS. 82A, 82B, 83A and 83B). Benign meningioma showed poor uptake compared to malignant meningioma (Figs 84A and B). Poor uptake was observed in patient with TB (FIG. 85A and FIG. 85B), but high uptake was observed in lung tumor (FIG. 86A, FIG. 86B, and FIG. 86C).

All of the compositions and/or methods disclosed and claimed herein can be made and executed without undue experimentation in light of the present disclosure. While the compositions and methods of this invention have been described in terms of preferred embodiments, it will be apparent to those of skill in the art that variations may be applied to the compositions and/or methods and in the steps or in the sequence of steps of the method described herein without departing from the concept, spirit and scope of the invention. More specifically, it will be apparent that certain agents which are both chemically and physiologically related may be substituted for the agents described herein while the same or similar results would be achieved. All such similar substitutes and modifications apparent to those skilled in the art are deemed to be within the spirit, scope and concept of the invention as defined by the appended claims.

REFERENCES

The following references, to the extent that they provide exemplary procedural or other details supplementary to those set forth herein, are specifically incorporated herein by reference.

5

Abrams, Juweid, Tenkate, "Technetium-99m-human polyclonal IgG radiolabeled via the hydrazino nicotinamide derivative for imaging focal sites of infection in rats," *J. Nucl. Med.*, 31:2022-2028, 1990.

10

Bakker, Krenning, Breeman, Kiper, Kooij, Reubi, Klijn, Visser, Docter, Lamberts, "Receptor scintigraphy with a radioiodinated somatostatin analogue: radiolabeling, purification, biologic activity and in vivo application in animals," *J. Nucl. Med.*, 31:1501-1509, 1990.

Blakenberg, Katsikis, Tait *et al.*, "In vivo detection and imaging of phosphatidylserine expression during programmed cell death," *Proc Natl. Acad. Sci USA*, 95:6349-6354, 1998.

15

Blakenberg, Katsikis, Tait, Davis, Naumovski, Ohtsuki, Kapiwoda, Abrams, Strauss, "Imaging of apoptosis (programmed cell death) with ^{99m}Tc annexin V," *J. Nucl. Med.*, 40:184-191, 1999.

Blondeau, Berse, Gravel, "Dimerization of an intermediate during the sodium in liquid ammonia reduction of L-thiazolidine-4-carboxylic acid," *Can J. Chem.*, 45:49-52, 1967.

20

Bolhuis, Lamers, Goey *et al.*, "Adoptive immunotherapy of ovarian carcinoma with Bs- MAB targeted lymphocytes. A multicenter study," *Int J Cancer*, 7:78-81, 1992.

Britton and Granowska, "Imaging of tumors, in tomography in nuclear medicine," *Proceedings of an International Symposium*, Vienna, Austria, IAEA, 91-105, 1996.

25

Bush, Jenkins, Allt, Beale, Bena, Dembo, Pringle, "Definitive evidence for hypoxic cells influencing cure in cancer therapy," *Br J Cancer*, (Suppl. III) 37:302-306, 1978.

Butterfield, Fuji, Ladd, Snow, Tan, Toner, "Segmented chelating polymers as imaging and therapeutic agents," *United States Patent 4,730,968*, March 24, 1998.

Campbell, Jones, Foulkes, Trowsdale, "Folate-binding protein is a marker for ovarian cancer," *Cancer Res*, 51:5329-5338, 1991.

30

Canevari, Miotti, Bottero, Valota, Colnaghi, "Ovarian carcinoma therapy with monoclonal antibodies," *Hybridoma*, 12:501-507, 1993.

Cherif, Yang, Tansey, Kim, Wallace, "Synthesis of [¹⁸F]fluoromisonidazole," *Pharm Res.*, 11:466-469, 1994.

- Coenen and Stocklin, "Evaluation of radiohalogenated amino acid analogues as potential tracers for PET and SPECT studies of protein synthesis," *Radioisot Klinik Forschung*, 18:402-440, 1988.
- 5 Coney, Mezzanzanica, Sanborn, Casalini, Colnaghi, Zurawski, "Chimeric mouse-human antibodies directed against folate binding receptor are efficient mediators of ovarian carcinoma cell killing," *Cancer Res*, 54:2448-2455, 1994.
- Davison, Jones, Orvig, Sohn, "A new class of oxotechnetium(+5) chelate complexes containing a TcON_2S_2 Core," *Inorg Chem*, 20:1629-1632, 1980.
- 10 Dickinson and Hiltner, "Biodegradation of poly(α -amino acid) hydrogel. II. In vitro," *J. Biomed Mater Res.*, 15:591, 1981.
- Dische, "A review of hypoxic-cell radiosensitization," *Int J Radiat Oncol Biol Phys*, 20:147-152, 1991.
- Fanciulli, Paggi, Bruno, et al., "Glycolysis and growth rate in normal and in hexokinase-transfected NIH-3T3 cells," *Oncol Res*, 6(9):405-9, 1994.
- 15 Franklin, Waintrub, Edwards, Christensen, Prendergrast, Woods, Bunn, Kolhouse, "New anti-lung-cancer antibody cluster 12 reacts with human folate receptors present on adenocarcinoma," *Int J Cancer-Supplement*, 8:89-95, 1994.
- Gatenby, Kessler, Rosenblum, Coia, Moldofsky, Hartz, Broder, "Oxygen distribution in squamous cell carcinoma metastases and its relationship to outcome of radiation therapy," *Int J Radiat Oncol Biol Phys*, 14:831-838, 1988.
- 20 Ginobbi, Geiser, Ombres, Citro, "Folic acid- polylysine carrier improves efficacy of c-myc antisense oligodeoxynucleotides on human melanoma (M14) cells," *Anticancer Res*, 17:29-35, 1997a.
- Goh, Pricher, Lobie, "Growth hormone promotion of tubulin polymerization stabilizes the microtubule network and protects against colchicine-induced apoptosis," *Endocrinology*, 25:4364-4372, 1998.
- 25 Goldsmith, "Receptor imaging: Competitive or complementary to antibody imaging," *Sem Nucl Med.*, 27:85-93, 1997.
- Goldsmith, Macapinlac, O'Brien, "Somatostatin receptor imaging in lymphoma," *Sem Nucl Med*, 25:262-271, 1995.
- 30 Gray, Conger, Elbert, Morsney, Scold, "The concentration of oxygen dissolved in tissues at the time of irradiation as a factor in radiotherapy," *Br J Radiol*, 26:638-648, 1953.
- Hall, "The oxygen effect and reoxygenation," In: E. J. Hall (ed.) *Radiobiology for the radiobiologist*, 3rd edition J.B. Lippincott Co., Philadelphia, PA, 137-160, 1988.

- Harada, Smith, Smith *et al.*, "Insulin-induced egr-1 and c-fos expression in 32D cells requires insulin receptor, Shc, and mitogen-activated protein kinase, but not insulin receptor substrate-1 and phosphatidylinositol 3-kinase activation," *J. Biol. Chem.* 271(47):30222-6, 1996.
- 5 Hay, Wilson, Moselen, Palmer, Denny, "Hypoxia-selective antitumor agents. Bis(nitroimidazolyl)alkanecarboxamides: a new class of hypoxia-selective cytotoxins and hypoxic cell radiosensitizers," *J Med. Chem.*, 37:381-391, 1994.
- Hermann, Patel. "Adaptive recognition by nucleic acid aptamers," *Science*, 287(5454):820-5, 2000.
- 10 Holm, Hansen, Hoier-Madsen, Sondergaard, Bzorek, "Folate receptor of human mammary adenocarcinoma," *APMIS*, 102:413-419, 1994.
- Hsueh and Dolnick, "Altered folate-binding protein mRNA stability in KB cells grown in folate-deficient medium," *Biochem Pharmacol*, 45:2537-2545, 1993.
- Imbert, "Discovery of podophyllotoxins," *Biochimie*, 80:207-222, 1998.
- 15 Jamar, Stoffel, Van Nerom, *et al.*, "Clinical evaluation of Tc-99m L,L-ethylenedicycysteine, a new renal tracer, in transplanted patients," *J Nucl Med*, 34:129P, 1993a.
- Jamar, Van Nerom, Verbruggen, *et al.*, "Clearance of the new tubular agent Tc-99m L,L-ethylenedicycysteine: Estimation by a simplified method," *J Nucl Med*, 34:129P, 1993b.
- 20 Kabasakal. "Technetium-99m ethylene dicysteine: a new renal tubular function agent," *Eur. J Nucl. Med.* 27(3):351-7, 2000.
- Kikukawa, Toyama, Katayama, *et al.*, "Early and delayed Tc-99m ECD brain SPECT in SLE patients with CNS involvement," *Ann Nucl Med.* 14(1):25-32, 2000.
- Koh, Rasey, Evans, Grierson, Lewellen, Graham, Krohn, Griffin, "Imaging of hypoxia in human tumors with [18F]fluoromisonidazole," *Int J Radiat Oncol Biol Phys*, 22:199-212, 1992.
- 25 Kranz, Patrick, Brigle, Spinella, Roy, "Conjugates of folate and anti-T-cell-receptor antibodies specifically target folate-receptor-positive tumor cells for lysis," *Proc Natl Acad Sci*, 92:9057-9061, 1995.
- Krenning, Kwokkeboom, Bakker, *et al.*, "Somatostatin receptor scintigraphy with [In-111-DTPA-D-Phe] and [I-123-Tyr]-octreotide: The Rotterdam experience with more than 1000 patients," *Eur J Nucl Med*, 7:716-731, 1995.
- 30 Lambert, Bakker, Reubi, Krenning, "Somatostatin receptor imaging in vivo localization of tumors with a radiolabeled somatostatin analog," *J. Steroid Biochem Mol Biol*, 37:1079-1082, 1990.

- Leamon and Low, "Cytotoxicity of momordin-folate conjugates in cultured human cells," *J Biol Chem*, 267:24966-24971, 1992.
- Leamon and Low, "Delivery of macromolecules into living cells: a method that exploits folate receptor endocytosis," *Proc Natl Acad Sci*, 88:5572-5576, 1991.
- 5 Leamon, Pastan, Low, "Cytotoxicity of folate-pseudomonas exotoxin conjugates toward tumor cells," *J Biol Chem*, 268:24847-24854, 1993.
- Lee and Low, "Delivery of liposomes into cultured KB cells via folate receptor-mediated endocytosis," *J Biol Chem*, 269:3198-3204, 1994.
- Lennon, Martin, Cotter, "Dose-dependent induction of apoptosis in human tumor cell lines by widely diverging stimuli," *Cell Prolif*, 24:203-214, 1991.
- 10 Lu, "Antimitotic agents," In: Foye, WO. Ed., "Cancer chemotherapeutic agents," Washington, DC: American Chemical Society, 345-368, 1995.
- Martin, Caldwell, Rasey, Grunbaum, Cerqueia, Krohn, Enhanced binding of the hypoxic cell marker [^{18}F]fluoromisonidazole in ischemic myocardium," *J Nucl Med*, 30:194-201, 1989.
- 15 Mathias, Hubers, Trump, Wang, Luo, Waters, Fuchs, Low, Green, "Synthesis of Tc-99m-DTPA-folate and preliminary evaluation as a folate-receptor-targeted radiopharmaceutical (Abstract)," *J Nucl Med*, (Supplement); 38:87P, 1997a.
- Mathias, Wang, Waters, Turek, Low, Green, "Indium-111-DTPA-folate as a radiopharmaceutical for targeting tumor-associated folate binding protein (Abstract)," *J Nucl Med*, (Supplement) 38:133P, 1997b.
- 20 Mathias, Wang, Lee, Waters, Low, Green, "Tumor-selective radiopharmaceutical targeting via receptor-mediated endocytosis of Gallium-67- deferoxamine-folate," *J Nucl Med*, 37:1003-1008, 1996.
- 25 Moller, Benecke, Flier. "Biologic activities of naturally occurring human insulin receptor mutations. Evidence that metabolic effects of insulin can be mediated by a kinase-deficient insulin receptor mutant," *J Biol Chem*. 15:266(17):10995-1001, 1991.
- Mochizuki, Inaki, Takeymoto, "Synthesis of polyglutamates containing 5-substituted uracil moieties," *Nucleic Acids Res.*, 16:121-124, 1985.
- 30 Nordmark, Overgaard, Overgaard, "Pretreatment oxygenation predicts radiation response in advanced squamous cell carcinoma of the head and neck," *Radiother Oncol*, 41:31-39, 1996.
- Offield, Jetton, Labosky, et al., "PDX-1 is required for pancreatic outgrowth and differentiation of the rostral duodenum," *Development*. 122(3):983-95, 1996.

- Orr, Kreisler, Kamen, "Similarity of folate receptor expression in UMSCC 38 cells to squamous cell carcinoma differentiation markers," *J Natl Cancer Inst*, 87:299-303, 1995.
- Patrick, Kranz, van Dyke, Roy, "Folate receptors as potential therapeutic targets in choroid plexus tumors of SV40 transgenic mice," *J Neurooncol*, 32:111-123, 1997.
- 5 Piper, McCaleb, Montgomery, "A synthetic approach to poly(glutamyl) conjugates of methotrexate," *J. Med. Chem.*, 26:291-294, 1983.
- Popovici, Mungiu, Trandafirescu, et al., "The influence of some antibiotics on hexokinase and pyruvate-kinase activity in the rat liver and kidney," *Arch Int Pharmacodyn Ther*.193(1):80-6, 1971.
- 10 Raderer, Becherer, Kurtaran, Angelberger, Li, Leimer, Weinlaender, Kornek, Kletter, Scheithauer, Virgolini, "Comparison of Iodine-123-vasoactive intestinal peptide receptor scintigraphy and Indium-111 CFT-102 immunoscintigraphy," *J. Nucl. Med.*, 37:1480-1487, 1996.
- Raffauf, Farren, Ulyot, "Colchicine. Derivatives of trimethylcolchicinic acid," *J. Am Chem Soc*, 75:5292-5294, 1953.
- 15 Rasey, Koh, Griesohn, Grunbaum, Krohn, "Radiolabeled fluoromisonidazole as an imaging agent for tumor hypoxia," *Int. J. Radiat Oncol. Biol Phys*, 17:985-991, 1989.
- Rasey, Nelson, Chin, Evans, Grunbaum, "Characterization of the binding of labeled fluoromisonidazole in cells in vitro," *Radiat Res*, 122:301-308, 1990.
- 20 Ratner and Clarke, "The action of formaldehyde upon cysteine," *J. Am Chem. Soc.*, 59:200-206, 1937.
- Reubi, Krenning, Lamberts *et al.*, "In vitro detection of somatostatin receptors in human tumors," *Metabolism*, 41:104-110 (suppl 2), 1992.
- Rogers, Bachorik, Nunn. "Neomycin effects on glucose transport by rat small intestine," *Digestion*. 1(3):159-64, 1968.
- 25 Ross, Chaudhuri, Ratnam, "Differential regulation of folate receptor isoforms in normal and malignant tissue in vivo and in established cell lines," *Cancer*, 73:2432-2443, 1994.
- Rowinsky, Cazenave, Donchower, "Taxol: a novel investigational antimicrotubule agent," *J. Natl. Cancer Institute*, 82(15):1247-1259, 1990.
- 30 Seabold, Gurl, Schurrer, Aktay, Kirchner, "Comparison of ^{99m}Tc-Methoxyisobutyl Isonitrile and ²⁰¹Tl Scintigraphy for Detection of Residual Thyroid Cancer After ¹³¹I Ablative Therapy," *J. Nucl. Med.*, 40(9):1434-1440, 1999.
- Shankar, Zhu, Baron et al., "Glucosamine infusion in rats mimics the beta-cell dysfunction of non-insulin-dependent diabetes mellitus," *Metabolism*. 47(5):573-7, 1998.

Stella and Mathew, "Derivatives of taxol, pharmaceutical compositions thereof and methods for preparation thereof," *United States Patent 4,960,790*, October 2, 1990.

Surma, Wiewiora, Liniecki, "Usefulness of Tc-99m-N,N'-ethylene-1-dicysteine complex for dynamic kidney investigations," *Nucl Med Comm*, 15:628- 635, 1994.

5 Tait and Smith, "Site-specific mutagenesis of annexin V: role of residues from Arg-200 to Lys-207 in phospholipid binding," *Arch Biochem Biophys*, 288:141-144, 1991.

Valk, Mathis, Prados, Gilbert, Budinger, "Hypoxia in human gliomas: Demonstration by PET with [^{18}F]fluoromisonidazole," *J Nucl Med*, 33:2133-2137, 1992.

10 Van Nerom, Bormans, Bauwens, Vandecruys, De Roo, Verbruggen, "Comparative evaluation of Tc-99m L,L-ethylenedicysteine and Tc-99m MAG3 in volunteers," *Eur J Nucl Med*, 16:417, 1990.

Van Nerom, Bormans, De Roo, *et al.*, "First experience in healthy volunteers with Tc-99m-L,L-ethylenedicysteine, a new renal imaging agent," *Eur J Nucl Med*, 20:738-746, 1993.

15 Verbruggen, Nosco, Van Nerom *et al.*, "Tc-99m-L,L-ethylenedicysteine: A renal imaging agent. I. Labelling and evaluation in animals," *J Nucl Med*, 33:551-557, 1992.

Verbruggen, Nosco, Van Nerom, Bormans, Adriacns, De Roo, "Evaluation of Tc-99m-L,L-ethylenedicysteine as a potential alternative to Tc-99m MAG3," *Eur J Nucl Med*, 16:429, 1990.

20 Villevalois-Cam, Tahiri, Chauvet, *et al.*, "Insulin-induced redistribution of the insulin-like growth factor II/mannose 6-phosphate receptor in intact rat liver," *J Cell Biochem*. 77(2):310-22, 2000

25 Virgolini, Raderer, Kurtaran, "Vasoactive intestinal peptide (VIP) receptor imaging in the localization of intestinal adenocarcinomas and endocrine tumors," *N Eng J Med*, 331:1116-1121, 1994.

Wang, Lee, Mathias, Green, Low, "Synthesis, purification, and tumor cell uptake of Ga-67 deferoxamine-folate, a potential radiopharmaceutical for tumor imaging," *Bioconjugate Chem*, 7:56- 62, 1996.

30 Wang, Luo, Lantrip, Waters, Mathias, Green, Fuchs, Low, "Design and synthesis of [^{111}In]DTPA-folate for use as a tumor-targeted radiopharmaceutical," *Bioconjugate Chem*, 8:673-679, 1997.

Wang, Wang, Ichijo, Giannakakou, Foster, Fojo, Wimalasena, "Microtubule-interfering agents activate c-Jun N-terminal kinase/stress-activated protein kinase through both Ras and apoptosis signal-regulating kinase pathways," *J. Biol. Chem.*, 273:4928-4936, 1998.

Weitman, Frazier, Kamen, "The folate receptor in central nervous system malignancies of childhood," *J Neuro-Oncology*, 21:107-112, 1994.

Weitman, Lark, Coney *et al.*, "Distribution of folate GP38 in normal and malignant cell lines and tissues," *Cancer Res*, 52:3396-3400, 1992a.

5 Weitman, Weinberg, Coney, Zurawski, Jennings, Kamen, "Cellular localization of the folate receptor: potential role in drug toxicity and folate homeostasis," *Cancer Res*, 52:6708-6711, 1992b.

Wester, Herz, Weber, Heiss, Schmidtke, Schwaiger, Stocklin, "Synthesis and radiopharmacology of -O(2-[¹⁸F]fluoroethyl)-L-Tyrosine for tumor imaging," *J. Nucl. Med.*, 40:205-212, 10 1999.

Westerhof, Jansen, Emmerik, Kathmann, Rijksen, Jackman, Schornagel, "Membrane transport of natural folates and antifolate compounds in murine L1210 leukemia cells: Role of carrier- and receptor- mediated transport systems," *Cancer Res*, 51:5507-5513, 1991.

15 Yang, Wallace, Cherif, Li, Gretzer, Kim, Podoloff, "Development of F-18-labeled fluoroerythronitroimidazole as a PET agent for imaging tumor hypoxia," *Radiology*, 194:795-800, 1995.

Yoshino, Takeda, Sugimoto, *et al.*, "Differential effects of troglitazone and D-chiroinositol on glucosamine-induced insulin resistance in vivo in rats," *Metabolism*. 48(11):1418-23, 20 1999.

CLAIMS

1. A composition for imaging comprising:

- a) a radionuclide label;
b) ethylenedicycysteine; and
c) a tissue specific ligand conjugated to said ethylenedicycysteine;

wherein said ethylenedicycysteine forms an N_2S_2 chelate with said radionuclide label.

2. The composition of claim 1, wherein said tissue specific ligand may be conjugated to said ethylenedicycysteine on one or both acid arms of the ethylenedicycysteine.

3. The composition of claim 1, wherein said radionuclide is ^{99m}Tc , ^{188}Re , ^{186}Re , ^{183}Sm , ^{166}Ho , ^{90}Y , ^{89}Sr , ^{67}Ga , ^{68}Ga , ^{111}In , ^{183}Gd , ^{59}Fe , ^{225}Ac , ^{212}Bi , ^{211}At , ^{64}Cu or ^{62}Cu .

4. The composition of claim 3, wherein said radionuclide is ^{99m}Tc .

5. The composition of claim 1, wherein said tissue specific ligand is an anticancer agent, DNA topoisomerase inhibitor, antimetabolite, tumor marker, folate receptor targeting ligand, tumor apoptotic cell targeting ligand, tumor hypoxia targeting ligand, DNA intercalator, receptor marker, peptide, nucleotide, organ specific ligand, antibiotic, antifungal, antibody, glutamate pentapeptide or an agent that mimics glucose.

6. The composition of claim 5, wherein said tissue specific ligand is an anticancer agent.

7. The composition of claim 6, wherein said anticancer agent may be selected from the group consisting of methotrexate, doxorubicin, tamoxifen, paclitaxel, topotecan, LHRH, mitomycin C, etoposide tomudex, podophyllotoxin, mitoxantrone, camptothecin, colehicine, endostatin, fludarabine, gemcitabine and tomudex.

8. The composition of claim 5, wherein said tissue specific ligand is a tumor marker.

9. The composition of claim 8, wherein said tumor marker is PSA, ER, PR, CA-125, CA-199, CEA AFP, interferons, BRCA1, HER-2/neu, cytoxan, p53, endostatin or a monoclonal antibody (e.g., antisense).

10. The composition of claim 5, wherein the tissue specific ligand is a folate receptor targeting ligand.
11. The composition of claim 10, wherein the folate receptor targeting ligand is folate, methotrexate or tomudex.
12. The composition of claim 11, further defined as ^{99m}Tc -EC-folate.
13. The composition of claim 11, further defined as ^{99m}Tc -EC-methotrexate.
14. The composition of claim 11, further defined as ^{99m}Tc -EC-tomodex.
15. The composition of claim 5, wherein the tissue specific ligand is a tumor apoptotic cell targeting ligand or a tumor hypoxia targeting ligand.
16. The composition of claim 15, wherein the tissue specific ligand is annexin V, colchicine, nitroimidazole, mitomycin or metronidazole.
17. The composition of claim 16, further defined as ^{99m}Tc -EC-annexin V.
18. The composition of claim 16, further defined as ^{99m}Tc -EC-colchicine.
19. The composition of claim 16, further defined as ^{99m}Tc -EC-nitroimidazole.
20. The composition of claim 16, further defined as ^{99m}Tc -EC-metronidazole.
21. The composition of claim 5, wherein the tissue specific ligand is glutamate pentapeptide (molecular weight 750-15,000).
22. The composition of claim 21, further defined as ^{99m}Tc -EC-glutamate pentapeptide.
23. The composition of claim 5, wherein the tissue specific ligand is an agent that mimics glucose.

24. The composition of claim 23, wherein the agent that mimics glucose is neomycin, kanamycin, gentamycin, paromycin, amikacin, tobramycin, netilmicin, ribostamycin, sisomicin, micromicin, lividomycin, dibekacin, isepamicin, astromicin, or an aminoglycoside.

25. The composition of claim 24, further defined as ^{99m}Tc -EC-neomycin.

26. The composition of claim 24, further defined as ^{99m}Tc -EC-kanamycin.

27. The composition of claim 24, further defined as ^{99m}Tc -EC-aminoglycosides.

28. The composition of claim 24, further defined as ^{99m}Tc -EC-gentamycin.

29. The composition of claim 24, further defined as ^{99m}Tc -EC-tobramycin.

30. The composition of claim 2, further comprising a linker conjugating EC to said tissue specific ligand.

31. The composition of claim 30, wherein the linker is a water soluble peptide, glutamic acid, aspartic acid, bromo ethylacetate, ethylene diamine or lysine.

32. The composition of claim 31, wherein the tissue specific ligand is estradiol, topotecan, paclitaxel, raloxifen, etoposide, doxorubicin, mitomycin C, endostatin, annexin V, LHRH, octreotide, VIP, methotrexate or folic acid.

33. A method of synthesizing a radiolabeled ethylenedicycysteine derivative for imaging comprising the steps:

- a) obtaining a tissue specific ligand;
- b) admixing said ligand with ethylenedicycysteine (EC) to obtain an EC-tissue specific ligand derivative; and
- c) admixing said EC-tissue specific ligand derivative with a radionuclide and a reducing agent to obtain a radionuclide labeled EC-tissue specific ligand derivative, wherein the EC forms an N_2S_2 chelate with the radionuclide.

34. The method of claim 33, wherein said reducing agent is a dithionite ion, a stannous ion or a ferrous ion.

35. A method for labeling a tissue specific ligand for imaging, comprising the steps:

- a) obtaining a tissue specific ligand;
- b) admixing the tissue specific ligand with ethylenedicysteine (EC) to obtain an EC-ligand drug conjugate; and
- c) reacting the drug conjugate with ^{99m}Tc in the presence of a reducing agent to form an N_2S_2 chelate between the ethylenedicysteine (with or without linker) and the ^{99m}Tc .

36. The method of claim 35, wherein the tissue specific ligand is an anticancer agent, DNA topoisomerase inhibitor, antimetabolite, tumor marker, folate receptor targeting ligand, tumor apoptotic cell targeting ligand, tumor hypoxia targeting ligand, DNA intercalator, receptor marker, peptide, organ specific ligand, antibiotic, antifungal, glutamate pentapeptide or an agent that mimics glucose.

37. The method of claim 36, wherein the reducing agent is a dithionite ion, a stannous ion or a ferrous ion.

38. A method of imaging a site within a mammalian body comprising the steps of administering an effective diagnostic amount of a composition comprising a ^{99m}Tc labeled ethylenedicysteine-tissue specific ligand conjugate and detecting a radioactive signal from the ^{99m}Tc localized at the site.

39. The method of claim 38, wherein the site is a tumor.

40. The method of claim 38, wherein the site is an infection.

41. The method of claim 38, wherein the site is breast cancer, ovarian cancer, prostate cancer, endometrium, heart, lung, brain, liver, folate (+) cancer, ER (+) cancer, spleen, pancreas, or intestine.

42. A kit for preparing a radiopharmaceutical preparation, said kit comprising a sealed container including a predetermined quantity of an ethylenedicysteine-tissue specific ligand conjugate composition and a sufficient amount of reducing agent to label the conjugate with ^{99m}Tc .

43. The kit of claim 42, wherein the ethylenedicysteine-tissue specific ligand conjugate composition further comprises a linker between the ethylenedicysteine and the tissue specific ligand.

44. The kit of claim 42, wherein the tissue specific ligand is an anticancer agent, DNA topoisomerase inhibitor, antimetabolite, tumor marker, folate receptor targeting ligand, tumor apoptotic cell targeting ligand, tumor hypoxia targeting ligand, DNA intercalator, receptor marker, peptide, organ ligand, antibiotic, antifungal, glutamate pentapeptide or an agent that mimics glucose.

45. The kit of claim 43, wherein the tissue specific ligand is estradiol, topotecan, paclitaxel, raloxifen, etoposide, doxorubicin, mitomycin C, endostatin, annexin V, LHRH, octreotide, VIP, methotrexate or folic acid.

46. The kit of claim 45, wherein the linker is a water soluble peptide, glutamic acid, polyglutamic acid, aspartic acid, polyaspartic acid, bromoethylacetate, ethylenediamine or lysine.

47. A reagent for preparing a scintigraphic imaging agent comprising a tissue specific ligand covalently linked to a ^{99m}Tc binding moiety.

48. The reagent of claim 47, wherein the ^{99m}Tc binding moiety is ethylenedicysteine.

49. The reagent of claim 48, wherein the tissue specific ligand is an anticancer agent, DNA topoisomerase inhibitor, antimetabolite, tumor marker, folate receptor targeting ligand, tumor apoptotic cell targeting ligand, tumor hypoxia targeting ligand, DNA intercalator, receptor marker, peptide, organ specific ligand, antibiotic, antifungal, glutamate pentapeptide or an agent that mimics glucose.

50. The reagent of claim 48, further comprising a linker between said tissue specific ligand and said ^{99m}Tc binding moiety.

51. A method of determining effectiveness of a candidate drug on a tumor, said method comprising:

- a) obtaining a candidate drug;
- b) conjugating said candidate drug with ethylenedicysteine (EC) to produce an EC-candidate drug conjugate;
- c) chelating said candidate drug conjugate with ^{99m}Tc to produce a ^{99m}Tc -EC-candidate drug conjugate;
- d) introducing said ^{99m}Tc -EC-candidate drug conjugate into a patient with a tumor; and
- e) imaging said patient to determine the effectiveness of the candidate drug against the tumor.

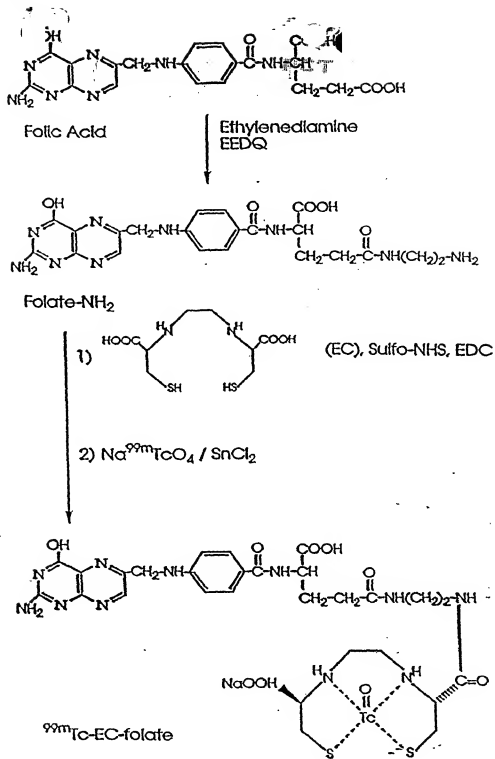


FIG. 1

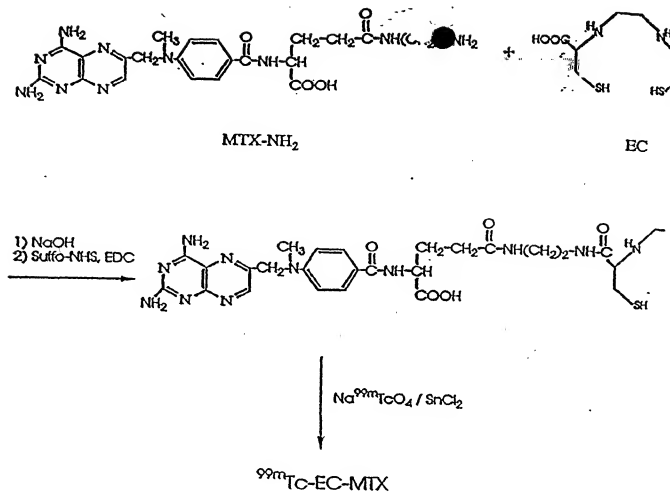


FIG 2

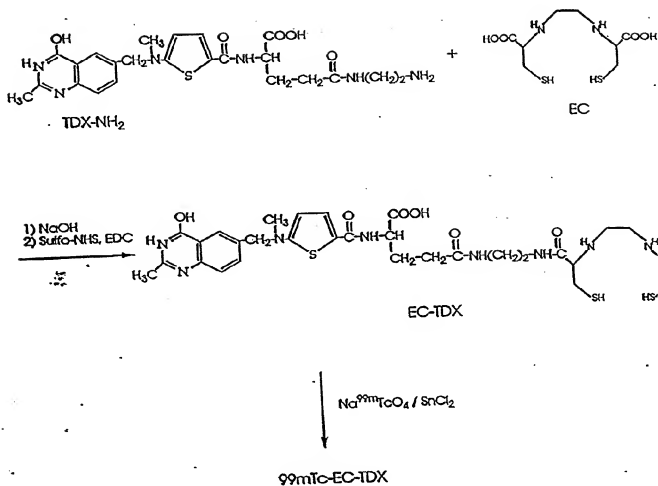


FIG. 3

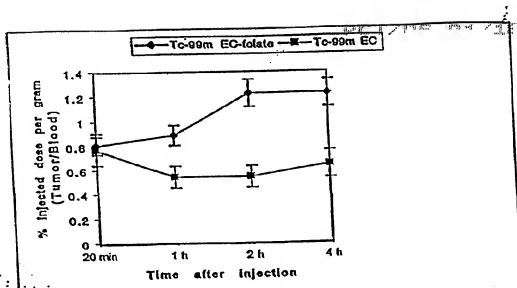


FIG. 4

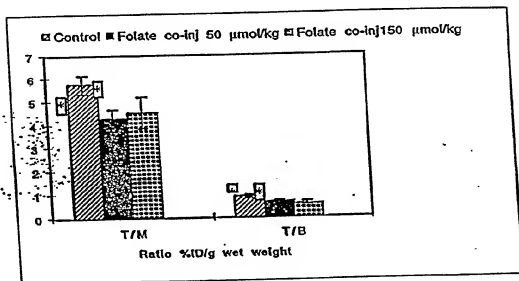


FIG. 5

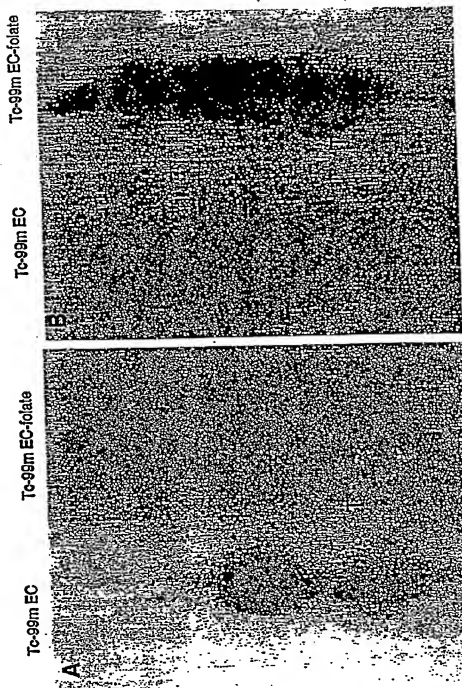


FIG. 6A

FIG. 6B

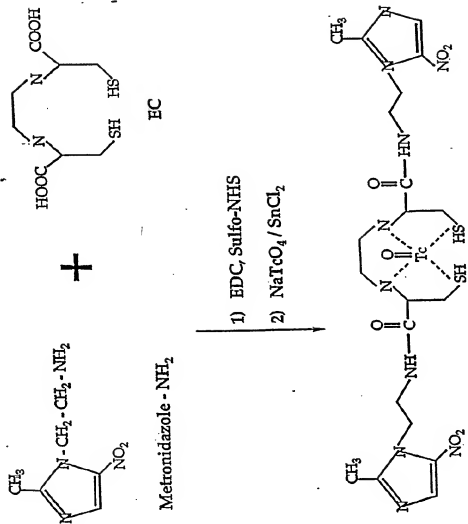


FIG. 7

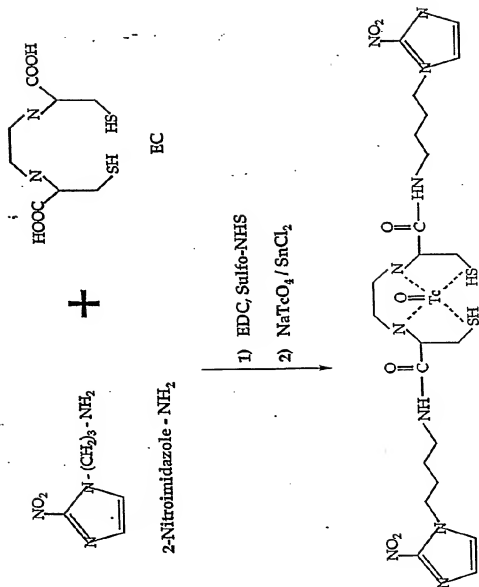
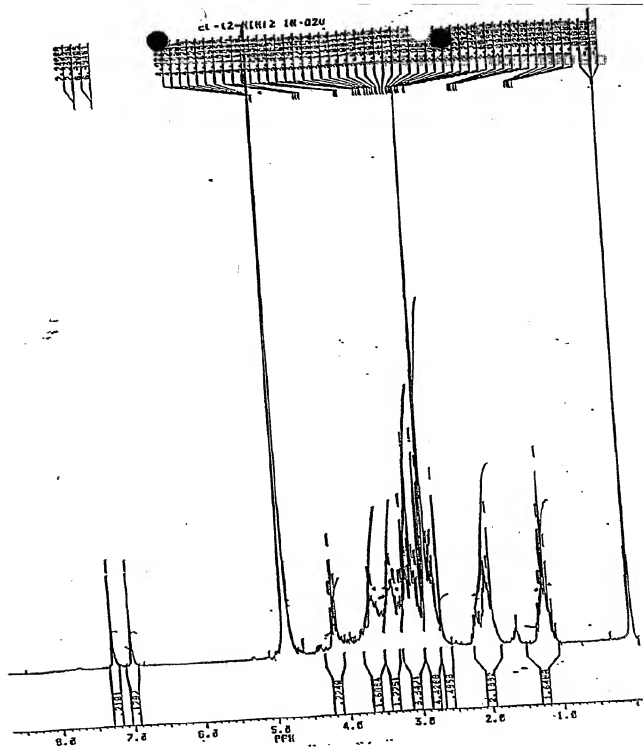


FIG. 8A



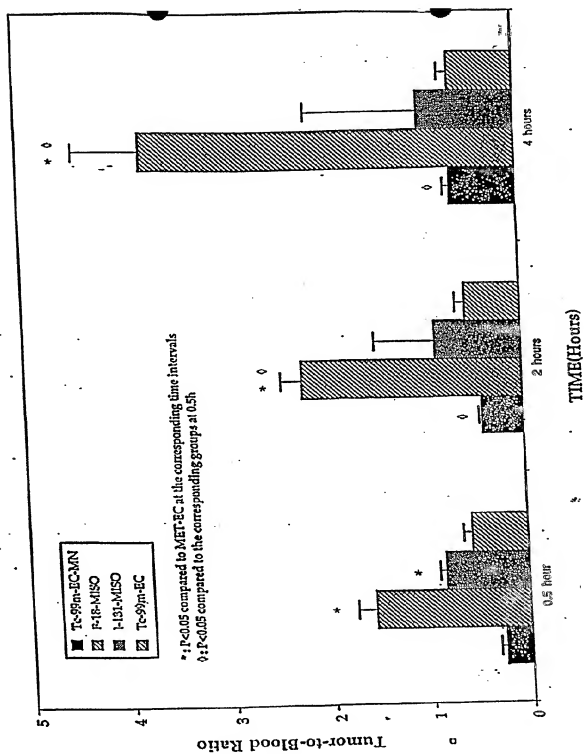


FIG. 9

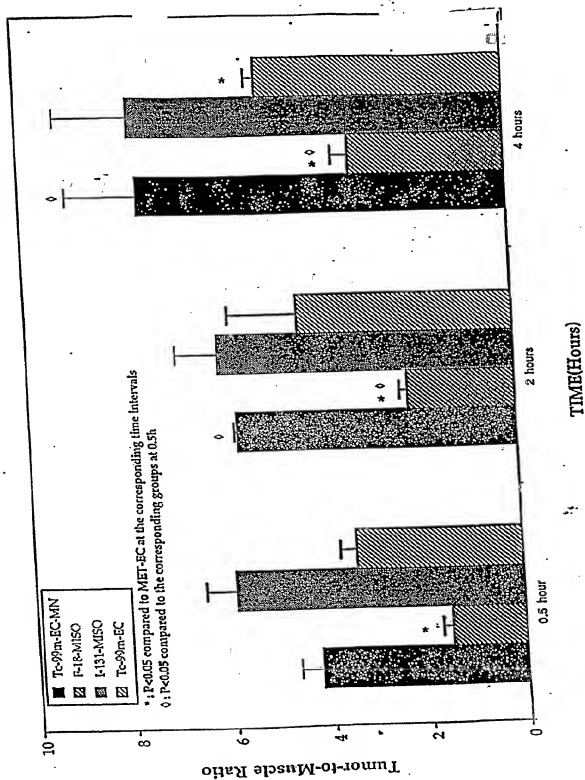


FIG. 10

FIG. 11A



FIG. 11B





FIG. 12

3-10-1999

Date: Mar 10 1999 Start time: 16:02
Data File:

Run time: 00:00:50
Plate: 1 Lane: 1

Elect Resolution: NORMAL

Stop counts: 50000

Stop Counts Region: 0.00 to 20.00 cm

Rf Calculations: Origin: 1.50 cm

Integration Parameters: Auto Integration

Peak slope: 1.0

Solvent Front: 19.00 cm

Min width: 0.1 Min %: 2.0

Total Count Region: 0.00cm to 20.00cm

Total Counts: 53170

Total CPM: 63810

Reg. #	Start (cm)	Stop (cm)	Center (cm)	Rf	Region Counts	Region CPM	% of Tot Reg	% Tot
1	0.60	4.40	2.50	0.06	4557	5468	9.02	8
2	8.20	16.80	12.56	0.63	45980	55180	90.98	86
TOTAL					50540	60650	100.00	95

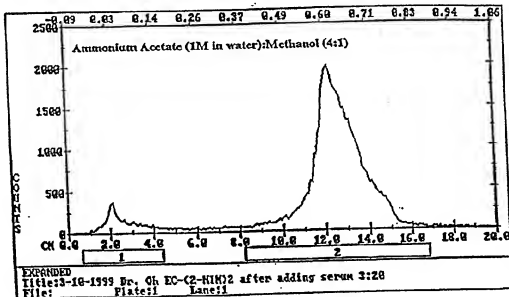


FIG. 13

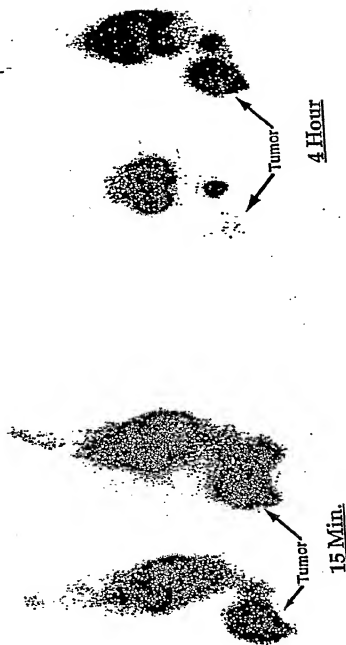
$^{99m}\text{Tc-EC-NIM}$ $^{99m}\text{Tc-EC}$ $^{99m}\text{Tc-EC-NIM}$ $^{99m}\text{Tc-EC}$ 

FIG. 14A

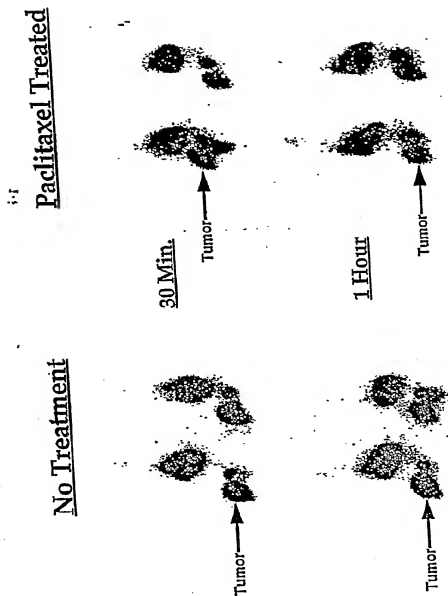


FIG. 14B

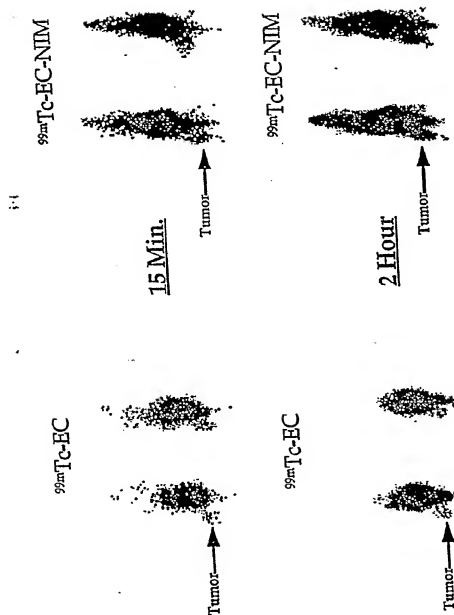


FIG. 15A

^{99m}Tc -EC-Nitroimidazole (NIM)
(100 μCi /mouse, iv.)

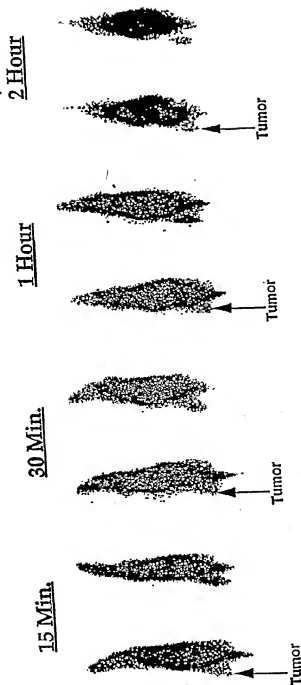


FIG. 15B

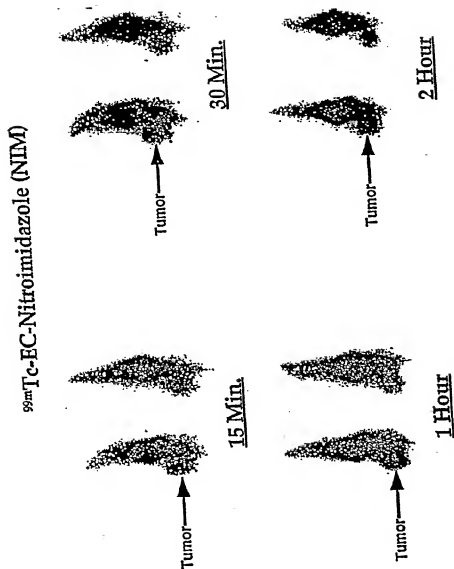


FIG. 15C

^{99m}Tc -EC-Nitroimidazole (NIM)
(100 μCi /mouse, iv.)

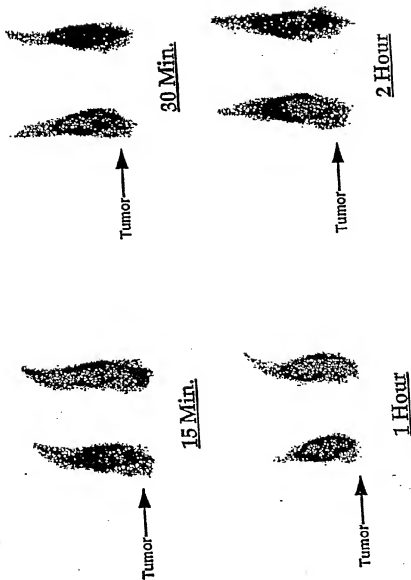
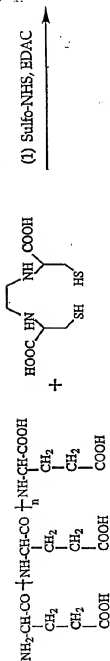
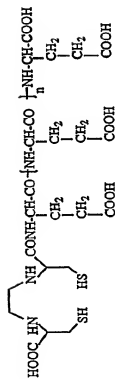


FIG. 15D



EC

L-GAP



EC-GAP

Synthesis of EC-GAP

FIG.
16

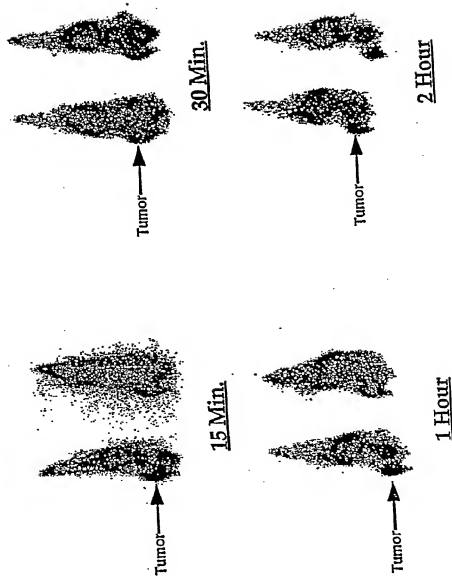


FIG. 17

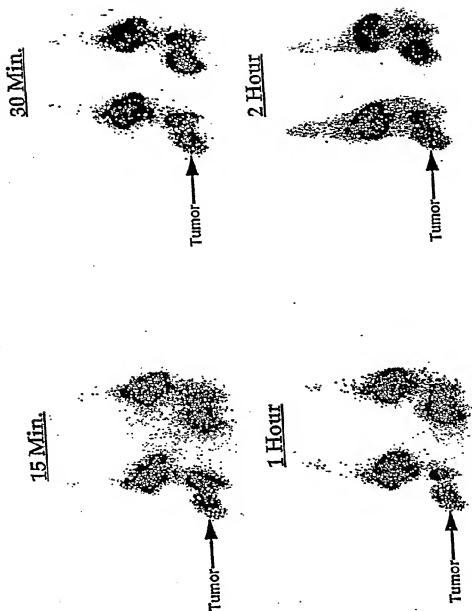


FIG. 18

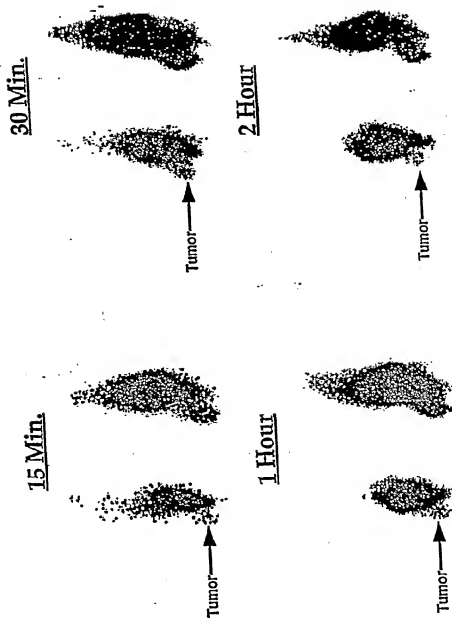


FIG. 19A

^{99m}Tc -EC-Annexin V
(100 μCi /mouse, iv.)

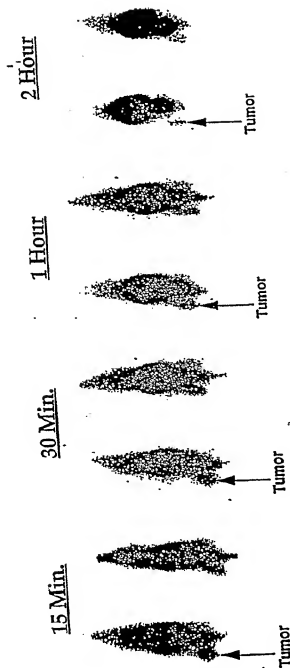


FIG. 19B

^{99m}Tc -EC-Annexin V30 Min. ^{99m}Tc -EC

Tumor→

 ^{99m}Tc -EC-Annexin V15 Min. ^{99m}Tc -EC

Tumor→

 ^{99m}Tc -EC-Annexin V2 Hour ^{99m}Tc -EC ^{99m}Tc -EC-Annexin V1 Hour ^{99m}Tc -EC

Tumor→



^{99m}Tc -EC-Annexin V
(100 μCi /mouse, iv.)

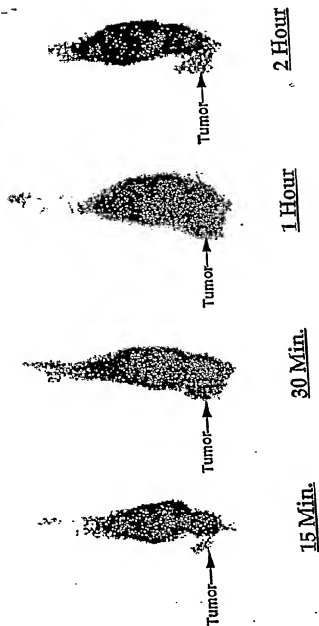


FIG. 20B

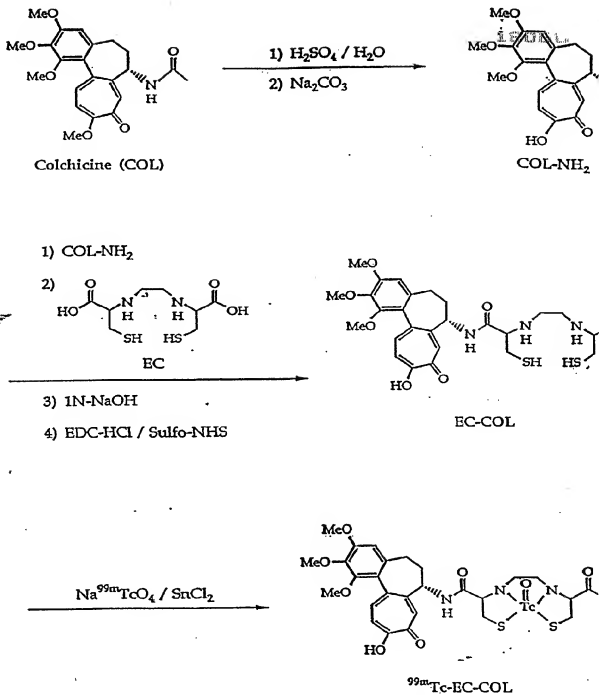


FIG. 21

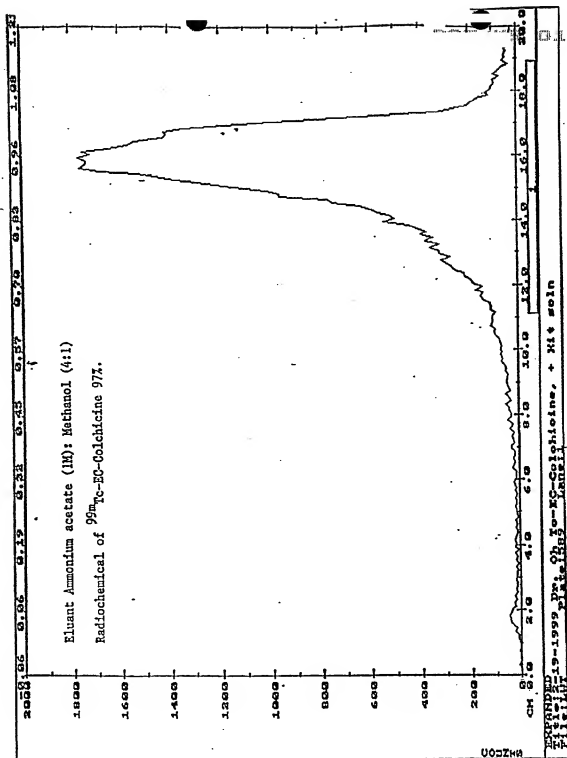


FIG. 22

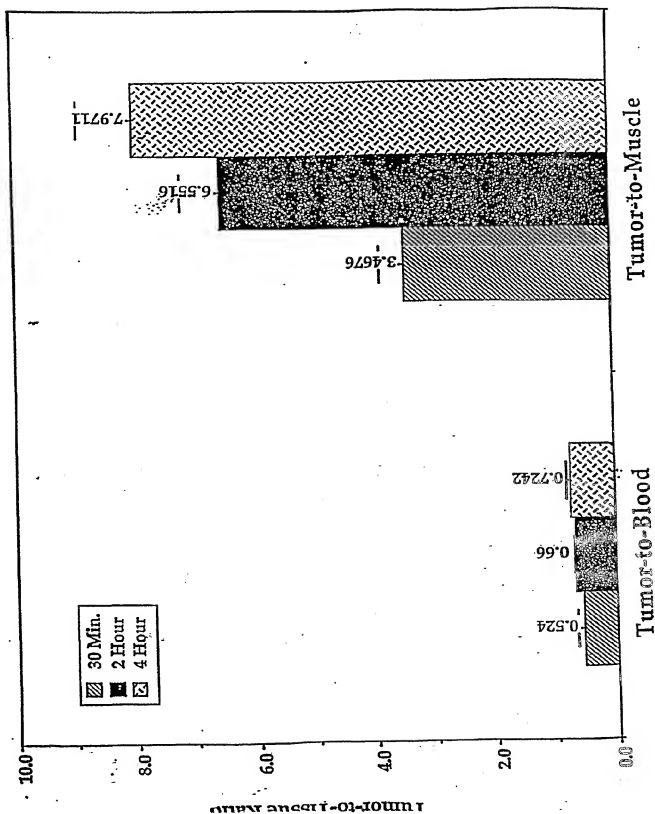


FIG. 23

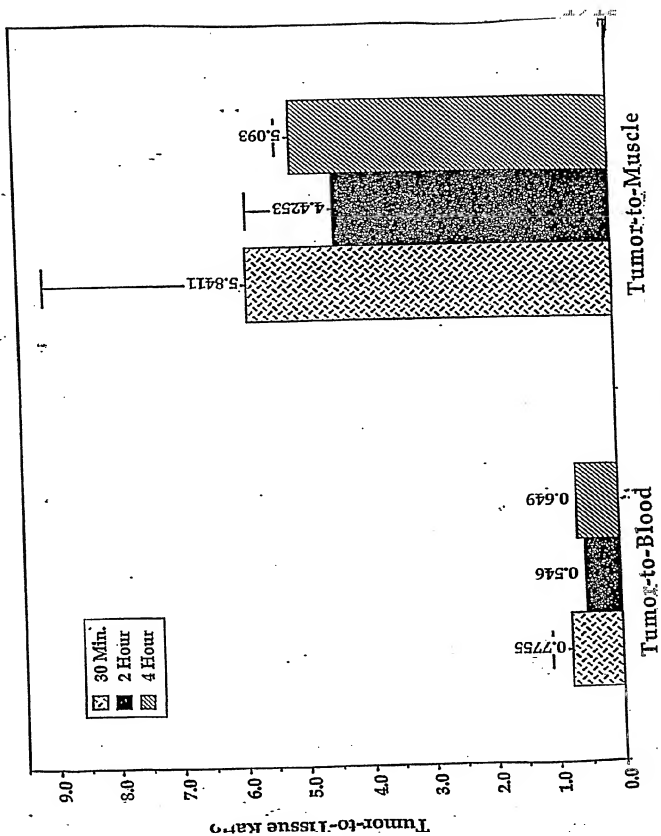


FIG. 24

^{99m}Tc-EC-Colchicine (1 Hour Postinjection)



FIG. 25

^{99m}Tc-EC (Control) (1 Hour Postinjection)

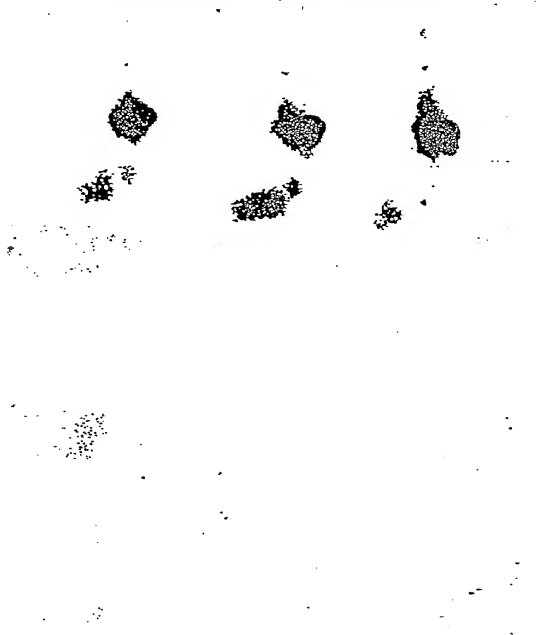
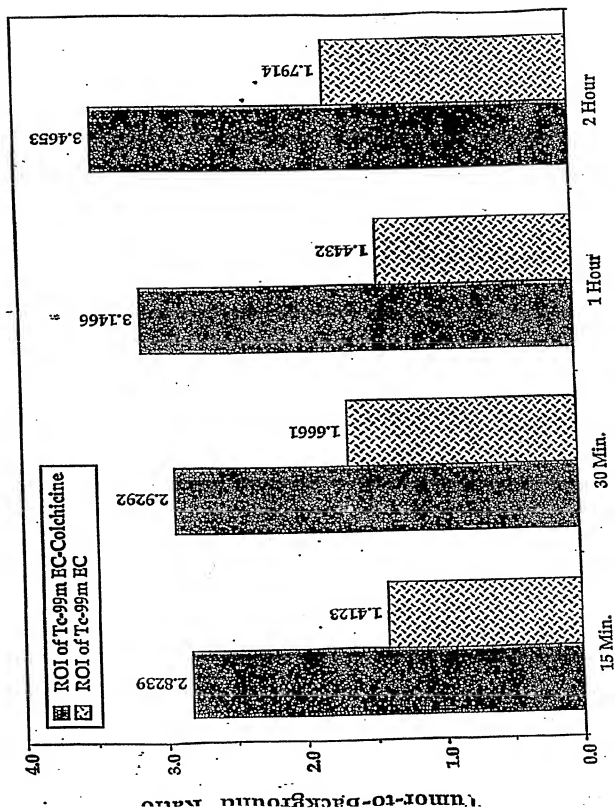


FIG. 26



Time

FIG. 27

FIG. 28

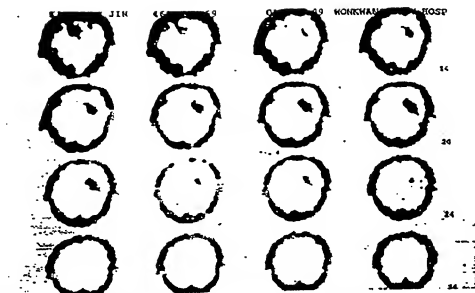


FIG. 29



FIG. 30

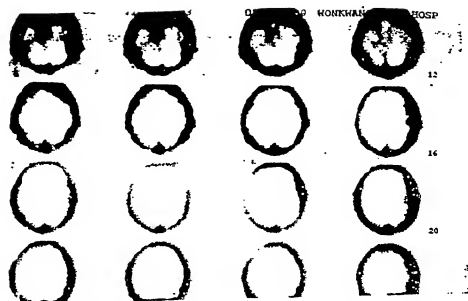


FIG. 31

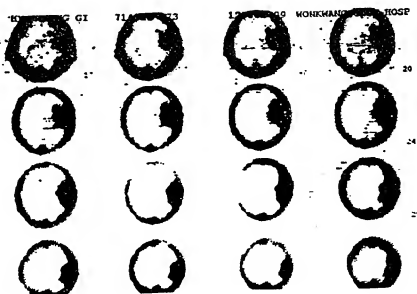




FIG. 32



FIG. 33

FIG. 34

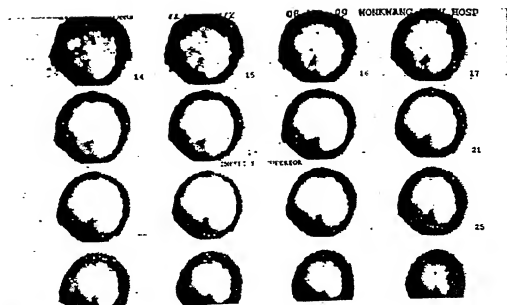


FIG. 35



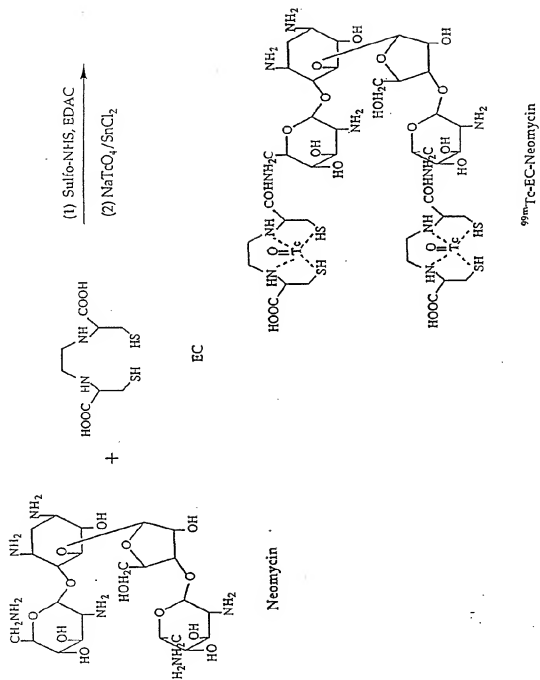
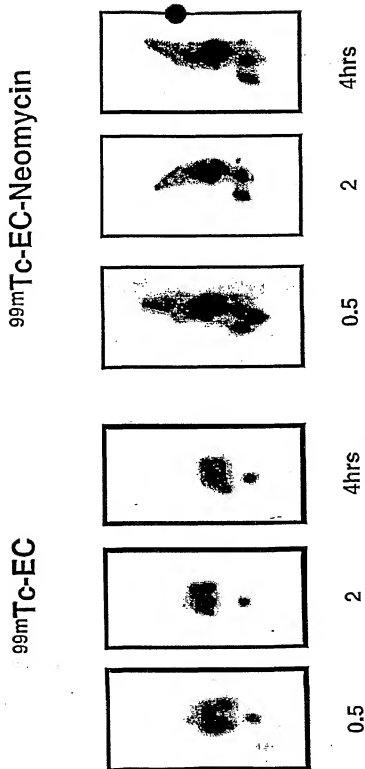


FIG. 36
Synthetic scheme of $^{99\text{m}}\text{Tc-EC-neomycin}$.



Planar image of breast tumor-bearing rats after administration of $^{99m}\text{Tc-EC}$ and $^{99m}\text{Tc-EC-Neomycin}$ (100 $\mu\text{Ci/rat}$, iv.) showed that the tumor could be well visualized from 0.5-4 hours postinjection.

Scintigraphic image of breast tumor-bearing rats after administration of $^{99m}\text{Tc-EC}$ and $^{99m}\text{Tc-EC-Neomycin}$ (100 $\mu\text{Ci/rat}$, iv.) showed that the tumor could be well visualized from

FIG. 37A

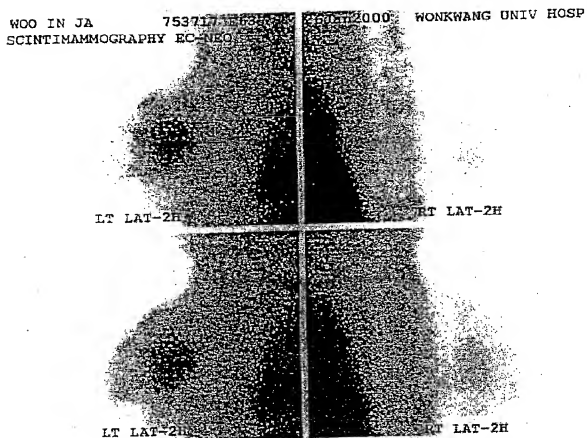


FIG. 37B

Scintimammography with ^{99m}Tc -EC-ncomycin (30 mCi, iv.) of a breast cancer patient. Images taken two hours post-injection.

EC

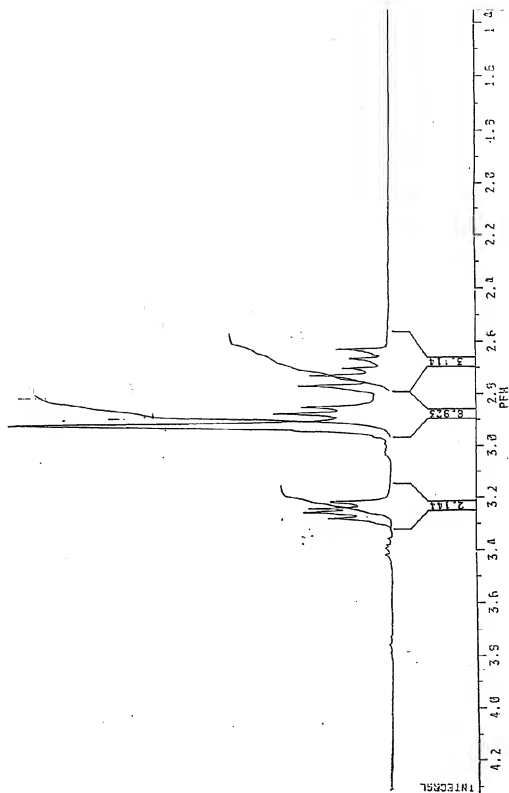
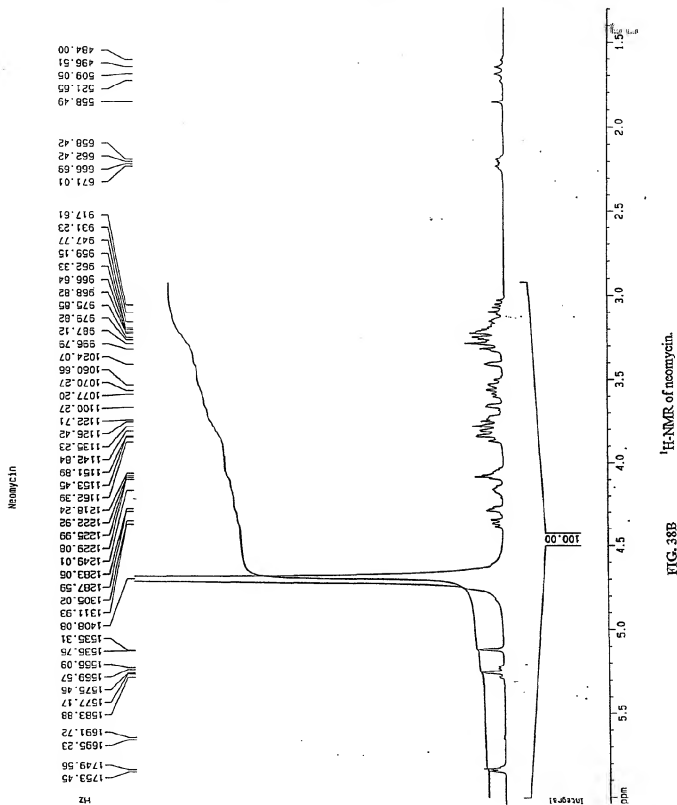
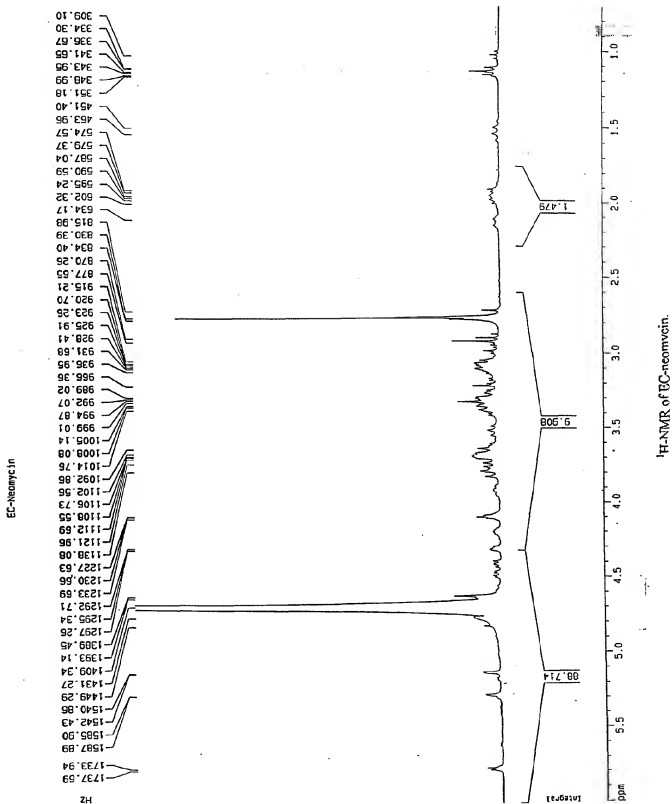
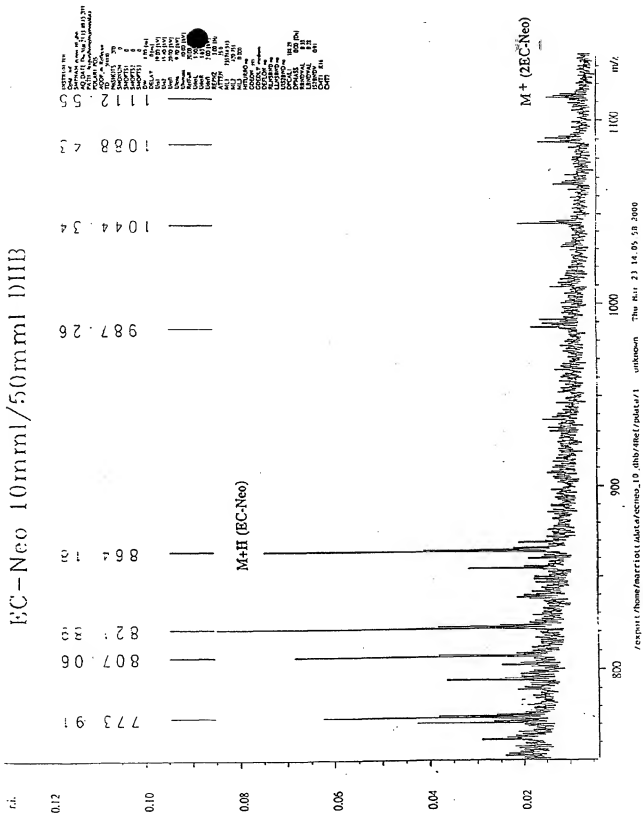
 ^1H -NMR of EC.

FIG. 38A







UV Wavelength Scan of EC

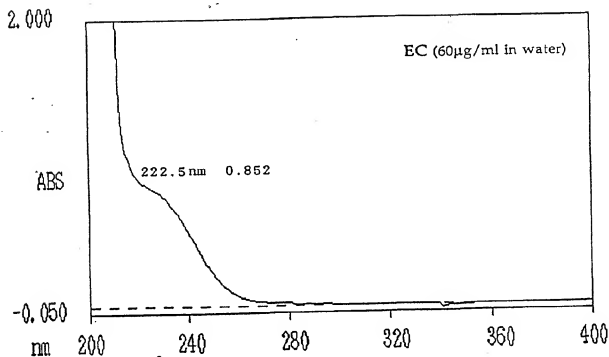


FIG. 40A

UV wavelength scan of EC.

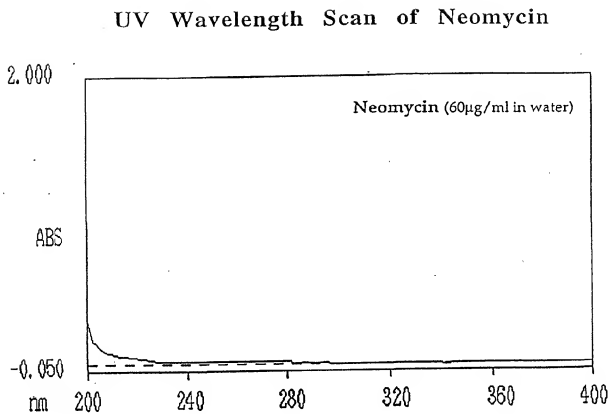


FIG. 40B

UV wavelength scan of neomycin.

UV Wavelength Scan of EC-Neomycin

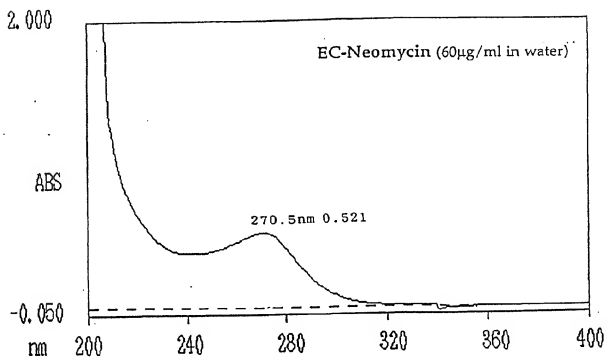


FIG. 40C

UV wavelength scan of EC-neomycin.

SUMMARY REPORT

EC-NEOMYCIN 30mg + EC

Tc-99m

METHANOL-AMMONIUM ACETATE

Date: Feb 03 2000

Start time: 12:45

Accum time: 00:03:01

Data File:

Plate: 1 Lane: 1

Elect Resolution: NORMAL

(Amp. Range: 0 - 2047)

Rf Calculations: Origin: 0.00 cm

Solvent Front: 20.00 cm

Integration Parameters: Auto Integration

Peak slope: 1.0

Min width: 0.1

Min %: 2.0

Total Count Region: 0.00cm to 20.00cm

Total Counts: 48360

Total CPM: 16030

Reg. #	Start (cm)	Stop (cm)	Center (cm)	Rf	Region Counts	Region CPM	% of Tot Reg	% of Tot Cnt
1	6.50	14.90	10.57	0.53	45000	14920	100.00	93.05
TOTAL					45000	14920	100.00	93.05

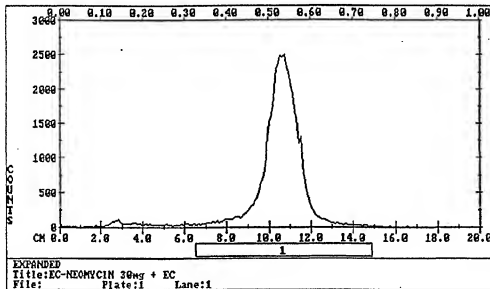


FIG. 41

Radio-TLC analysis of ^{99m}Tc -EC-neomycin.

^{99m}Tc-EC-NEO

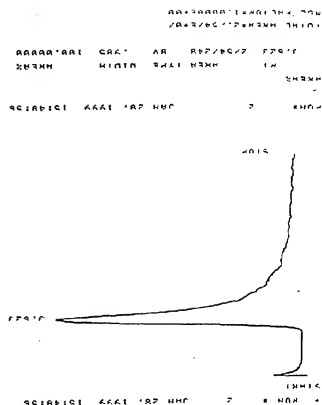
Column: Bio-Rad Carbohydrate, Aminex HPX-87C, 250x4mm

Eluent: H₂O

Flow Rate: 0.4ml/min

Detector: Radiochemical

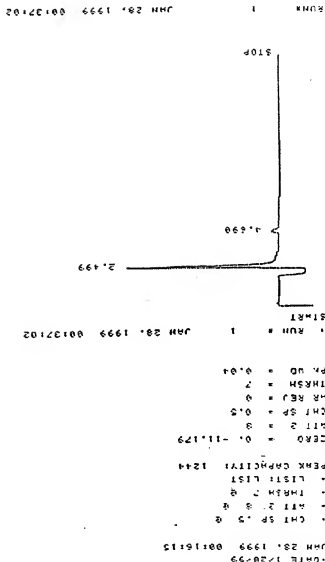
Temp: 85.0°C

HPLC analysis of ^{99m}Tc-EC-neomycin (radioactive detector).

UTC 40

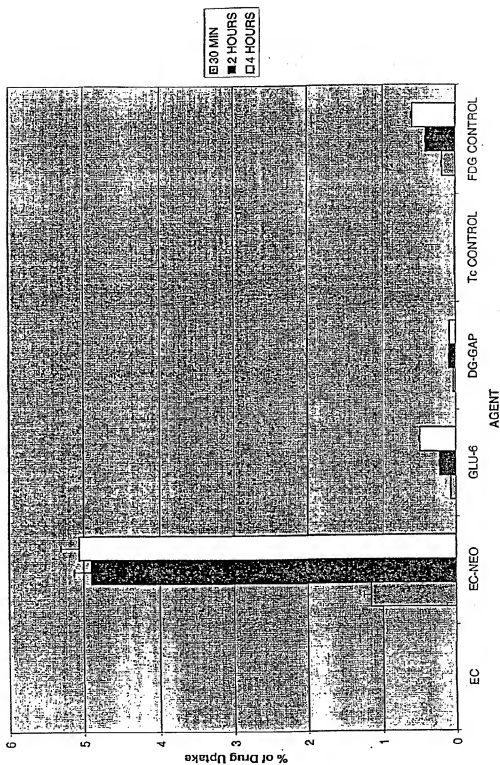
Column: Bio-Rad Carbohydrate,
Aminex HPX-87C, 250x4mm
Eluent: H₂O
Flow Rate: 0.4ml/min
Detector: UV, 254nm
Temp: 85.0°C

¹⁸F-FDG



HPLC analysis of ¹⁸F-FDG (UV 254 nm).

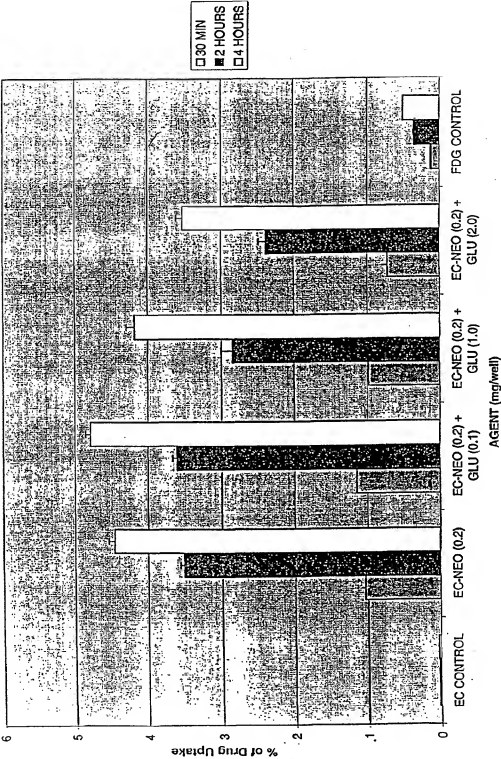
% of Drug Uptake in Lung Cancer Cell Line (A549)



In vitro cellular uptake assay of a series of ^{99m}Tc -EC-drug conjugates in lung cancer cell line. ^{99m}Tc -EC-neomycin showed

FIG. 46

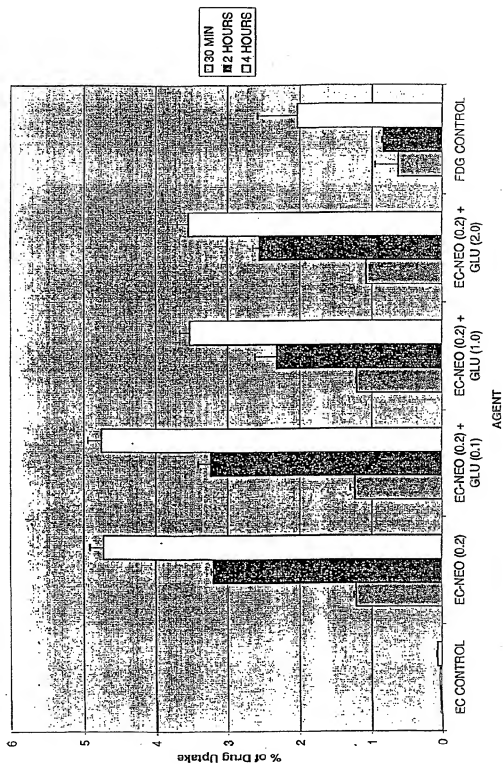
% of Drug Uptake in Human Lung Cancer Cell Line (A549)



Effect of glucose on cellular (A549) uptake of ^{18}F -EC- neomycin and ^{18}F -FDG.

FIG. 47

% of Drug Uptake in Human Lung Cancer Cell Line (H1299)

Effect of glucose on cellular (H1299) uptake of ^{67}Ga -Tc-EC-

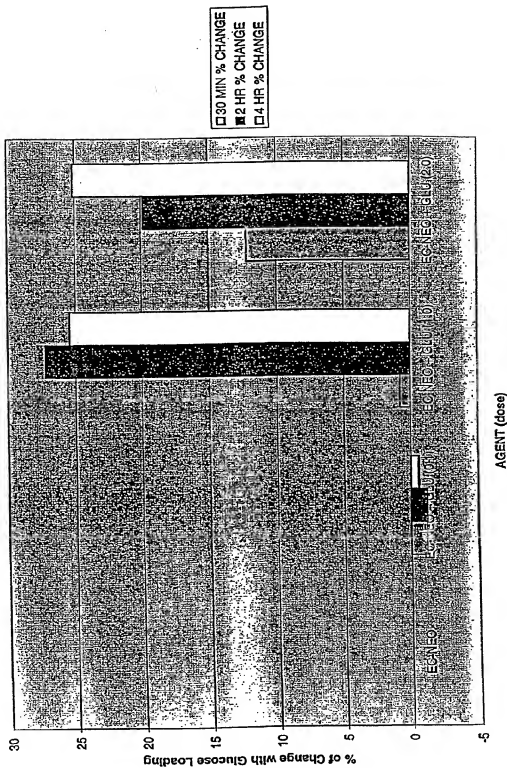
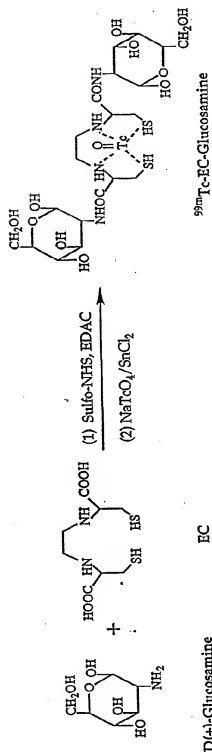
Effects of Glucose Loading on ^{99m}Tc -EC-Neomycin in Human Lung Cancer Cell Line (H1299)

FIG. 48B

FIG. 49
Synthesis of ^{99m}Tc -EC-Glucosamine

Hexokinase Assay of Glucose

WAVELENGTH SCAN/0

03/01/00 14:41

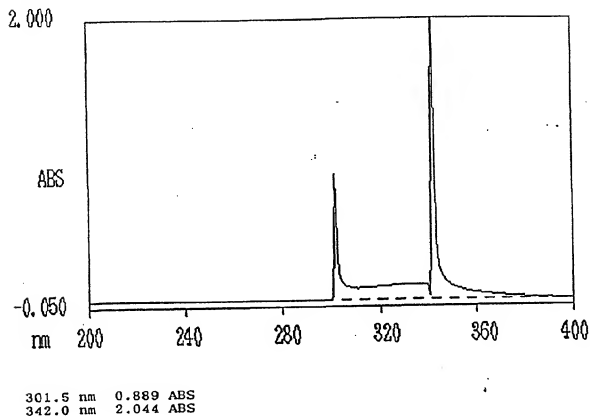


FIG. 50

Hexokinase Assay of Glucosamine

WAVELENGTH SCAN/0

03/01/00 14:50

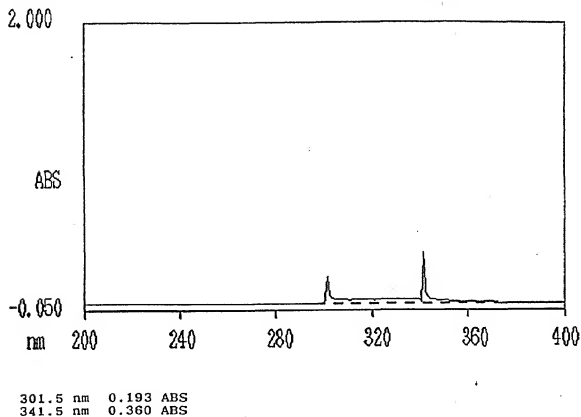


FIG. 51

Hexokinase Assay of EC-Glucosamine

WAVELENGTH SCAN/0

03/01/00 14:45

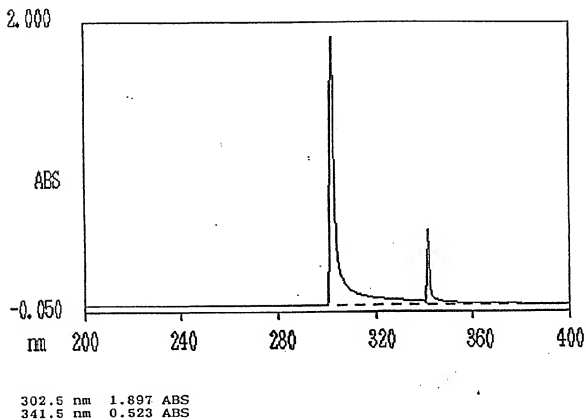
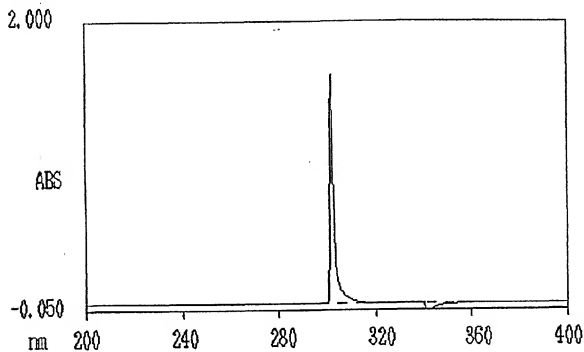


FIG. 52

Hexokinase Assay of EC-GAP-Glucosamine

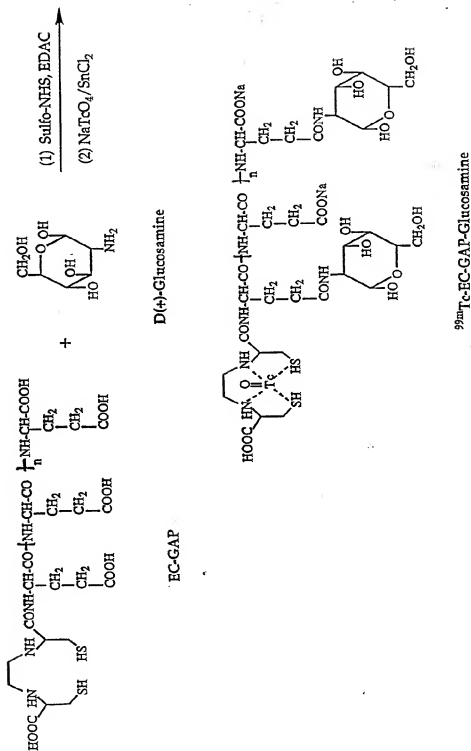
WAVELENGTH SCAN/0

03/01/00 15:37



302.0 nm 1.620 ABS

FIG. 53

FIG. 54 Synthesis of ^{99m}Tc-EC-GAP-Glucosamine

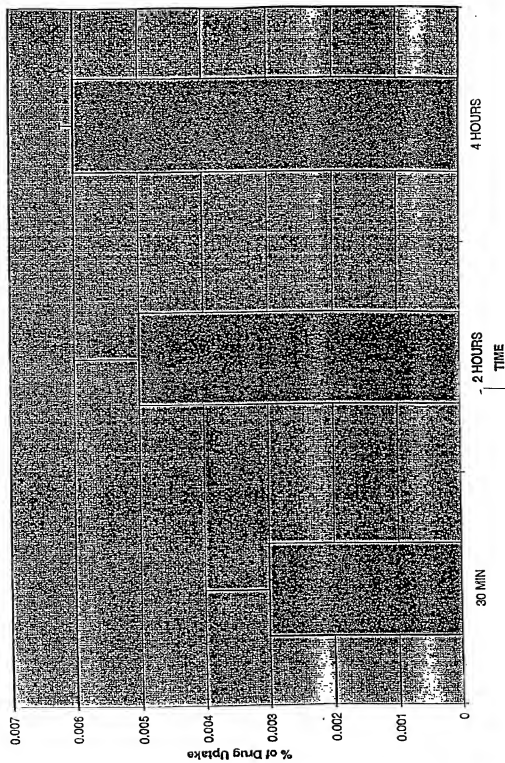
In Vitro Cellular Uptake of ^{56m}Co -EC in Human Lung Cancer Cell Line (A549)

FIG. 55A

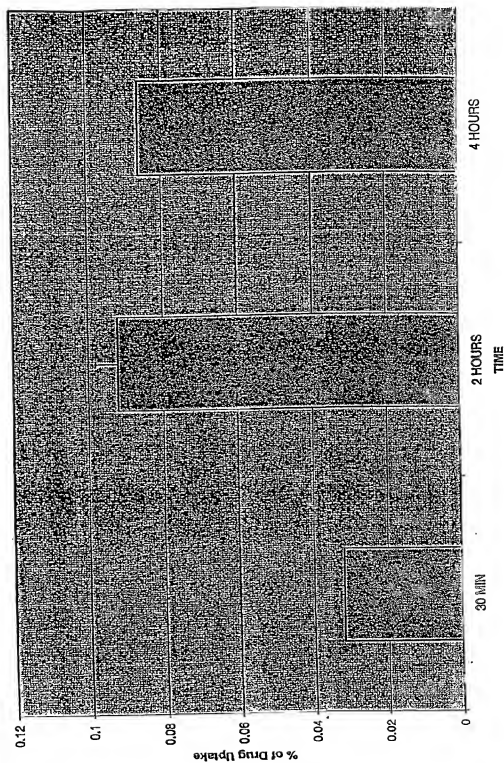
In Vitro Cellular Uptake of ^{89m}Tc -EC-DG-GAP in Human Lung Cancer Cell Line (A549)

FIG. 55B

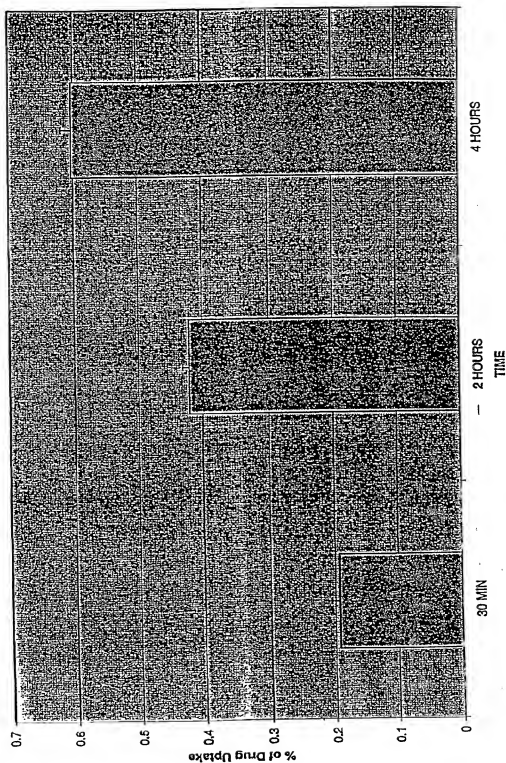
In Vitro Cellular Uptake of ^{18}F FDG in Human Lung Cancer Cell Line (A549)

FIG. 55C

Tumor-to-tissue count density ratios of ^{99m}Tc -EC-GAP in breast tumor-bearing rats
(n=3/interval; 10 μCi /rat, IV)

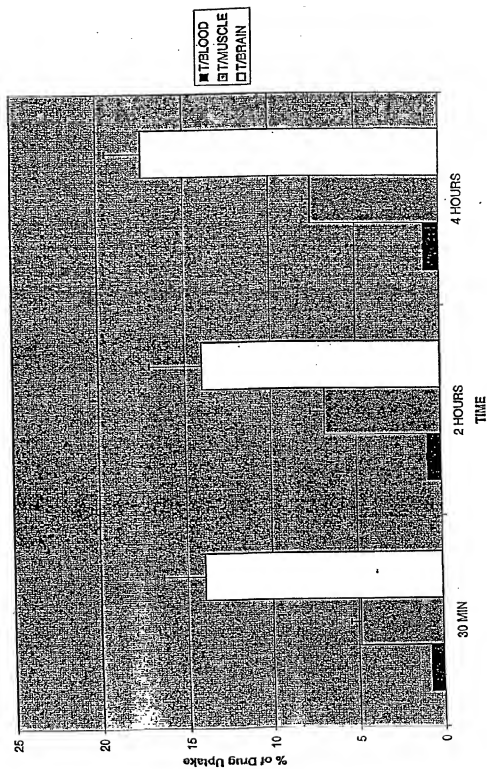


FIG. 56

In Vitro Cellular Uptake of ^{18}F FDG with Glucose Loading at 2 Hours Post-Injection in Breast Cancer Cell Line (13762)

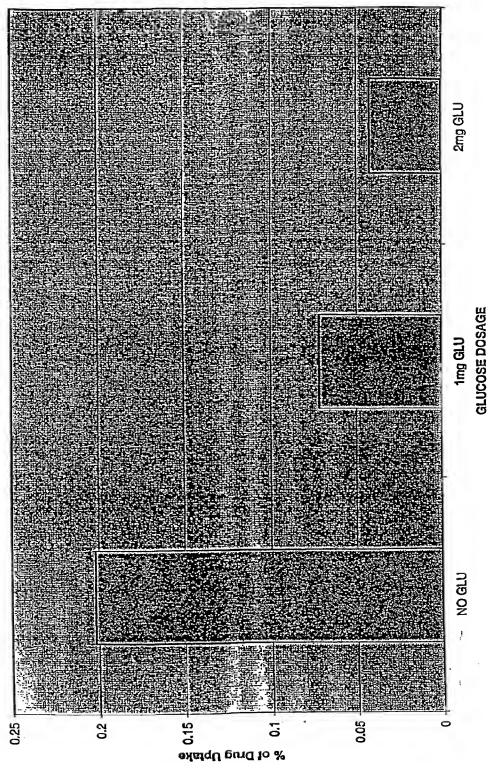


FIG. 57

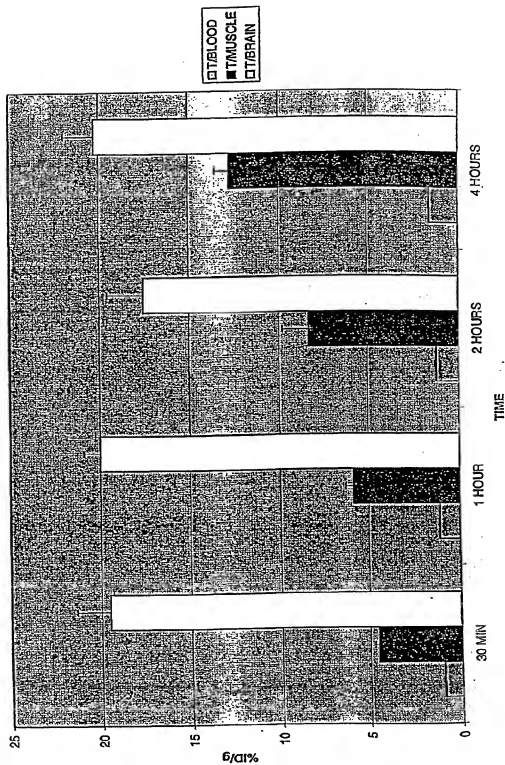
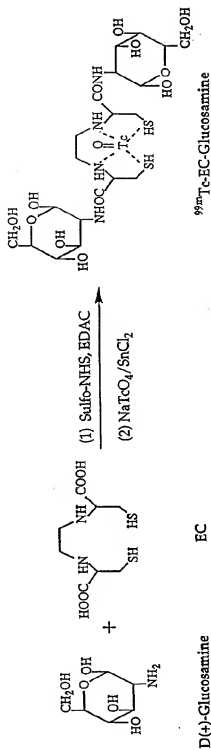
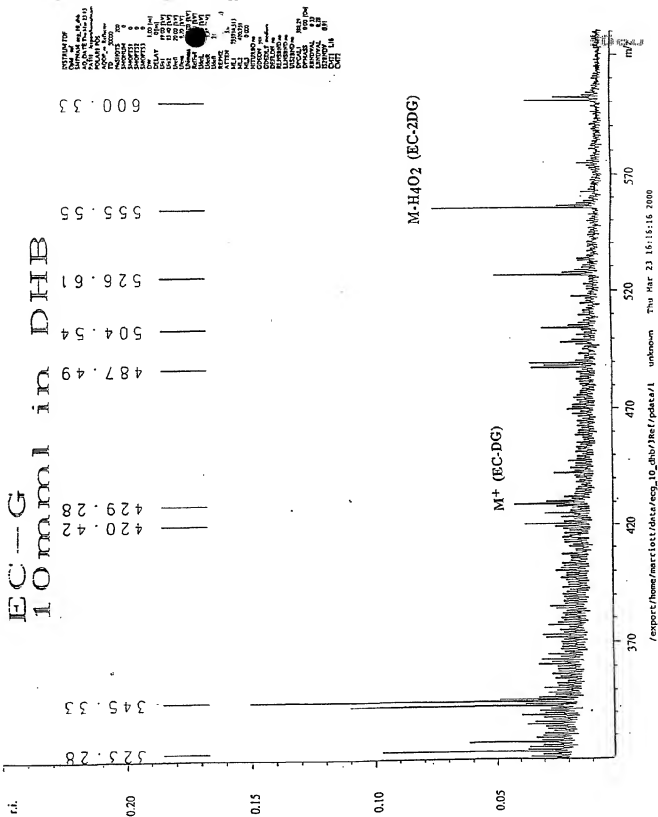
% Uptake of ^{99m}Tc -EC-Neomycin in Breast Tumor-Bearing Rats

FIG. 58

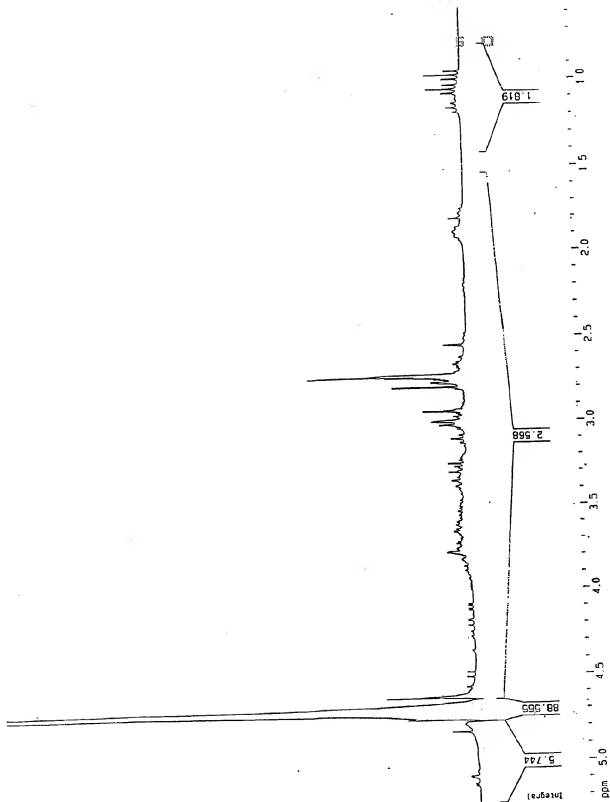


Synthetic scheme of $^{99\text{m}}\text{Tc-EC-d-oxxyglucose}$.

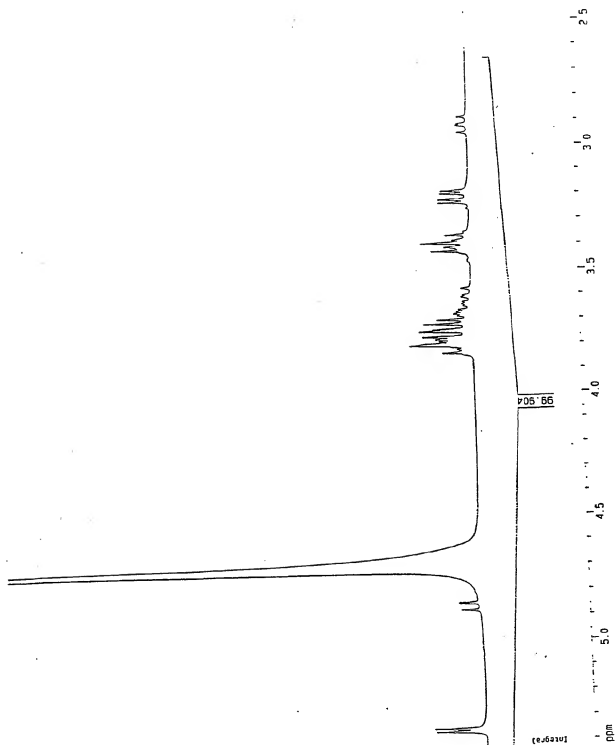
FIG. S9



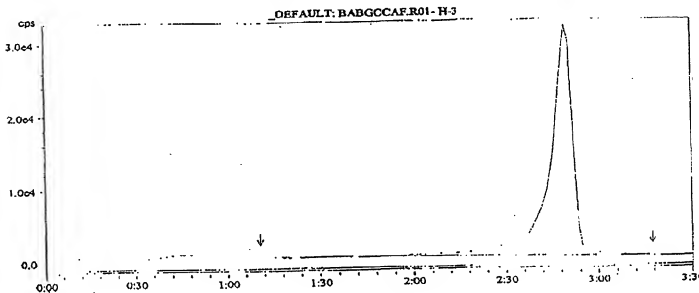
90-33



Glucosamine



0653528488 0653528488 17137453372 PAGE: 01
 04-03 10:55 MON FROM: MON KJ HOSP
 Method: DEFAULT File: BABGCCAF.R01 Raw data User: EC-Glucosemi (72-EC-56-01-18060)



Regions: BABGCCAF.R01

Channel: H-3		Detector:					
Name	Start	End	RT	Height (cps)	Area (Counts)	%Total (%)	%ROI (%)
Bkg 1	0: 00-	2: 19	1: 09	539.7			
Rgn 1	2: 19-	3: 02	2: 47	31608.2	263570.8	97.99	100.00
Bkg 2	3: 02-	3: 27	3: 14	250.1			
1 Peak					263570.8	97.99	100.00
Total Area	= 268986.1 Counts						
Bkg Area	= 89999.9 Counts						
Unallocated	= 5415.3 Counts (2.01%)						

Trace Parameters: BABGCCAF.R01-H-3

Trace Display Smoothing: 0.0 s
 Trace Display Shift: 0.0 s
 Trace Display Factor: 1.000
 Channel Shift: 0.0 s
 Channel Factor: 1.000

Regions were added manually.

FIG. 63

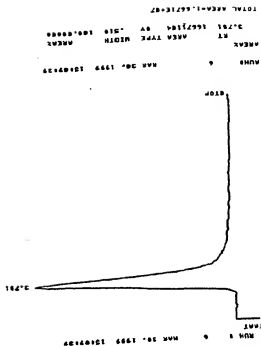
Radio-TLC analysis of ^{99m}Tc -EC-DG.

^{99m}Tc -EC-deoxyglucose

5.00 x 10⁴ cps
4 ml/min. H₂O at
95°C
Radioactive 5cm
EC-Deoxy-Glucose
TC-99m

Radioactive 5cm

EC-TC-99m



5.00 x 10⁴ cps
4 ml/min. H₂O at
95°C
Radioactive 5cm
EC-Deoxy-Glucose
TC-99m

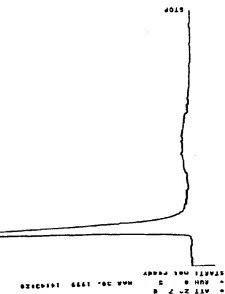


FIG. 64
HPLC analysis of ^{99m}Tc -EC-deoxyglucose and ^{99m}Tc -EC-
(radioactive detector)

FIG. 65

HPIC analysis of ^{99m}Tc -EC-deoxyglucose and ^{99m}Tc -EC
(radioactive detector, mixed).

• ATT 2• BREAK

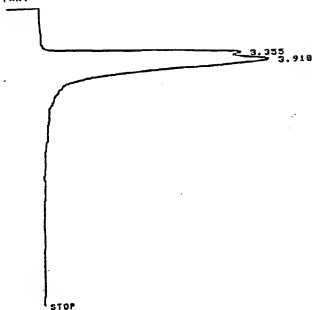
•
BREAK

• LIST: ATT 2• = 7

• ATT 2• 8 8

• RUN 1 7 MAR 30, 1999 15:32:37

START



Radioactive Scan

Mixed Tc-^{99m}
EC-Deoxy-Glucose
EC

^{99m}Tc -EC-deoxyglucose + ^{99m}Tc -EC
(mixed)

RUN# 7 MAR 30, 1999 15:32:37

AREA#	RT	AREA TYPE	WIDTH	AREA%
1	3.355	22173760	BY .440	58.46186
2	3.918	21767872	VV .307	49.53814

TOTAL AREA=4.3942E+07
MUL FACTOR=1.0000E+00

Hexokinase Assay of Glucose

WAVELENGTH SCAN/0

03/01/00 14:41

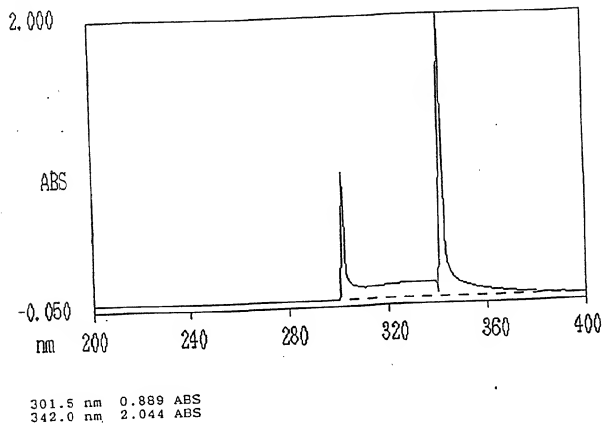


FIG. 66 Hexokinase assay of glucose.

Hexokinase Assay of FDG

WAVELENGTH SCAN/0

03/09/00 14:34

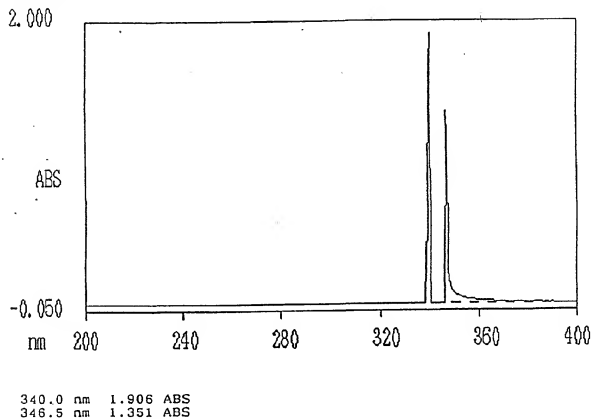


FIG. 67

Hexokinase assay of FDG.

Hexokinase Assay of EC-Glucosamine (EC-DG)

WAVELENGTH SCAN/0

03/01/00 14:45

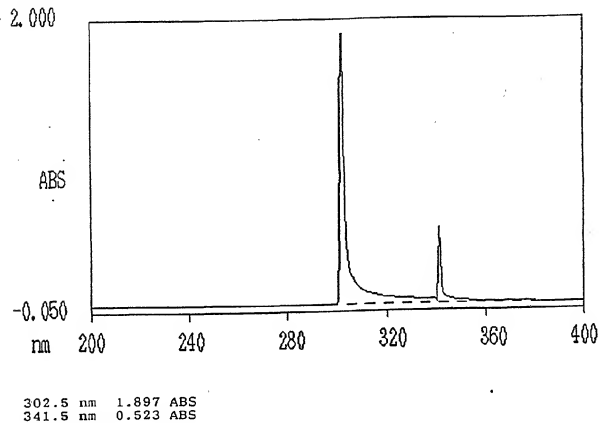


FIG. 68

Hexokinase assay of EC-DG.

% of Drug Uptake in Lung Cancer Cell Line (A549)

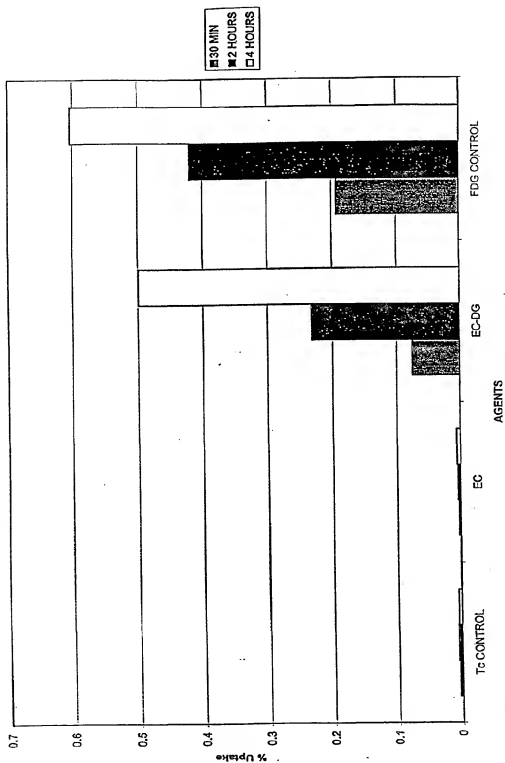
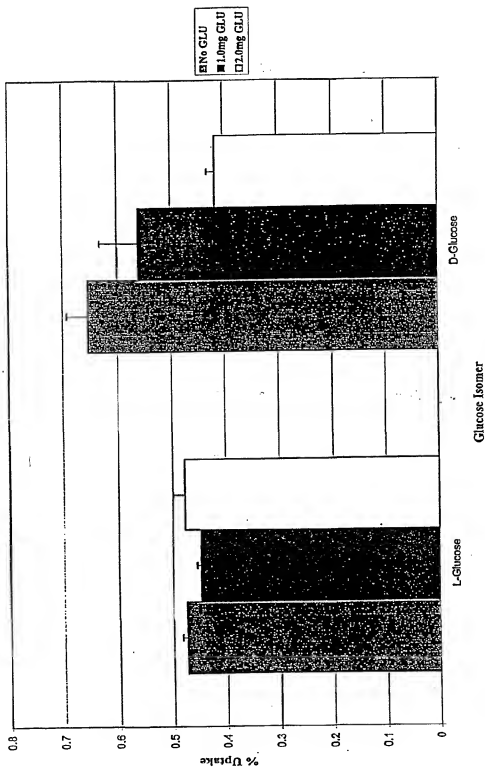


FIG. 69 In vitro cellular uptake assay of ^{99m}Tc -EC-deoxyglucose, ^{99m}Tc -EC and ^{18}F -FDG in lung cancer cell line (A549). ^{99m}Tc -EC-DG

In Vitro Cellular Uptake of ^{99m}Tc -EC-DG in Breast Cancer Cells after Glucose Loading (2 hours
Incubation; 2×10^5 cells/well; 50,000 cells/well; 0.5mL/well)



Effect of d- and l-glucose on breast cellular (13762 cell line) uptake
of ^{99m}Tc -EC-DG.

FIG. 70

In Vitro Cellular Uptake of ^{18}F FDG in Breast Cancer Cells after Glucose Loading (2 hours incubation; $2\mu\text{Ci}/\text{well}$; 50,000 cells/well; $5\text{mL}/\text{well}$)

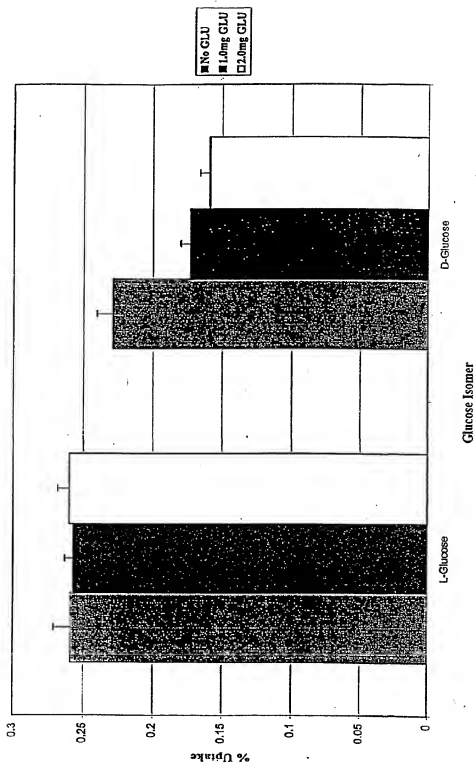


FIG. 71 Effect of d- and l-glucose on breast cellular (13762 cell line)

In Vitro Cellular Uptake of ^{18}F FDG in Lung Cancer Cells after Glucose Loading (2 hours incubation;
 2×10^5 cells/well; 50,000 cells/well; 5mL/well)

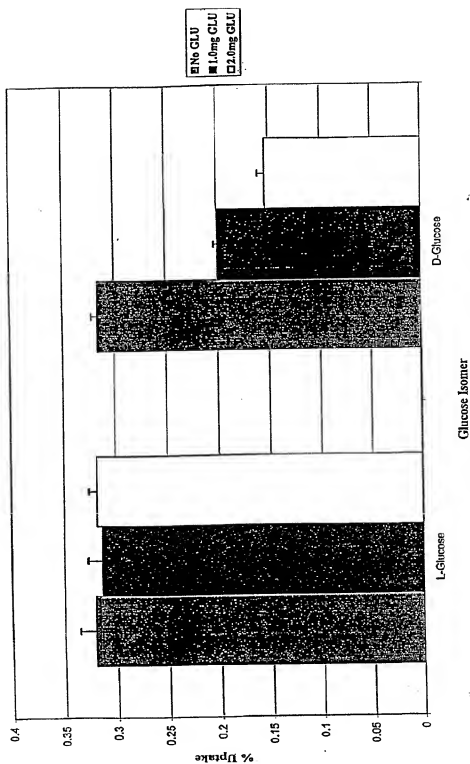
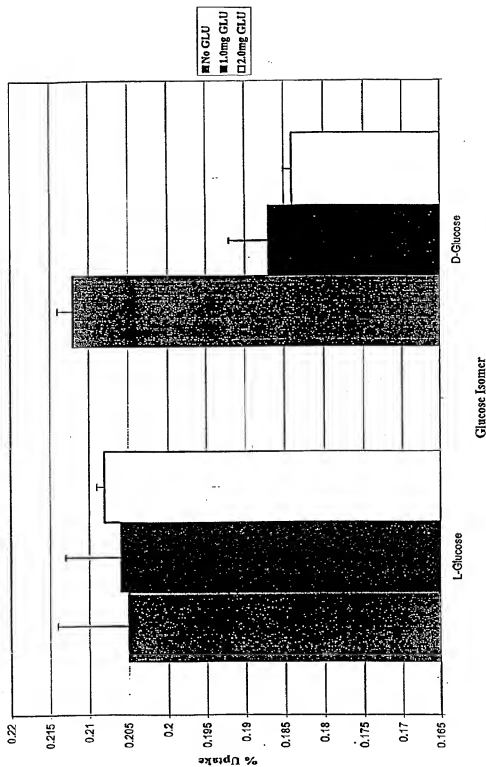


FIG. 72 Effect of d- and l-glucose on lung cancer (A549 cell line) uptake of

FIG. 72

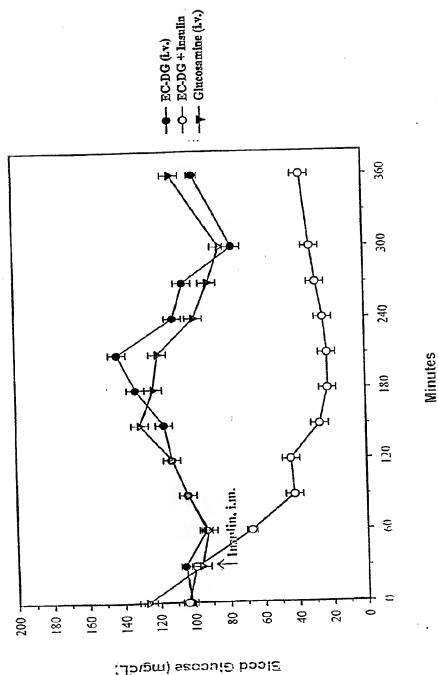
In Vitro Cellular Uptake of ^{99m}Tc -EC-DG in Lung Cancer Cells after Glucose Loading (2 hours incubation; $2\mu\text{Ci}/\text{well}$; 50,000 cells/well; $0.5\text{mL}/\text{well}$)



Effect of d- and l-glucose on breast cellular (AS49 cell line) uptake

FIG. 73

Effect of Intravenous Injection of Glucosamine and EC-DG on Blood Glucose Level in Rats



Effect of *in vivo* blood glucose level induced by glucosamine and

FIG. 74

Effect of Intravenous Injection of FDG and Insulin on Blood Glucose Level in Rats

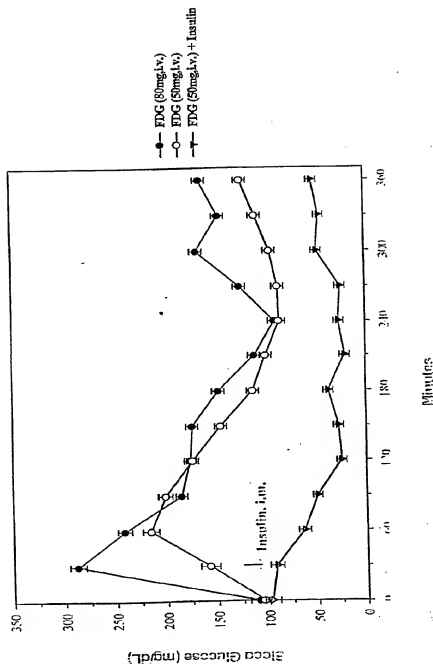
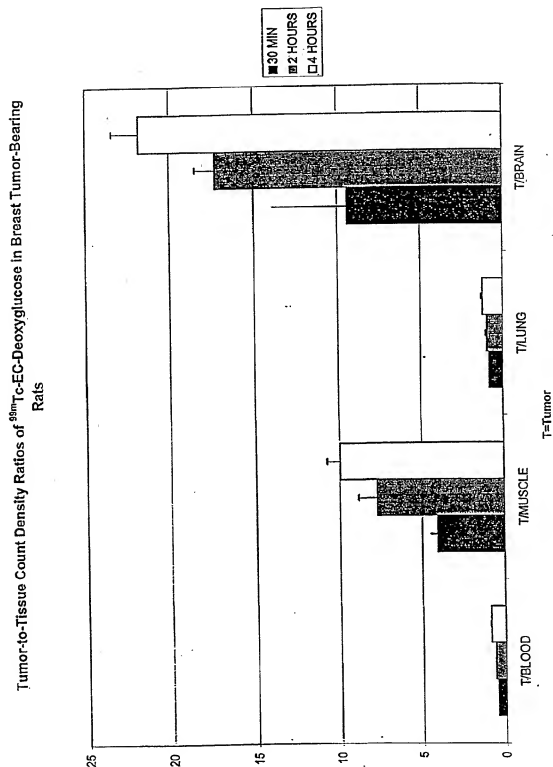


FIG. 75 Effect of *in vivo* blood glucose level induced by FDG (1.2 and 1.9

FIG. 76 Tumor-to-tissue count density ratios of ^{99m}Tc -EC-deoxyglucose in

In Vivo Uptake of ^{99m}Tc -EC-Deoxyglucose in Breast Tumor-Bearing Rats

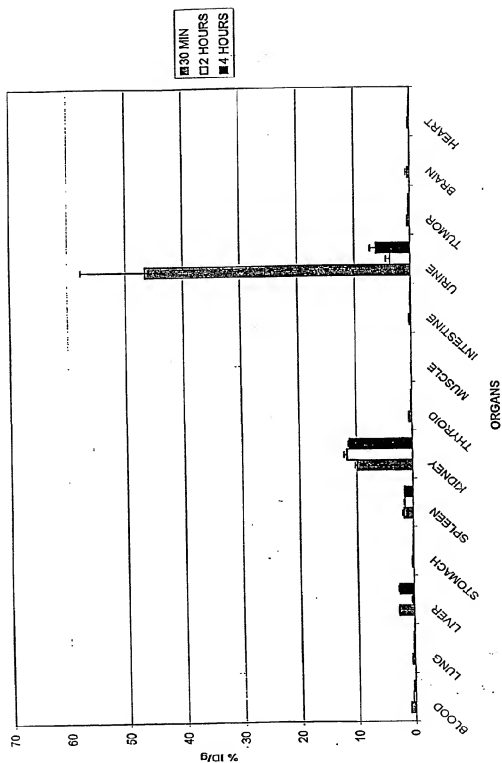


FIG. 77 In vivo biodistribution of ^{99m}Tc -EC-deoxyglucose in breast tumor-

In Vivo Uptake of ^{99m}Tc -EC-Deoxyglucose in Lung Tumor-Bearing Nude Mice

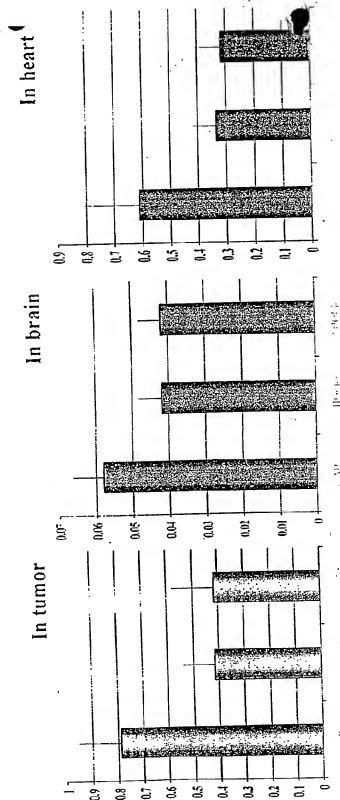


FIG. 78 In vivo tissue uptake of ^{99m}Tc -EC-deoxyglucose in lung tumor-bearing mice.

In Vivo Uptake of ^{99m}Tc -EC-Neomycin in Lung Tumor-Bearing Nude Mice

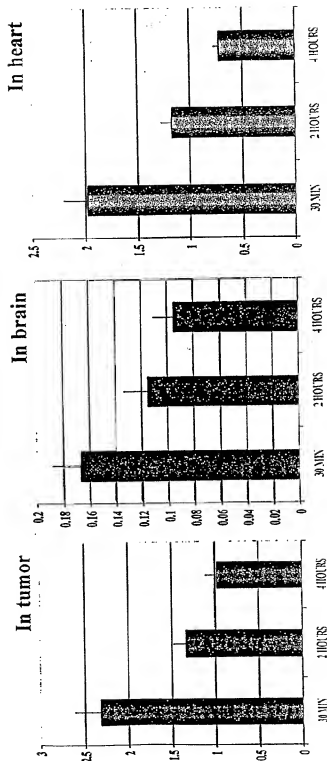


FIG. 79 In vivo tissue uptake of ^{99m}Tc -EC-neomycin in lung tumor-bearing mice.

In Vivo Uptake of ^{18}F FDG in Lung Tumor-Bearing Nude Mice

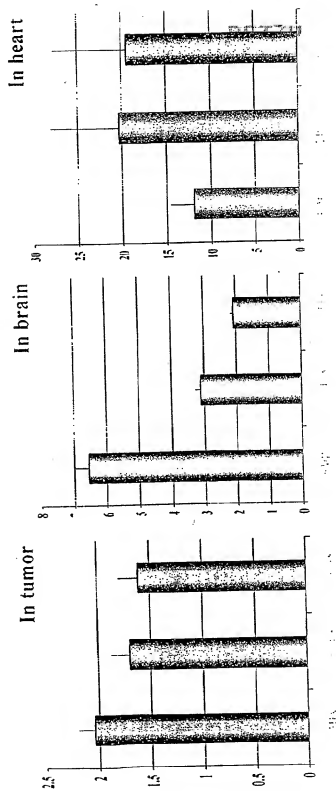
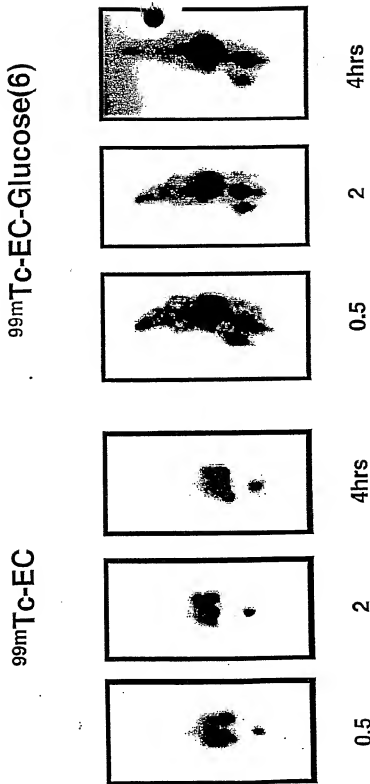


FIG. 80 In vivo tissue uptake of ^{18}F FDG in lung tumor-bearing mice.

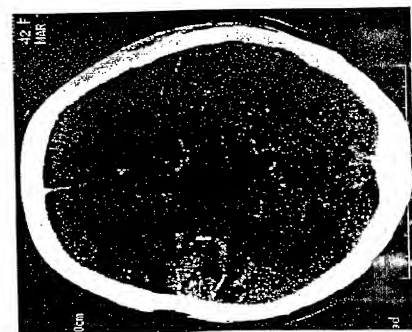


Planar image of breast tumor-bearing rats after administration of $^{99m}\text{Tc-EC}$ and $^{99m}\text{Tc-EC-Glucose(6)}$ ($100\mu\text{Ci/rat, iv.}$) showed that the tumor could be well visualized from 0.5-4 hours postinjection.

FIG. 81 Planar image of breast tumor-bearing rats after administration of $^{99m}\text{Tc-EC}$ and $^{99m}\text{Tc-EC-4-deoxyglucose}$ ($100\mu\text{Ci/rat, iv.}$) showed

Case 11/42

Dx : anaplastic astrocytoma



Pre OP



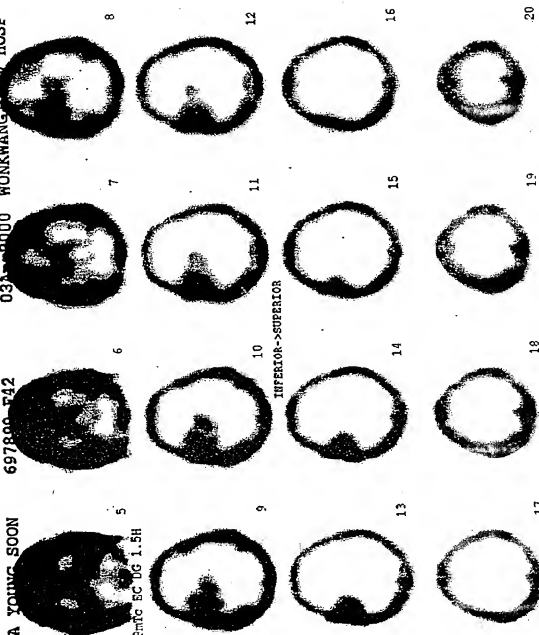
Post OP

031-0000 WONKWANG INTL HOSP

697800-F42

NA YOUNG SOON

90mc EC DG 1.5H

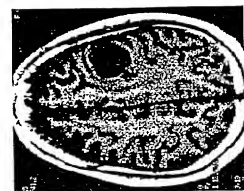


EC-DG Scan

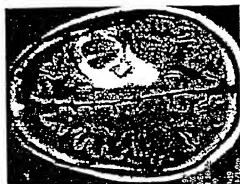
POD-25D

Figure 2, 1/61

Low anaplastic astrocytoma with hemorrhage



Pre -OP



Post-OP



FIG. 83A MRI of a patient with hemorrhagic astrocytoma.

WONKWANG UNIV HOSP

00Apr2000

790085 E-1

SEO JOK RI

16

15

14

13

DATE EC DG 1.5H

20

19

18

17

INFERIOR-SUPERIOR

24

23

22

21

28

27

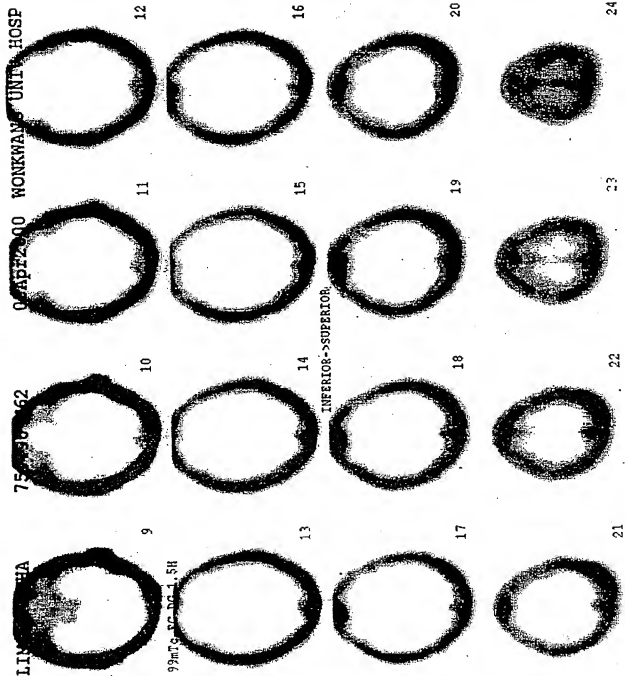
26

25

LC-DG Scan POD-26D

Case 5 : M/62
Dx : Meningioma



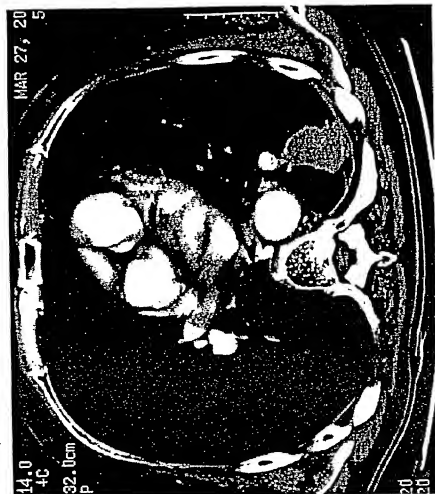


 scan with ^{99m}Tc-VC-DG of a patient with benign meningioma

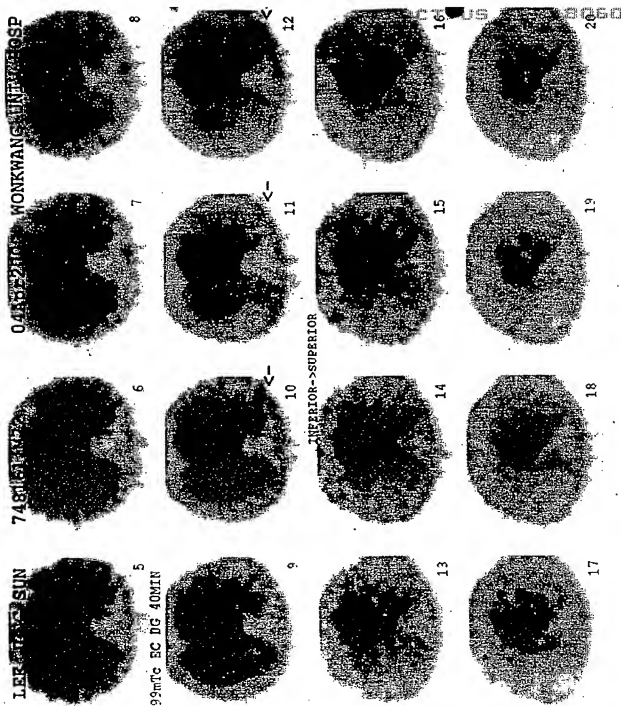
Case 1. M/F

Ur: Pul. nodule (only necrotic material on biopsy)

TB pleurisy



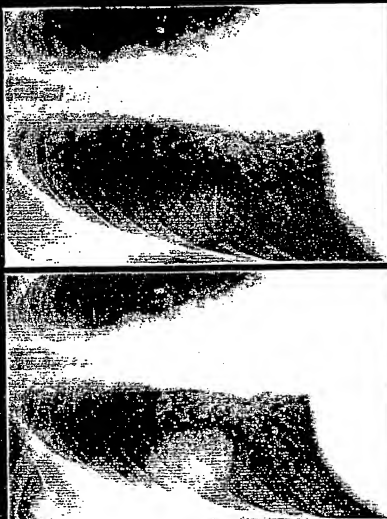
seen of a patient with TB in liver



Conclusion: The 99mTc-EC-DG of a patient with TB showed no focal

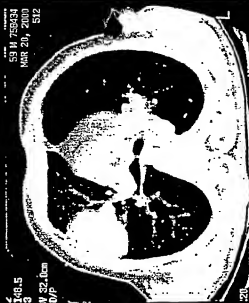
Case 5 : 59/M

Dx: Squamous carcinoma



Pre RTX

Post RTX



Pre RTX



Post RTX

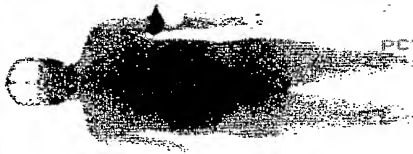
JUNG KI WOON

758434 M59

10Apr2000

WONKWANG UNIV HOSP

EC DG 1H



PCT/US 01/18060

ANT

ANT

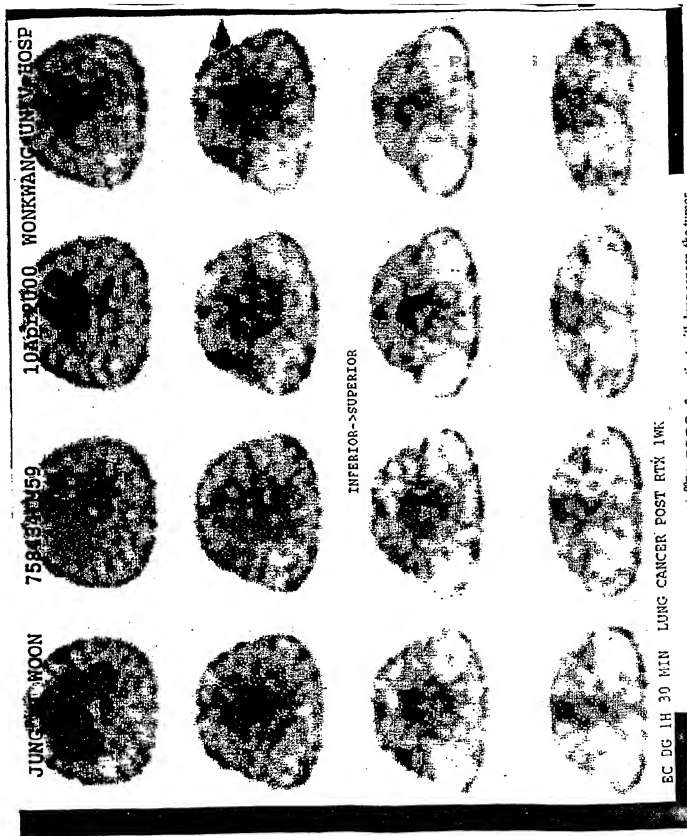
ANT

ANT

LUNG CANCER POSTI RTX 1WK

Whole body images of ^{99m}Tc -EC-DG of a patient with lung

FIG. 8GB



SPECT with ^{99m}Tc -EC-DG of a patient with lung cancer, the tumor